MOLECULAR MECHANISMS OF

FLT3-ITD-INDUCED LEUKEMOGENESIS

Sarah Cassidy Nabinger

March, 2012

Accepted by the Faculty of Indiana University, in partial
fulfillment of the requirements for the degree of Doctor of Philosophy.

_____

Rebecca J. Chan, MD/PhD, Chair

Doctoral Committee

_____

Kenneth Cornetta, MD

January 11th, 2012

_____

Nuria Morral, PhD

_____

Reuben Kapur, PhD

ACKNOWLEDGEMENTS

ABSTRACT

Sarah Cassidy Nabinger

MOLECULAR MECHANISMS OF

FLT3-ITD-INDUCED LEUKEMOGENEISIS

Internal tandem duplications in FMS-like receptor tyrosine kinase (FLT3-ITDs) are seen in approximately 25% of all acute myeloid leukemia (AML) patients. FLT3-ITDs induce FLT3 ligand (FL)-independent cellular hyperproliferation, promiscuous and aberrant activation of STAT5, and confer a poor prognosis in patients; however, the molecular mechanisms contributing to FLT3-ITD-induced malignancy remain largely unknown.

The protein tyrosine phosphatase, Shp2, is important for normal hematopoiesis as well as hematopoietic stem cell (HSC) differentiation, engraftment, and self-renewal. Furthermore, FLT3-ITD- or constitutive active STAT5-expressing CD34+ cells demonstrate enhanced hematopoietic stem cell self-renewal. Together with the previous findings that Shp2 is critical for normal hematopoiesis, that dysregulated Shp2 function contributes to myeloid malignancies, and that Shp2 has been shown to interact with WT-FLT3 tyrosine 599, which is commonly duplicated in FLT3-ITDs, a positive role for Shp2 in FLT3-ITD-induced signaling and leukemogenesis is implied.

I demonstrated that Shp2 is constitutively associated with the reported FLT3-ITDs, N51-FLT3 and N73-FLT3, compared to WT-FLT3; therefore, I hypothesized that increased Shp2 recruitment to N51-FLT3 or N73-FLT3 contributes to hyperproliferation

and hyperactivation of STAT5. I also hypothesized that Shp2 cooperates with STAT5 to activate STAT5 transcriptional targets contributing to the up-regulation of pro-leukemic proteins. Finally, I hypothesized that reduction of Shp2 would result in diminished N51-FLT3-induced hyperproliferation and activation of STAT5 *in vitro*, and prevent FLT3-ITD-induced malignancy *in vivo*. I found that genetic disruption of *Ptpn11*, the gene encoding Shp2, or pharmacologic inhibition of Shp2 with the novel Shp2 inhibitor, II-B08, resulted in significantly reduced FLT3-ITD-induced hematopoietic cell hyperproliferation and STAT5 hyperphosphorylation. I also demonstrated a novel role of Shp2 in the nucleus of FLT3-ITD-expressing hematopoietic cells where Shp2 and STAT5 co-localized at the promoter region of STAT5-transcriptional target and pro-survival protein, Bcl-X$_L$. Furthermore, using a Shp2$^{flox/flox}$;Mx1Cre+ mouse model, I demonstrated that reduced Shp2 expression in hematopoietic cells resulted in an increased latency to and reduced severity of FLT3-ITD-induced malignancy. Collectively, these findings demonstrate that Shp2 plays an integral role in FLT3-ITD-induced malignancy and suggest that targeting Shp2 may be a future therapeutic option for treating FLT3-ITD-positive AML patients.

Rebecca J. Chan, MD/PhD, Chair

TABLE OF CONTENTS

LIST OF TABLES

LIST OF FIGURES

CHAPTER ONE

INTRODUCTION

Acute Myeloid Leukemia

Acute myeloid leukemia (AML) is a disease predominantly affecting older

individuals and accounts for about 25% of all leukemias in adults in the western world

(Deschler and Lubbert 2006; Estey and Dohner 2006). Patients with AML often present

with an overabundance of myeloid cells, anemia, and thrombocytopenia. Generally,

afflicted individuals may be overly tired, have an increase in bruising or bleeding,

recurrent fever, infections, or unexplained weight loss. In the recent past, the incidence

of patients over 65 with AML was over 9 times higher than that of patients under 65

years old (Deschler and Lubbert 2006) (Figure 1.1). Furthermore, patients under 65 years

old had a 34.4% 5-year survival rate, while patients over 65 years old, had a dismal

survival rate of merely 4.3% (Deschler and Lubbert 2006) (Figure 1.2). As the mean age

of the population continues to increase, there is a growing population of older

individuals, making better treatments and curative therapies for AML urgently needed. It

is extremely important to recognize the difficulty in treating older patients with AML.

As patients age, they tend to develop multiple co-morbidities and, thus, become less

tolerant of harsh chemotherapy and radiation (Deschler and Lubbert 2006; Estey and

Dohner 2006; Melchert 2006). Because of these complications, older patients are often

ineligible for cytotoxic therapy and are only treated with supportive, rather than curative,

care. Therefore, it is imperative that therapies with reduced toxicity and increased

efficacy are developed to treat AML patients.
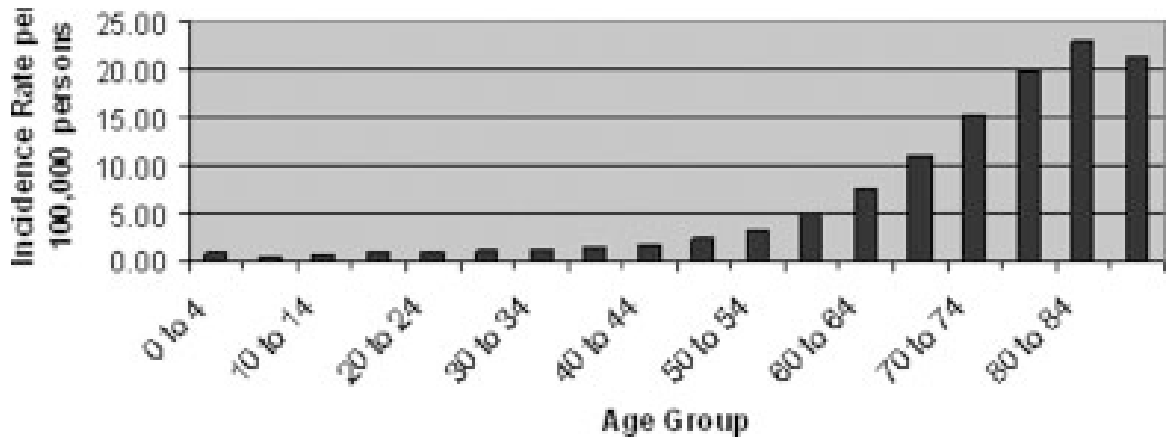
Figure 1.1: AML is predominantly diagnosed in aging individuals

Incidence of AML diagnosis represented as the number of people diagnosed with AML out of 100,000. Figure is adapted from Deschler et al. (Deschler and Lubbert 2006).
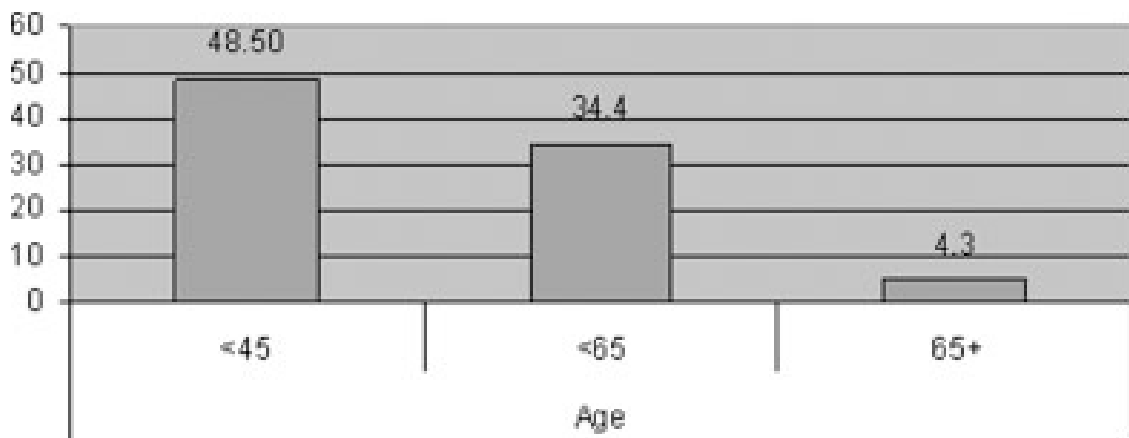
Figure 1.2: 5-year survival rate of AML patients by age group

The 5-year survival rate of AML patients is divided into 3 age groups: under 45 (<45), under 65 (<65), and over 65 (65+) years old and is displayed as percent survival. Figure adapted from Deschler et al. (Deschler and Lubbert 2006).

2

AML and FLT3 Mutations

Internal tandem duplications in FMS-like tyrosine kinase (FLT3-ITD) are insertions of several amino acids into or around the juxtamembrane domain and are present in approximately 25% of all AML patients (Kelly, Liu et al. 2002; Georgiou, Karali et al. 2006; Heiss, Masson et al. 2006; Rocnik, Okabe et al. 2006; Small 2006). The WT-FLT3 amino acid sequence of the juxtamembrane domain is shown in figure 1.3 with several examples of FLT3-ITDs, their specific duplications, and insertion sites into the juxtamembrane domain. It is well-known that these FLT3-ITDs contribute to a poor prognosis. Figure 1.4 displays a Kaplan Meijer curve from a study by Abu-Duhier and colleagues comparing the FLT3-ITD status of AML patients (FLT3-ITD-positive or negative) with survival (Abu-Duhier, Goodeve et al. 2000). There was an obvious decrease in the survival of patients that were FLT3-ITD+ compared to AML patients that were FLT3-ITD- with a p-value of 0.0002.

FLT3-ITD mutations result in constitutive FLT3 phosphorylation, FLT3 ligand (FL)-independent cellular hyperproliferation, and aberrant activation of signal transducer and activator of transcription 5, STAT5 (Mizuki, Schwable et al. 2003; Chung, Morrone et al. 2005; Kato, Iwama et al. 2005; Rocnik, Okabe et al. 2006; Choudhary, Brandts et al. 2007). STAT5 is a transcription factor which is known to activate pro-cycling molecules such as Cyclin D1 (Joung, Lim et al. 2005) and anti-apoptotic proteins such as Bcl-X_L (Beverly and Varmus 2009; Mizukawa, Wei et al. 2011). We wish to investigate the molecular mechanism(s) underlying the transforming capacity of FLT3-ITDs in an effort to develop novel, molecularly-targeted, and less toxic therapies for individuals with FLT3-ITD-positive AML.
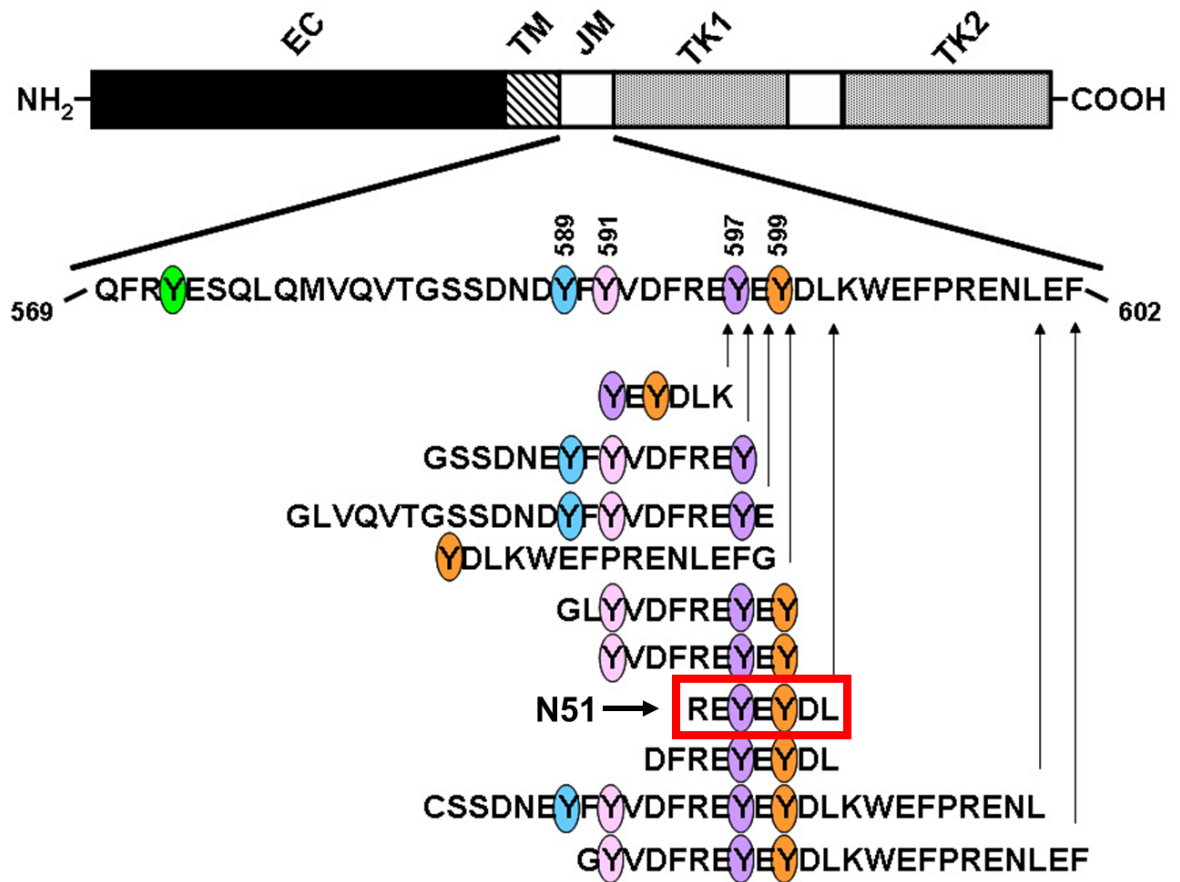
Figure 1.3: Examples of FLT3-ITDs

The WT-FLT3 receptor is shown in the schematic with listing the amino acid sequence of the jutamembrane domain highlighting the different tyrosine residues. Below the WT-FLT3 sequence are the amino acid sequences and where they are inserted of several reported FLT3-ITDs. We will frequently use the FLT3-ITD, N51-FLT3.
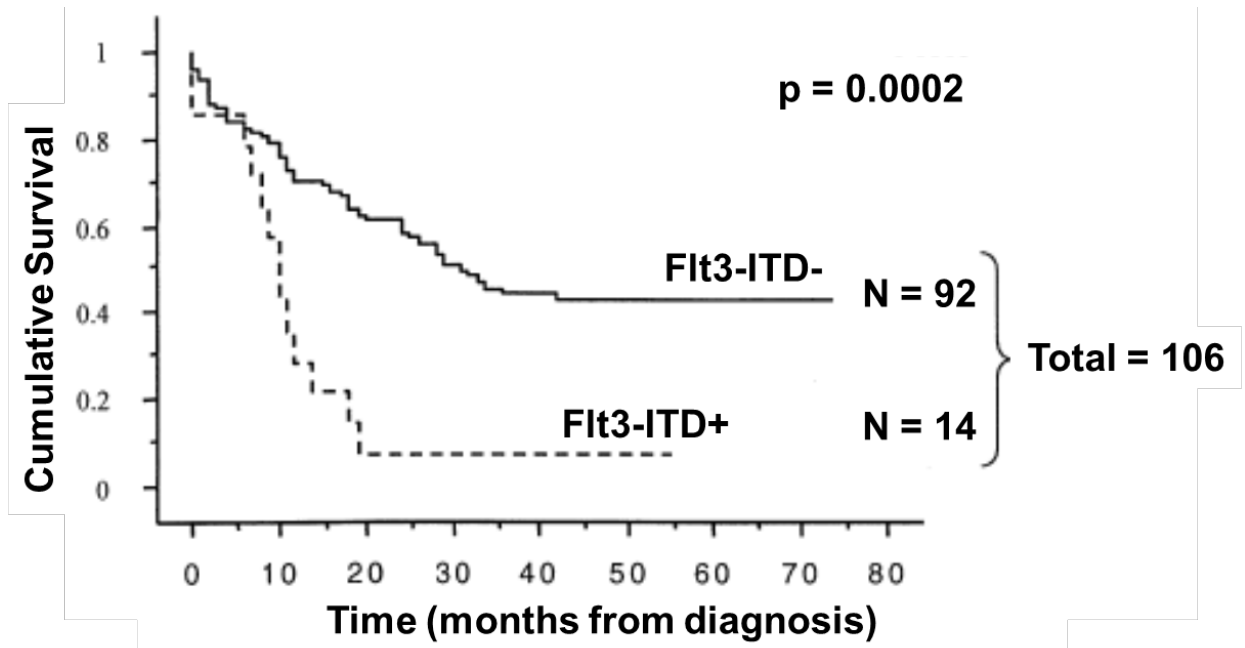
Figure 1.4: Cumulative Survival of FLT3-ITD-negative (-) vs. FLT3-ITD-positive (+) patients

Data is presented as cumulative survival of AML patients that are either FLT3-ITD+ or FLT3-ITD-. P-value derived from log-rank test; figure adapted from Abu-Duhier et al., Br. J. Haematol., 2000.

Wildtype FLT3

To better understand the potential signaling aberrations of the FLT3-ITDs, we will first explore data presented on wildtype (WT) FLT3. FMS-like tyrosine kinase 3, FLT3, is a member of the class III receptor tyrosine kinase family which also includes platelet-derived growth factor receptor (PDGFR) and stem cell growth factor receptor, c-Kit. FLT3 is normally expressed on immature hematopoietic progenitor cells and contributes to proliferation, survival, and differentiation. Upon stimulation with FLT3 ligand (FL), FLT3 forms a homodimer and autophosphorylates itself resulting in the activation of downstream signaling cascades.

Wildtype FLT3 Recruits the Protein Tyrosine Phosphatase, Shp2

To better understand the molecular mechanism of normal FLT3 function, Heiss et al. investigated the wildtype (WT) FLT3 receptor. They determined that activated WT-FLT3 recruits the protein tyrosine phosphatase, Shp2, via autophosphorylation of tyrosine 599 (Y599) in the juxtamembrane domain (Heiss, Masson et al. 2006). To do this, the autophosphorylation sites in the juxtamembrane domain of WT-FLT3 were mapped, identifying tyrosines 572, 589, 591, and 599 as sites of autophosphorylation *in vivo*. Next, tyrosine (Y) residues were mutated to phenylalanine (F) and WT-FLT3, FLT3-Y589F and FLT3-Y599F constructs were stably transduced into 32D cells. Upon examination of FLT3 ligand (FL)-induced responses, it was determined that Y589F and Y599F exhibited distinct FL-dependent phenotypes. Stimulation of WT-FLT3 induced Erk activation which remained high in cells expressing the Y589F construct; however in cells expressing the Y599F construct, Erk activation was diminished. This suggested that

phosphorylation of Y599 specifically contributes to Erk activation. Next, the authors

determined that Shp2 directly associates with pY599 in biochemical experiments.

Protein extracts from 32D-WT-FLT3 and 32D-FLT3-Y599F cells were prepared and

incubated with glutathione S-transferase (GST)-conjugated Shp2. These proteins were

separated on SDS-PAGE, transferred to nitrocellulose membrane, and probed for FLT3.

These studies demonstrated that Shp2 was recruited to WT-FLT3 but not FLT3-Y599F.

This further strengthened their argument that Shp2 associates with Y599 in the

juxtamembrane domain of FLT3. Finally, they measured cell growth by MTT [3-(4,5-

dimethylthiazol-2-yl)-2,5-diphenyltetrazolium bromide] assays to demonstrate that FL

stimulation results in increased cell numbers in WT-FLT3 32D cells. However, FL

stimulation of 32D-FLT3-Y599F cells did not induce cell growth.

Thus, these studies suggest that in WT-FLT3 receptor signaling, Shp2 binds Y599

and this interaction is required for Erk activation and normal FL-stimulated cell growth

(Heiss, Masson et al. 2006). Interestingly, Y599 is conserved in all members of the class

III receptor tyrosine kinase family, and mutation of tyrosine 577 (Y577) in PDGFR (the

tyrosine homologous to Y599), leads to constitutive receptor tyrosine phosphorylation

and ligand-independent cellular proliferation (Irusta, Luo et al. 2002). These findings

suggest that Y599 in FLT3 may be important in FL-independent growth and when

duplicated in FLT3-ITDs, may contribute to FLT3-ITD-induced leukemogenesis.

Protein Tyrosine Phosphatase Shp2

Shp2 is a ubiquitously expressed cytosolic signaling molecule encoded by the

gene *Ptpn11*. It has two Src homology 2 (SH2) domains (N-terminal and C-terminal)

located in the amino end and a phosphatase domain localized to the carboxyl terminus (Figure 1.5). Shp2 is important in a wide variety of cell processes including cell proliferation, differentiation, cell cycle maintenance, and migration. One simplistic schematic of Shp2 activation is shown in Figure 1.5. Upon Shp2 activation, Ras is activated which leads to the downstream activation of signaling molecules Raf and Mek which ultimately activates mitogen-activated protein kinase, MAPK also known as Erk (Figure 1.5).

Approximately 50% of individuals with the congenital disorder, Noonan syndrome (NS), bear germline gain-of-function mutations in *PTPN11*, and NS patients have an increased incidence of juvenile myelomonocytic leukemia (JMML). Somatic gain-of-function mutations in Shp2 have also been associated with other malignancies in addition to myeloid leukemia (Tartaglia, Niemeyer et al. 2003; Bentires-Alj, Gil et al. 2006), and wildtype Shp2 has been shown to be over-expressed in several human AML cases (Xu, Yu et al. 2005). These data demonstrate that Shp2 is implicated in human diseases and leukemogenesis. Given that leukemia is a proliferative disease of the stem and hematopoietic progenitor cells, we next investigated the known functions of Shp2 in normal stem cell function and hematopoiesis.
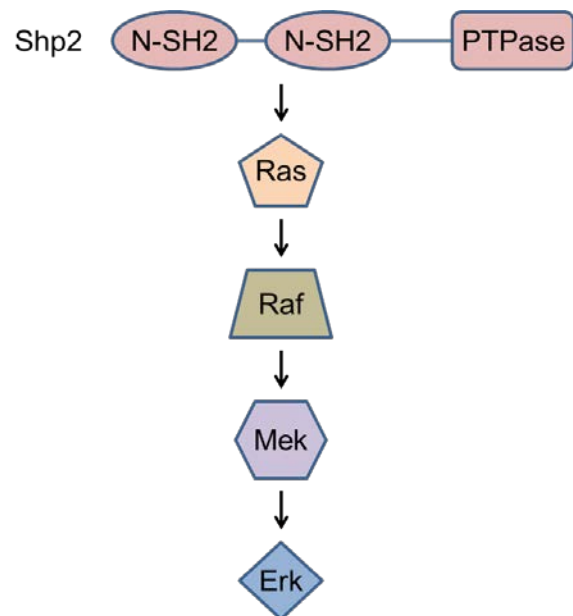
Figure 1.5: Schematic representation of Shp2 activation (adapted from (Chen, Sung et al. 2006))

Shp2 in Normal Hematopoiesis and in Hematopoietic Stem Cell Function

Shp2 is an essential, ubiquitously expressed protein tyrosine phosphatase as evidenced by the fact that *Shp2-/-* animals are embryonic lethal (Saxton, Henkemeyer et al. 1997). Using ES cells bearing an exon 3 deletion from *Ptpn11* resulting in an in-frame deletion of amino acids 46-110 within the N-terminal SH2 domain of the mature Shp2 protein, Qu et al. demonstrated that embryoid body (EB) differentiation in the form of erythroid and myeloid development was impaired compared to WT ES cells (Qu, Shi et al. 1997). They further went on to use *Shp2-/-* -WT chimeric animals to demonstrate that *Shp2-/-* ES cells failed to contribute to hematopoietic progenitors in fetal liver and bone marrow, resulted in deficient yolk sac hematopoiesis, and resulted in multiple developmental defects of chimeric animals (Qu, Yu et al. 1998). Finally, Chan et al. demonstrate a role of Shp2 in the initial steps of ES cell differentiation (Chan, Johnson et al. 2003) using the previously described truncated-Shp2-bearing ES cells. Furthermore, using haploinsufficient *Shp2+/-* animals, it was demonstrated that *Shp2+/-* bone marrow cells have reduced hematopoietic stem cell (HSC) repopulating units and reduced self-renewal after transplantation into lethally irradiated hosts compared to that of WT bone marrow (Chan, Li et al. 2006). Collectively these data suggest that Shp2 is important in normal hematopoiesis by promoting differentiation from very early stages of ES cell development and by supporting HSC function and self-renewal.

As previously mentioned, complete Shp2 knock out is embryonic lethal, therefore, Shp2$^{flox/flox}$ animals were designed and studied by Geng-Sheng Feng's lab (Zhang, Chapeau et al. 2004). Initially they crossed these Shp2$^{flox/flox}$ animals with a neuronal-specific Cre to examine the loss of Shp2 in brain tissues. These Shp2$^{flox/flox}$

animals were later crossed with Mx1Cre+ transgenic animals and used to demonstrate that a loss of Shp2 results in cytopenia in peripheral blood, bone marrow, and spleen (Zhu, Ji et al. 2011). They also demonstrated that Shp2 deficient HSCs failed to reconstitute lethally irradiated recipients and that this defect is cell-autonomous, collectively supporting the importance of Shp2 in self-renewal, homing, and survival (Zhu, Ji et al. 2011). In a similar Shp2-deficient mouse model developed in the Ben Neel lab, Mx1Cre+;*Ptpn11*$^{\text{flox/flox}}$ animals also demonstrated that loss of Shp2 results in a rapid decrease of HSCs and hematopoietic progenitors from all lineages in a dose-dependent and cell autonomous manner (Chan, Cheung et al. 2011). These complementary studies demonstrate that Shp2 is an important factor in normal hematopoiesis contributing to self-renewal, maturation, and differentiation of HSC/progenitors. Given that acute leukemia is a disease of dysregulated HSCs and given the importance of Shp2 in HSC function, we rationalized that dysregulated Shp2 function in the context of FLT3-ITD+ leukemia may promote leukemogenesis by supporting aberrant HSC function. This hypothesis was further supported by previous findings that FLT3-ITDs as well as constitutively activated STAT5, the most robust neomorphic signal found in FLT3-ITD+ cells, also leads to increased HSC self-renewal.

The Role of STAT5 and FLT3-ITD in Hematopoietic Stem Cell Function

Moore and colleagues published two important studies examining the function of STAT5 and FLT3-ITD using human cord blood CD34+ cells. CD34+ cells were transduced with constitutive active STAT5 and used to demonstrate that CD34+ cells expressing active STAT5 have increased self-renewal and contribute to increased

proliferation and generation of erythroid progenitors (Schuringa, Chung et al. 2004). In

another study, CD34+ cord blood cells were transduced with either WT-FLT3 or N51-

FLT3 and the N51-FLT3-transduced cells had a proliferative advantage and were able to

generate early cobblestone areas which maintained self-renewal upon plating into

secondary and tertiary cobblestone area-forming cell (CAFC) assays (Chung, Morrone et

al. 2005). Although the authors did not directly examine the molecular mechanisms,

these data provide evidence that either FLT3-ITD and/or hyperactive STAT5 contribute

to increased HSC self-renewal. Given that AML is a clonal disorder of undifferentiated

myeloid blasts that is maintained and propagated by a small population of leukemic cells

with stem cell qualities, these findings may at least partially explain why FLT3-ITDs

(which are associated with constitutive active STAT5) induce such a robust leukemia.

Constitutive Activation of STAT5 in FLT3–ITD Mutants

The most well know aberration in FLT3-ITDs is the promiscuous activation of

STAT5, which is only modestly activated in WT-FLT3 signaling; however, the molecular

mechanism by which STAT5 is robustly activated in the presence of FLT3-ITDs is

unknown. There are four tyrosines in the juxtamembrane domain of wild type FLT3

(Y589, Y591, Y597, and Y599) which are comonly duplicated in FLT3-ITDs such as

those published examples of FLT3-ITDs illustrated in figure 1.3. Notice that Y599 is

very commonly duplicated among the reported FLT3-ITDs (Figure 1.3).

Multiple studies have demonstrated that FLT3-ITDs induce constitutive activation

of STAT5 (Kiyoi and Naoe 2002; Mizuki, Schwable et al. 2003; Chung, Morrone et al.

2005; Kato, Iwama et al. 2005; Rocnik, Okabe et al. 2006; Choudhary, Brandts et al.

2007), in contrast to physiologic FLT3 receptor signaling, which only modestly induces STAT5 activation (Zhang and Broxmeyer 2000; Chung, Morrone et al. 2005). Rocnik et al. purified histidine-tagged cDNA encoding amino acids 580-993 of wild type FLT3 and performed *in vitro* autophosphorylation reactions. Residues Y591, Y726, Y942, Y955 and Y969 were phosphorylated, while Y589, Y597, Y599, Y768, Y793, Y865, Y889, Y726, and Y955 were not. To better understand the role of each tyrosine in FLT3-ITD-induced transformation, Rocnik and coworkers used a specific FLT3-ITD called N51-FLT3 (Figure 1.3), which contains a duplication of 7 amino acids including Y597 and Y599 and modified several of the identified tyrosine residues to phenylalanine. Using WT-FLT3, N51-FLT3, and N51-FLT3-Y589/591F they found that mutations Y589F and Y591F together significantly reduced STAT5 activation compared to N51-FLT3 in both Baf3 and 32D cells. Additionally, when they transplanted bone marrow cells transduced with the three constructs (WT-FLT3, N51-FLT3, or N51-FLT3-Y589/591F) into mice and tracked survival over time, the N51-FLT3 mice acquired myeloproliferative disease with a latency of 40-60 days; however, the WT-FLT3 or N51-FLT3-Y589/591-transplanted mice showed no signs of myeloproliferative disease with follow-up to 240 days (Rocnik, Okabe et al. 2006). Therefore, they concluded that Y589 and Y591 are responsible for N51-FLT3-induced constitutive STAT5 activation and contribute to the transformation capacity of N51-FLT3 *in vivo* (Rocnik, Okabe et al. 2006).

Tyrosines 589 and 591 are Important for Autoinhibition of FLT3

Upon examination of the crystal structure of autoinhibited wild type FLT3, Griffith and colleagues observed that the juxtamembrane (JM) domain contains two key

tyrosines, Y589 and Y591, which are located in the JM-Switch motif and bind another segment of the receptor called the C-lobe. This binding stabilizes the JM domain association with the structural elements of the receptor and maintains the kinase in its inactive confirmation (Griffith, Black et al. 2004). When Y589 and Y591 become phosphorylated, they are unable to bind the C-lobe and, thus FLT3 undergoes a conformational change to its active form (Griffith, Black et al. 2004). In other words, Y589 and Y591 must be phosphorylated for FLT3 to become activated. Therefore, mutations of Y589 and Y591 to phenylalanine, which precludes phosphorylation at these site, would clearly permit FLT3-ITD to remain permanently autoinhibited. Consequently, it is not unexpected FLT3-ITD-Y589/591F used by Rocnik and colleagues prevents receptor phosphorylation, activation, and myeloproliferative disease *in vivo* (Rocnik, Okabe et al. 2006). Although these studies are informative by demonstrating the importance of Y589 and Y591 in maintaining FLT3 in the inactive conformation, these studies do not define what signaling molecules may be aberrantly recruited to mutant FLT3 or how the aberrantly recruited signaling moleucles may contribute to FLT3-ITD-induced transformation and leukemogenesis.

Shp2 Positively Regulates STAT5

While some studies have demonstrated that Shp2 inactivates STAT5 (Yu, Jin et al. 2000; Chen, Wen et al. 2003), other studies have shown that Shp2 plays a positive role in STAT5 activation and signaling (Chughtai, Schimchowitsch et al. 2002; Ke, Lesperance et al. 2006). In a conditional mouse model (Shp2$^{flox/flox}$ crossed with MMTV-Cre transgenic mice), *Shp2-/-* mammary gland cells exhibited reduced phoshpho-STAT5

(P-Stat5) in response to lactation compared to control animals (Ke, Lesperance et al. 2006). Immunoprecipitation experiments revealed that upon prolactin stimulation of control mice, the prolactin receptor (PRLR) recruits Jak2 and Shp2 to form a complex. However, Shp2-deficient mice are unable to form this complex suggesting Shp2 is important in the PRLR-Jak2 activation of STAT5 (Ke, Lesperance et al. 2006). In another study, Chughtai and colleagues demonstrated that STAT5 was phosphorylated and associated with Shp2 in a dose-dependent manner in either murine mammary epithelial (CH11) or human mammary carcinoma (T47D) cell lines in response to prolactin (PRL) stimulation (Chughtai, Schimchowitsch et al. 2002). To understand the role of the SH2 domains in Shp2, 293 cells were transiently transfected with plasmids encoding the prolactin receptor (PRLR), STAT5, Jak2 and either wild type Shp2 or Shp2 containing point mutations in the N-terminal SH2 domain (SHP2-R32K) or the C-terminal SH2 domain (SHP2-R138K). Total cell lysates were immunoprecipitated with α-Shp2 and blotted with α-STAT5 to look for a Shp2-STAT5 association in response to PRL. The association between STAT5 and Shp2-R138K was significantly reduced while interaction between STAT5 and Shp2-R32K appeared normal. Similarly prepared cell lysates were analyzed by western blot analysis for phosphorylation of STAT5. Cells overexpressing WT-Shp2 or Shp2-R32K exhibited a strong activation of STAT5 upon PRL stimulation; however, this activation was not induced in cells overexpressing Shp2-R138K. Thus, the C-terminal SH2 domain of Shp2 is required for physical association and phosphorylation of STAT5 in response to PRL (Chughtai, Schimchowitsch et al. 2002). Further studies demonstrated that Shp2 was found in a nuclear protein complex with STAT5 at the STAT5-responsive β-casein promoter. These studies provide

evidence that in mammary epithelial cells Shp2 plays a positive role in STAT5 signaling and may do so by promoting STAT5 function in the nucleus. While robust Shp2 expression has been detected in the nuclear fraction of human AML samples, its role in the nucleus in the setting of AML has never been investigated; therefore, we hypothesized that in response to FLT3-ITDs, perhaps Shp2 associates with and activates STAT5 to promote pro-leukemogenic STAT5-target genes such as Bcl-X_L and Cyclin-D1 (Figure 1.6).
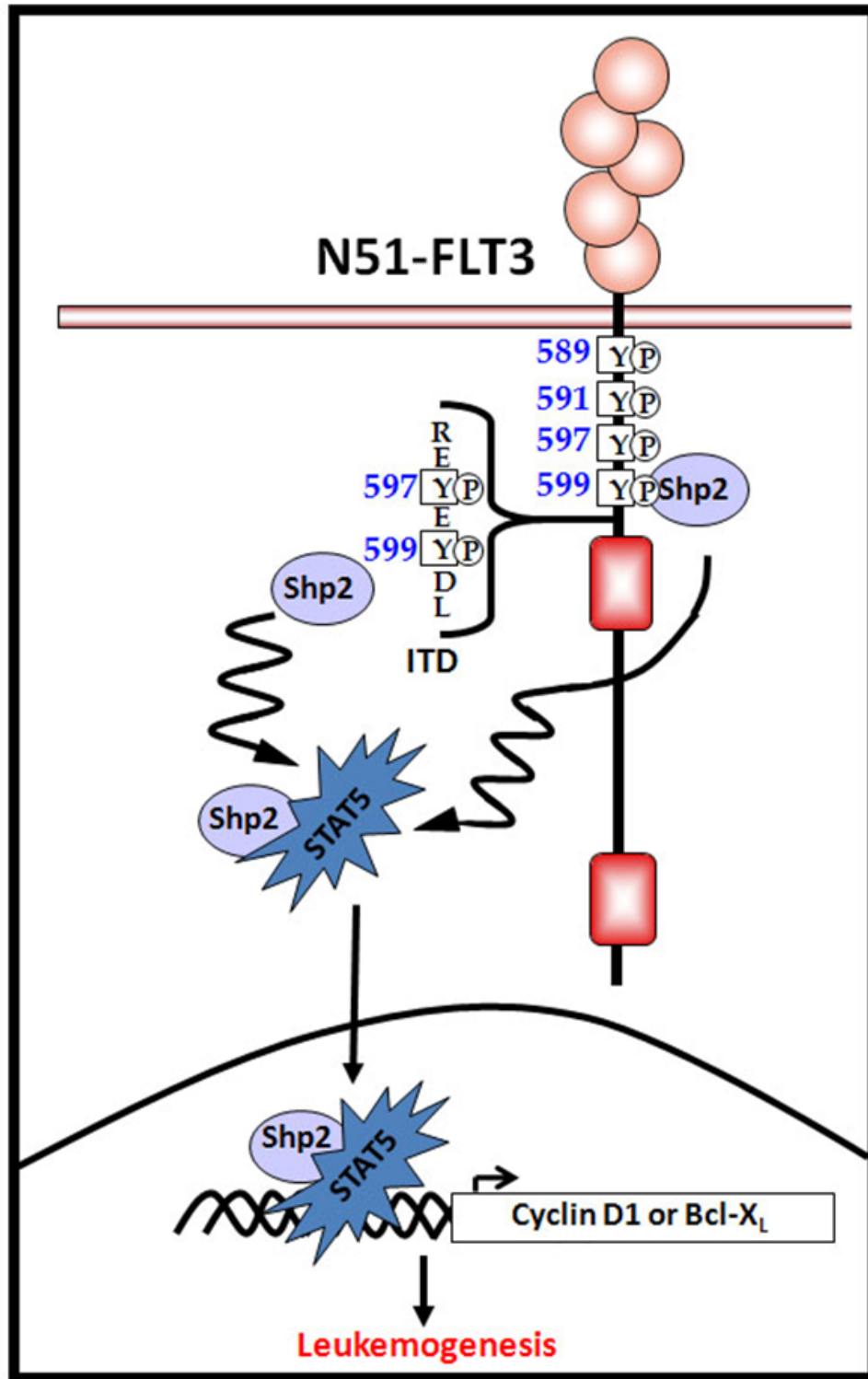
Figure 1.6: Schematic representation of proposed N51-FLT3 molecular mechanism

Summary and Significance

While FLT3-ITD-positive AML contributes to a poor prognosis in patients, the molecular mechanisms contributing to FLT3-ITD-induced leukemogenesis remain largely unknown. Multiple studies have demonstrated that Shp2 functions physiologically in FLT3 receptor signaling (Zhang and Broxmeyer 1999; Zhang, Mantel et al. 1999; Heiss, Masson et al. 2006). We provide novel data demonstrating that Shp2 is constitutively associated with FLT3-ITDs, N51-FLT3 and N73-FLT3, suggesting that increased Shp2 function contributes to FLT3-ITD-induced cellular transformation.

Since Shp2 has been shown to be important in HSC engraftment, self-renewal, homing, and maturation (Qu, Shi et al. 1997; Qu, Yu et al. 1998; Chan, Johnson et al. 2003; Chan, Li et al. 2006; Chan, Cheung et al. 2011), and is increasingly being identified as a key transforming molecule in leukemogenesis (Bentires-Alj, Paez et al. 2004; Chan, Leedy et al. 2005; Mohi, Williams et al. 2005; Schubbert, Lieuw et al. 2005; Xu, Yu et al. 2005; Chan and Feng 2007), it has become an attractive potential target in anti-leukemia therapies. Additionally, given that leukemia is a disease caused by dysregulated HSC/progenitor function, and that Shp2, FLT3-ITDs, and constitutively activated STAT5 have been shown to promote HSC self-renewal, we reasoned that dysregulated Shp2, in the context of FLT3-ITD-poisitve AML may induce constitutive activation of STAT5 and its subsequent molecular targets.

The role of Shp2 in STAT5 activation and hyperactivation in response to WT-FLT3 and FLT3-ITD receptor stimulation, respectively, is unknown. In some studies, Shp2 has been shown to inactivate STAT5 (Yu, Jin et al. 2000; Chen, Wen et al. 2003). However, paradoxically, other studies show that Shp2 positively regulates STAT5 (Ali,

Chen et al. 1996; Berchtold, Volarevic et al. 1998; Chughtai, Schimchowitsch et al. 2002; Ke, Lesperance et al. 2006). Thus, the role of Shp2 in STAT5 activation appears to be cell type- and pathway-dependent. Importantly, IL-3- and GM-CSF-stimulation of myeloid cells bearing leukemia-associated Shp2 gain-of-function mutations induces hyperactivation of STAT5 (Mohi, Williams et al. 2005), suggesting that Shp2 plays a positive role in STAT5 activation in the setting of leukemogenesis.

Our main goal is to better understand these molecular mechanisms contributing to FLT3-ITD-positive leukemogenesis in order to determine molecular targets and/or molecular-based therapeutic options to treat FLT3-ITD+ AML patients. Our studies specifically address the following hypotheses:

1. Increased recruitment of Shp2 to N51-FLT3 and N73-FLT3 contributes to ligand-independent cellular proliferation and the constitutive STAT5 activation.

2. Shp2 forms a complex with STAT5 in the nucleus of FLT3-ITD-bearing hematopoietic cells to activate STAT5 transcriptional targets contributing to pro-leukemic functions.

3. Genetic loss of Shp2 results in reduced cellular hyperproliferation and reduced activation of STAT5, and consequently prevents FLT3-ITD-induced myeloproliferative disease (MPD) or increases the latency to disease onset *in vivo*.

4. Pharmacologic inhibition of Shp2 results in decreased hyperproliferation and hyperactivation of STAT5, and prevents FLT3-ITD-induced malignancy *in vivo*.

Overall, our hypothesis is generalized by the schematic diagram in Figure 1.6. Duplication of Shp2 binding residue, Y599, in FLT3-ITDs contributes to increased recruitment of Shp2 to the mutant receptor and this increased Shp2 recruitment contributes to aberrant activation of STAT5. Subsequently, Shp2 cooperates with STAT5 in the nucleus to activate STAT5 target genes and promote hyperproliferation and leukemic signals.

In addressing these hypotheses, we have used functional analyses to determine the proliferative potential of FLT3-ITD-bearing cell lines and primary cells compared to WT-FLT3-expressing cells. We also used functional assays to examine FLT3-ITD-induced hyperproliferation after targeting Shp2 by either shRNAs targeting Shp2, genetic disruption of Shp2, or blocking the phosphatase activity of Shp2 by treatment with the pharmacologic inhibitor, II-B08.

To determine the consequences of loss of Shp2 biochemically, immunoprecipitation assays were used to demonstrate an increased recruitment of Shp2 to N51-FLT3 and N73-FLT3, and the association of Shp2 and STAT5 in total cell lysates. We further used immunoblot analysis to determine the levels of phosphorylated- and total-Shp2 protein expression, and the activation of STAT5.

To study the potential role of Shp2 in the nucleus of FLT3-ITD-expressing cells, immunofluorescence and chromatin immunoprecipitation (ChIP) assays were utilized to demonstrate nuclear co-localization of Shp2 with phospho-STAT5 and the presence of Shp2 at the STAT5-responsive promoter, *BCL2L1*, which regulates expression of the pro-survival protein, Bcl-X$_L$.

To examine the contribution of Shp2 in FLT3-ITD-induced myeloproliferative disorder (MPD) *in vivo*, Shp2$^{flox/flox}$;Mx1Cre genetic knock out animals were utilized by examining the effect of *in vivo* deletion of Shp2 on the latency to malignancy in animals transplanted with N51-FLT3-transduced Shp2$^{flox/flox}$;Mx1Cre cells. Finally, using a syngeneic N51-FLT3 transplant model, we examined the effect of *in vivo* treatment with the Shp2 pharmacologic inhibitor, II-B08.

Significance

While acute myeloid leukemia is a relatively rare disease, it accounts for approximately 40% of all leukemias in the western world. Therapies to treat patients with FLT3-ITD-positive acute myeloid leukemia typically involve harsh regimens of chemotherapy and radiation and even then prognosis remains poor, rendering supportive care often one of the only remaining options.

Our efforts to identify Shp2 as an important, targetable signaling molecule for molecularly targeted therapeutic treatment of these patients are significant because they allow us to better understand the molecular mechanisms contributing to FLT3-ITD+ cellular transformation. Ultimately, this has enabled us to study genetic deletion of Shp2 and the use of a pharmacologic inhibitor targeted to Shp2 in order to demonstrate that targeting Shp2 may have therapeutic benefits to FLT3-ITD+ AML patients. Because Shp2 has been implicated in many different types of malignancies as well as congenital disorders, a better understanding of its molecular mechanisms in FLT3-ITD+ AML opens the possibilities for potential therapeutic options for these other Shp2-related disorders.

CHAPTER TWO

MATERIALS AND METHODS

A. Materials

1. Plasmids

a. pMSCV

pMSCV: WT-, N51-, and N73-FLT3 constructs were expressed using the Murine Stem Cell Virus (pMSCV) plasmid. cDNA from human WT-FLT3, or patient-derived FLT3-ITDs, N51-FLT3, or N73-FLT3 were expressed in the bicistronic pMSCV vector, co-expressing green fluorescent protein (GFP) as a marker. FLT3-ITDs "N51-FLT3" and "N73-FLT3" have insertions/duplications of the following amino acids: "REYEYDL" and "GLYVDFREYEY" respectively.

2. Primers

Standard PCR reactions were performed using oligonucleotides synthesized by Invitrogen.

Table 2.1: Genotyping primers

Gene	Forward (5′-3′)	Reverse (5′-3′)
Shp2flox	5'-ACGTCATGATCCGCTGTCAG-5'	5'-ATGGGAGGGACAGTGCAGTG-3'
Cre	5'-CTGGCAATTTCGGCTATACGTAACAGGGTG-3'	5'-GCCTGCATTACCGGTCGATGCAACGAGTG-3'
Shp2^{null}	5'-AAGAGGAAATAGGAAGCATTGAGGA-3'	5'-TAGGGAATGTGACAAGAAAGCAGTC-3'

Table 2.2: Quantitative PCR primers

Gene	Forward (5′-3′)	Reverse (5′-3′)
Bcl-X$_L$	5'-CCCAGGGAGTGACTTTCCGAGG-3'	5'-TCGAAAGCACCAGTGGACTCTGA-3'

3. Patient Samples

Patient, peripheral blood, or bone marrow aspirate samples were obtained with prior patient consent. Using ficol gradient, low density mononuclear cells were isolated and given to us by Dr. Scott Boswell's lab under the Institutional Review Board (IRB) #9812-11 (Principle investigator, Dr. Larry Cripe).

4. shRNA plasmids

shRNA vectors are pRS plasmids with the shRNA driven by the U6 promoter for mammalian cell expression. Four different shRNA sequences targeted to Shp2 were given as well as an empty vector control and a scrambled, non-targeting control and are seen in the table below:

Table 2.3: shRNA Plasmids

ID	Name	shRNA sequence
TI525710	Shp2 shRNA-10	TAGTGAAACGGTCATTCAGCCACTGAATA
TI525711	Shp2 shRNA-11	GTTTGAGACGCTCCAGCAACAGGAATGCA
TI525712	Shp2 shRNA-12	ATGGATGTCCAGCACTACATAGAGACGCT
TI525713	Shp2 shRNA-13	CTGGCGGATGGTGTTCCAGGAGAACTCTC
TR20003	Shp2 shRNA-vector	None
TR30003	Shp2-shGFP scrambled	Not given

5. Mice

a. C57Bl/6

C57Bl/6 mice were received from Harlan and used to isolate wild type bone marrow low density mononuclear cells.

b. Shp2$^{flox/flox}$

Shp2$^{flox/flox}$ animals were given to us by Dr. Gen-Sheng Feng and crossed with Mx1-Cre animals which we received from Dr. Reuben Kapur.

c. Mx1-Cre+

Mx1-Cre animlas were a generous gift from Dr. Reuben Kapur.

d. F1 (C57/BoyJ F1)

F1 transplant recipient mice were purchased from the In Vivo Therapeutics Core at

Indiana University School of Medicine.

6. Antibodies

Table 2.4: Primary Antibodies

Primary Antibodies	Company	Clone
T-Akt	Cell Signaling	N/A
P-Akt (S473)	Cell Signaling	587F11
P-Erk	Cell Signaling	N/A
T-Erk	Cell Signaling	N/A
P-STAT5 (Y694)	Cell Signaling	N/A
T-STAT5	Cell Signaling	3H7
T-STAT5 (Chip assay)	Santa Cruz	N-20
FLT3	Santa Cruz	C-20
T-Shp2	Santa Cruz	C-18
P-Shp2(Y580)	Cell Signaling	N/A
Ras	Millipore	RAS 10
GAPDH	Biodesign International	6C5
PARP1	Santa Cruz	A-20
P-STAT5-APC (PY694)	BD	N/A
APC Mouse IgG1, *k* isotype	Biolegend	N/A
Annexin-V-APC	BD Pharmingen	N/A
CD45.1-PE	eBioscience	A20
Rat IgG2a Isotype (PE)	eBioscience	eBR2a
CD45.2-APC	eBioscience	104
Rat IgG2a Isotype (ACP)	eBioscience	eBR21

Table 2.5: HRP Secondary Antibodies

Secondary Antibody	Vendor
Goat Anti-Rabbit IgG HRP	Santa Cruz
Goat Anti-Mouse IgG HRP	Santa Cruz

7. Kits

Table 2.6: Kits

Kit	Vendor	Catalog Number
NE-PER Nuclear/Cytoplasmic Extraction Kit	Thermo Scientific	PI-78833
ChIP assay kit	Millipore	17-295
Hematopoietic progenitor and stem cell enrichment kit	EasySep, Stem Cell Technologies	19756
Plasmid Maxi-Prep Kit	Invitrogen	K210007
SuperSignal West Dura Extended Duration Substrate	Thermo Scientific	34076
Mini-prep kit	Qiagen	27106
TOPO TA Cloning Kit for Sequencing	Invitrogen	K459501
Profection Mammalian Transfection System	Promega	E1200
Ras Activation Assay Kit	Millipore	17-218
Nucleofector Kit V	Amaza/Lonza	VCA-1003
Annexin V Apoptosis Kit	BD Pharmigen	556547

B. Methods

1. Cell Culture

a. 32D Cells

32D cells, American Type Culture Collection (ATCC) were cultured in IMDM
(Invitrogen), 10% FBS (HyClone), 1% Penicillin/streptomycin (Invitrogen), and 10ng/ml
IL-3 (PeproTech). Cells were grown at 37˚C and 5% CO_2. Cells were split every 2-4
days.

b. Baf3 Cells

Baf3 cells (ATCC), were maintained in IMDM (Invitrogen) supplemented with 10% fetal
bovine serum (FBS) (HyClone), 1% penicillin/streptomycin (Gibco), and 5ng/ml IL-3
(PreproTech). Cells were grown at 37˚C and 5% CO_2. Cells were split every 2-4 days.
Baf3 cells expressing WT-, N51-, or N73-FLT3 express neomycin resistance and are
therefore also cultured with 40µl/ml genetecin (Invitrogen).

c. HL-60

HL-60 cells (ACTT) are cultured in RPMI (Invitrogen), supplemented with 10% FBS
(HyClone) and 1% Penicillin/streptomycin at 37˚C and 5% CO_2. Cells were split every
2-4 days.

d. MV411

MV411 cells are cultured in McCoy's 5A media (Invitrogen), 10% FBS (HyClone), and
1% Penicillin/streptomycin (Invitrogen). Cells were grown at 37˚C and 5% CO_2. Cells
were split every 2-4 days.

e. Primary Low Density Mononuclear Cells (LDMNCs)

Primary murine LDMNCs are cultured in MEM-alpha (Invitrogen), 20% FBS (HyClone), 2% Penicillin/streptomycin (Invitrogen), Granulocye-Colony Stimulating Factor (G-CSF), Stem Cell Factor (SCF) and Thrombopoietin (TPO) at 100ng/ml concentration each. LDMNCs are maintained at 37˚C and 5% CO_2. LDMNCs are grown for up to a maximum of 9-10 days, changing their media every 2-4 days.

f. Macrophage Progenitors

Primary LDMNCs are cultured in IMDM (Invitrogen), 20% FBS (HyClone), 1% Penicillin/streptomycin, and 50ng/ml macrophage-colony stimulating factor (M-CSF) for 7-10 days at 37˚C and 5% CO_2 to generate adherent macrophage progenitors. Macrophage progenitors require additional media after 2-3 days to supplement their growth before they become adherent. A full media change is required after they become adherent at day 5-6, and every 2-3 days thereafter.

g. Phoenix-GP Packaging Cells

Phoenix-GP cells are cultured in DMEM (Invitrogen), supplemented with 10% FBS (HyClone), 1% L-glutamine, and 2% penicillin/streptomycin on gelatin-coated, tissue culture treated 10-cm plates at 37˚C and 5% CO_2. Cells are split every 2-3 days.

2. Thymidine Incorporation Assays

Cell were starved for 4-6 hours (Baf3 cells overnight) in serum-free IMDM and then plated into thymidine incorporation assays ($1-5 \times 10^4$ cells/200 ul) either at baseline (no growth factor) or in the presence of 50 or 100ng/ml FLT3 ligand (FL), with or without indicated inhibitors and incubated overnight at 37˚C. The following morning, cells were

pulsed with 1µCi tritiated thymidine and incubated for 5-6 hours at 37˚C. Thymidine incorporation was determined using automated 96-well cell harvester (Brandel, Gaithersburg, MD).

3. Retroviral Supernatant Production

Pheonix-GP packaging cell lines are grown in DMEM + 10% FBS + 1% L-glutamine (Gibco, 25030) and 2% penicillin/streptomycin. Retroviral supernatants were produced by transfecting the phoenix cells with retroviral vector plasmids using calcium phosphate transfection (ProFection® Mammalian Transfection System, Promega, Madison, WI). Supernatants, collected at 48, 60 and 72 hours post-transfection were filtered through 0.45 micron filters and concentrated 1:4 by ultra-centrifugation.

4. Retroviral Transduction

a. Primary murine cells

Low density mononuclear (LDMNCs) cells were transduced with 2ml pMSCV, pMSCV-WT-FLT3 or pMSCV-N51-FLT3 retroviral supernatant, supplemented with 100ng/ml TPO, SCF, and G-CSF in retronectin-coated, 6cm non-tissue culture plates for 24 hours at 37˚C. After 24 hours, cells were collected, transduced again, (fresh retroviral supernatant and growth factors), and incubated overnight at 37˚C. The following morning, cells were collected and plated back into prestimulation media for 24 hours.

b. Baf3 cells

Baf3 cells were transduced similarly to LDMNCs (above) with the following modifications. Cells were supplemented with 10ng/ml IL-3 and plated into 6-well plates.

They were then spun for 1 hour at 1,200 rpm to help ensure the virus and cells were in very close proximity to each other prior to incubation at 37˚C.

5. Cell Sorting

Retrvirally transduced cells are collected and sorted using fluorescence-activated cell sorting (FACS) analysis, collecting enhanced green fluorescent protein positive (EGFP+) cells.

6. Immunoprecipitation and Immunoblots

0.5-1mg total cell lysates were immunoprecipitated with anti-FLT3, anti-Shp2, or anti-STAT5 and protein-A sepharose beads (Cl-4B, GE Healthcare) in HNTG buffer (20mM Hepes (pH 7.5), 150mM NaCl, 1% Triton X-100, 10% glycerol, plus fresh inhibitors (1mM Na_3VO_4, 0.1mM $ZnCl_2$, 1mM PMSF, 10µl/ml sigma protease inhibitor)) overnight while rotating at 4˚C. The following day, beads were centrifuged and washed several times with cold HNTG buffer, and immunoprecipitated proteins resuspended in sample buffer. IP products were run on SDS-PAGE gels, and blots were probed with indicated primary antibody, incubated with secondary antibody, and imaged.

7. Apoptosis Assay

Sorted, EGFP+, bone marrow LDMNCs expressing either WT-FLT3 or N51-FLT3 were prestimulated for 24-48 hours. Cells were then collected and counted. 225,000 cells were plated into 12-well non tissue culture plates in baseline (2%FBS-IMDM) media or in the presence of DMSO (4.5µl) 5µM, 15µM, or 30µM II-B08 in a total volume of

500µl and incubated overnight at 37˚C. The following day cells were carefully collected into individual 5ml polystyrene tubes (FACS tubes), washed with PBS and resuspended in 100µl 1X buffer (BD Pharmingen FITC-Apoptosis Detection Kit I #556547 with APC-Annexin-V #51-65874X (556420)) supplemented with 5µl propidium Iodide (BD#51-66211E(556463)) and 5µl Annexin-V-APC. Cells were incubated in the dark at room temperature for 30 minutes to stain. Finally, 200-400µl of 1X buffer was added and FACS analysis performed using the FACSCalibur APC flow cytometry machine.

8. Phospho-STAT5 staining

Sorted, EGFP+ WT-FLT3 or N51-FLT3-expressing polyI/polyC-treated Shp2$^{flox/flox}$;Mx1-Cre- or Shp2$^{flox/flox}$;Mx1-Cre+ cells were fixed in 1.5% formaldehyde (stock 37%) at room temperature for 10 minutes at 37˚C. Cells were then collected, centrifuged and resuspend in 100% ice cold methanol at 4˚C at a concentration of 1×10^6 cells/ml methanol, vortexed, and incubated at 4˚C for 10 minutes. 3ml of FACS buffer was added to each tube and cells were pelleted and washed a second time with 3ml FACS buffer. Cells were then resuspend in 100µl of FACS buffer, split into two tubes and either 20µl conjugated antibody (BD, Alexa Fluor 647 mouse Anti-STAT5 (PY694), or 1µl isotype (Biolegend APC Mouse IgG1, *k* isotype) added. Cells were kept in the dark at room temperature for 30 minutes to stain and then washed with 3ml FACS buffer. Finally, cells were resuspend in 500µl FACS buffer and analyzed using the Accuri flow cytometer.

9. Transplants

Bone marrow LDMNCs were isolated from Shp2$^{flox/flox}$;Mx1cre+animals (C57Bl/6

background) and subjected to negative selection for isolation of lineage negative (Lin-)

cells for enrichment of hematopoietic progenitors and stem cells. Lin- cells were

retrovirally transduced with pMSCV-N51-FLT3 and sorted to homogeneity as described

above. 1 x 10^6 transduced cells were transplanted by intravenous injection with 150,000

supporting splenocytes into lethally irradiated (1100cGy split dose) F1 recipient animals.

Transplanted animals were permitted to recover for 4 weeks, and then animals were

separated into two groups with equal CD45.2 chimerism, EGFP expression, and WBC

counts for treatment with either PBS (positive control animals) or 300µg polyI/polyC for

deletion of *Ptpn11* floxed sequences (experimental animals). Animals were followed for

12 months with assessment of chimerism every 4-6 weeks and evaluation of spleen size

and histopathological diagnosis at the time of death.

10. Statistical Analysis *in vivo*

The Leukemia Specific Survival is analyzed using the Kaplan Meier estimation method

where leukemia related death are the events. Both Mice that are alive at the last day of

follow-up are incorporated into the analysis with time to event censored as the last day

known alive. Mice whose deaths are not related to leukemia are also incorporated into

the analysis with time to event censored as the death time. P-values are generated using

the log-rank tests. Statistical significance is set at 0.05 level.

11. Immunofluorescence

Briefly, 1.2 x 10^6 MV4-11 or HL-60 cells were loaded into 35-mm glass-bottom

microwell dishes (MatTek Cultureware, Ashland, MA; Gamma irradiated, TK0275),

centrifuged at 1400rpm for 5min at room temperature, fixed with cold methanol/acetone

(1/1) for 10 minutes at -20˚C, and air dried at room temperature for 15min. Cells were

blocked with 2%BSA, 10% goat serum in PBS, incubated with anti-Shp2 (BD

Biosciences, #610621) or anti-phosphorylated STAT5 (Cell Signaling Technology,

#9314), secondarily stained with Alexa-647 goat anti-mouse and Alexa-488 goat anti-

rabbit, respectively, and counterstained with DAPI 5µg/mL. Cells were imaged on

Olympus FV1000-MPE confocal/multiphoton microscope (Olympus America Inc, Center

Vally, PA0 using UPLAPO 60X W/NA:1.20 objective Lens. Samples were scanned at

405nm, 488nm, 635nm excitation wavelength, and images were collected at 461nm,

520nm, and 668nm emission wavelength, respectively. The system is mounted on an

Olympus IX81 inverted microscope stand. Images shown are representative of at least 2

independent experiments. MetaMorph (Universal Imaging, Downington, PA) was used

for image handling.

12. Chromatin Immunoprecipitation Assay

Chromatin immunoprecipitation (ChIP) assays were performed using a ChIP assay kit

(Upstate Biotechnolgy). Briefly, MV411 and HL60 cells were treated with 1%

formaldehyde for cross-linking followed by preparation of cellular extracts using lysis

buffer (1% SDS, 10 mM EDTA, and 50 mM Tris-HCL, pH 8.1). Extracts were sonicated

to shear chromatin DNA to produce 500-1000 bp DNA fragments followed by incubation

with anti-STAT5, anti-Shp2, or normal rabbit IgG (Millipore) and salmon sperm DNA/Protein A agarose in ChIP dilution buffer (0.01% SDS, 1.1% Triton X-100, 1.2 mM EDTA, 16.7 mM Tris-HCL, pH 8.1, and 167 mM NaCl) overnight at 4˚C. Immunoprecipitates were collected by gentle centrifugation, washed, and eluted with low and high stringency buffers. Histone-DNA crosslinks were reversed by heating for 4 hours at 65˚C, proteins were digested by treatment with proteinase K, and DNA was recovered by phenol/chloroform extraction. Quantitative PCR using SYBR green was conducted using forward primer 5'-CCC AGG GAG TGA CTT TCC GAG GAA-3' and reverse primer 5'-TCG AAA GCA CCA GTG GAC TCT GA-3', which generate a 90 bp band spanning the human *BCL2L1* promoter including two interferon γ activation sites (gAS, consensus sequence TTCN2-N4GAA) by which STAT5 has been shown to transactivate gene expression. Immunoprecipitated fragments were expressed as a percentage of the total chromatin used in the sample. Amplified fragments were additionally electrophoresed on agarose gels to validate fragment size and fragments were subcloned for sequence verification of the predicted *BCL2L1* promoter fragment.

13. Ras Activation Assay

Ras Activation Assays were performed using the manufactures directions (Millipore, catalog number 17-218). Briefly, cells were treated in the absence or presence of the indicated amount of II-B08 for 5 or 60 minutes. Cells were then collected on ice, washed with ice cold PBS, and lysed in MLB buffer. Lysates were centrifuge to remove any cellular debris (supernatant retained), quantified immediately and immunoprecipitation set up for a 45-minute incubation with Ras Assay Reagent (Raf-1 RBD agarose). Next,

beads were centrifuged and washed 3 times with MLB. Beads were finally resuspended in sample buffer to liberate the pull-down products, boiled, and run by immunoblot analysis, probing with anti-Ras antibody.

CHAPTER THREE

REDUCED SHP2 EXPRESSION INHIBITS FLT3-ITD-INDUCED

HYPERPROLIFERATION IN BAF3 CELLS

Introduction

It is well established that FLT3-ITDs confer a poor prognosis in all AML patients, including the elderly (Whitman, Archer et al. 2001). Elderly patients are at an increased susceptibility to mortality from AML for several reasons. First of all, AML is more prevalent in aging individuals and the elderly are more likely to have co-morbidities, such as diabetes and heart disease, rendering standard chemotherapy and radiation regimens too harsh for these patients to sustain. Therefore, we are interested in better understanding the molecular mechanisms contributing to FLT3-ITD-induced leukemogenesis in order to identify novel and less toxic therapeutic approaches which may be beneficial in treating FLT3-ITD-positive AML patients.

Baf3 cells are an immortalized, murine, pro-B, IL3-dependent cell line. They do not endogenously express FLT3 receptors, therefore they are an attractive model to examine the effects of FLT3-ITDs. Baf3 cells are particularly useful because they can be easily cultured to generate large amounts of cells for biochemical assays. They are also easily transfected or transduced to express additional proteins of interest. Baf3 cells expressing WT-FLT3, N51-FLT3, and N73-FLT3 were a generous gift from Dr. Seiji Fukuda (Fukuda, Broxmeyer et al. 2005) and were used for the following studies. The transduced Baf3 cells express a neomycin resistance gene in addition to the FLT3 cDNA and are therefore cultured in the presence of 40µl/ml geneticine to maintain stable cell lines.

Given that FLT3-ITD often duplicate Y599, the site of Shp2 recruitment to WT-FLT3, we hypothesized that in the presence of N51- and N73-FLT3 there would be an increased association of Shp2 to the mutant FLT3 receptor and this interaction would contribute to the activation of STAT5 and its transcriptional targets. I used these cells in biochemical studies to examine the potential interaction between the protein tyrosine phosphatase, Shp2, and FLT3 or STAT5. I also conducted functional assays examining if knockdown of Shp2 expression resulted in reduced FLT3-ITD-induced hyperproliferation. Finally, using a human, FLT3-ITD-positive cell line, MV411, I examined the nuclear association of Shp2 and its potential co-localization with STAT5 at STAT5-responsive promoter element *BCL2L1*.

Results

Baf3 cells stably expressing N51-FLT3 or N73-FLT3 are hyperproliferative

Previous studies had indicated that the FLT3-ITD mutants, N51 and N73, confer ligand-independent hyperproliferation and STAT5 hyperphosphorylation; however, we wished to verify these findings in the N51-FLT3- and N71-FLT3-transduced cell lines. Therefore, we examined the proliferation of Baf3 cell lines stably expressing WT-FLT3, N51-FLT3, or N73-FLT3 (Figure 3.1A). Each cell line was starved overnight in serum-free IMDM and then plated into thymidine incorporation assays ($1\text{-}5 \times 10^4$ cells/200μl) either at baseline (no growth factor) or in the presence of 50 or 100ng/ml FLT3 ligand (FL) and incubated overnight at 37˚C. The following morning, cells were pulsed with 1 μCi tritiated thymidine and incubated for 5-6 hours at 37˚C. Thymidine incorporation was determined using automated 96-well cell harvester (Brandel, Gaithersburg, MD). WT-FLT3-expressing Baf3 cells were quiescent at baseline and demonstrated increased

proliferation in a FL-dependent manner (Figure 3.1A). However, both N51-FLT3- and

N73-FLT3-expressing Baf3 cells were constitutively hyperproliferative at baseline and

could not be further induced to proliferate by FL stimulation (Figure 3.1A). We next

prepared total cell lysates from each cell line to examine FLT3 expression levels. Total

cellular extracts were electorphoresed by sodium dodecyl sulfate-polyacrylamide gel

electrophoresis (SDS-PAGE), transferred to nitrocellulose and probed with α-FLT3

(Figure 3.1B). Expression levels of WT-FLT3 and N73-FLT3 were very similar

suggesting the hyperproliferation of N73-FLT3 is due to the contribution of the gain-of-

function FLT3-ITD. The protein expression of N51-FLT3 was, however, higher than that

of WT-FLT3 or N73-FLT3, which may partially explain the increased level of N51-

induced hyperproliferation compared to that of N73-FLT3, particularly in the absence of

FL (Figure 3.1A).
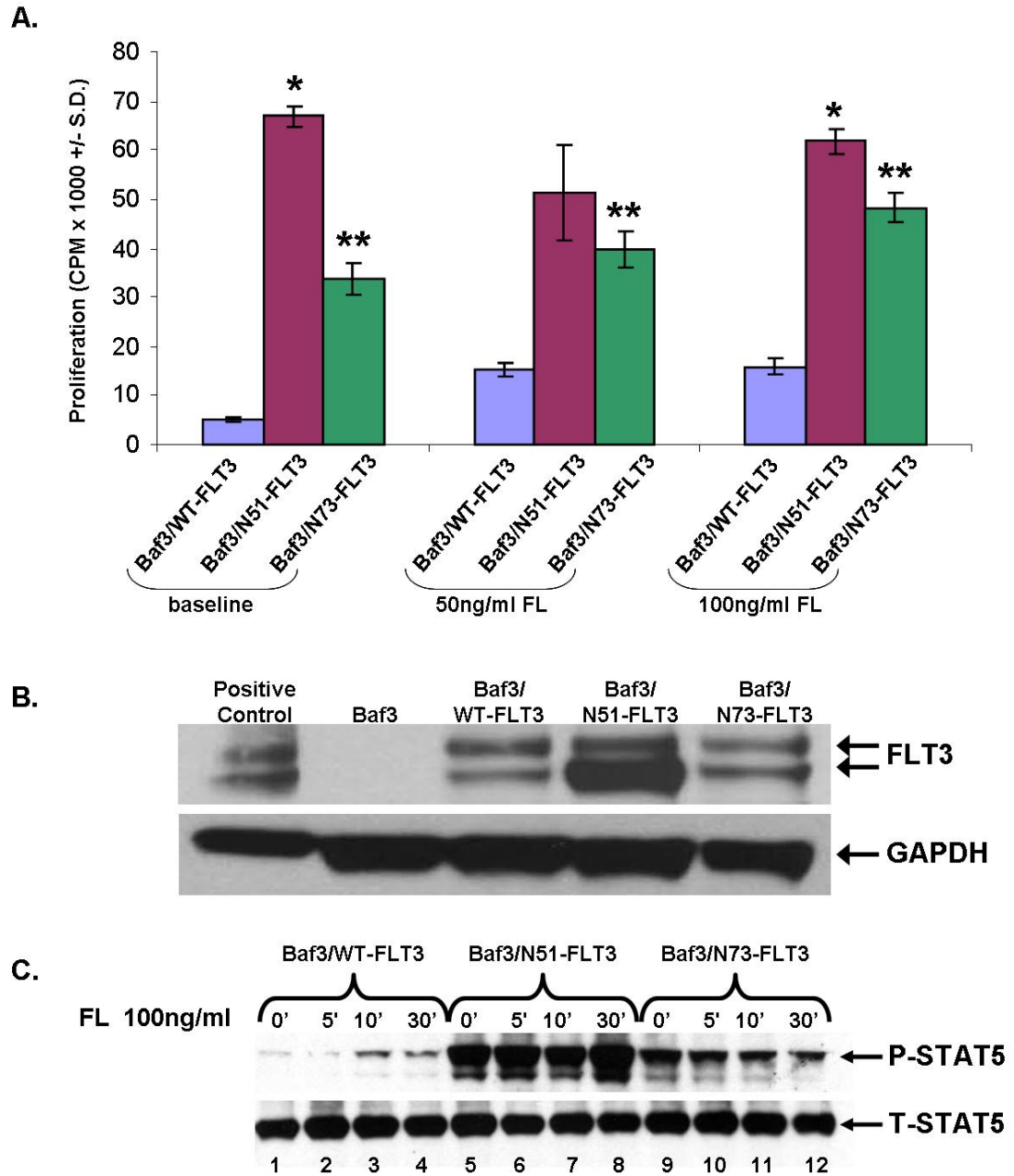
Figure 3.1: Baf3 cells expressing N51- or N73-FLT3 are hyperproliferative and express constitutively activated STAT5

(A) Baf3 cells expressing WT-, N51-, or N73-FLT3 were subjected to thymidine incorporation assays in the absence (baseline) or presence of 50 or 100ng/ml FL; N=4; statistics were determined by unpaired, two-tailed T-test; *p<0.001 for N51 vs WT **p<0.001 for N73 vs. WT, at baseline and in response to FL at 50ng/ml and 100ng/ml. (B) Immunoblot analysis of total cell lysates from nascent Baf3 cells, or those expressing WT-, N51-, or N73-FLT3, probed with α-FLT3 or α-GAPDH. (C) Immunoblot demonstrating phospho (P)-STAT5 in WT-, N51-, and N73-FLT3-expressing Baf3 cells.

37

Baf3/N51-FLT3 and Baf3/N73-FLT3 cells exhibit constitutive activation of STAT5

It has been well demonstrated that in the presence of FLT3-ITDs, STAT5 is constitutively activated (Mizuki, Schwable et al. 2003; Chung, Morrone et al. 2005; Kato, Iwama et al. 2005; Rocnik, Okabe et al. 2006; Choudhary, Brandts et al. 2007). To further investigate the molecular mechanism underlying the hyperproliferation of N51- and N73-FLT3, we used the WT-FLT3-, N51-FLT3-, and N73-FLT3-transduced Baf3 cell lines for biochemical analysis. Cells were starved overnight in IMDM. The following morning, cells were collected (baseline) and stimulated for 5, 10, or 30 minutes with FL (100ng/ml). Total cell lysates were electorphoresed by SDS-PAGE, transferred to nitrocellulose membrane, and probed with α-P-STAT5 or α-T-STAT5. Figure 3.1C demonstrates that STAT5 is modestly activated by WT-FLT3 in response to FL stimulation (lanes 1-4). However, STAT5 is constitutively phosphorylated in cells expressing N51-FLT3 (lanes 5-8) and N73-FLT3 (lanes 9-12) independent of FL stimulation. Consistent with increased baseline proliferation and increased FLT3 expression, the N51-FLT3-transduced cells demonstrate the most robust level of STAT5 activation. Collectively, our results are consistent with previous studies that FLT3-ITDs induce FL-independent constitutive activation of STAT5.

Co-immunoprecipitation reveals that Shp2 is constitutively associated to FLT3 in Baf3 cells expressing N51-FLT3 or N73-FLT3 and in the human FLT3-ITD+ cell line, MV411

Since Y599 of WT-FLT3 was shown to recruit Shp2 in biochemical studies (Heiss, Masson et al. 2006), and since Y599 is commonly duplicated in FLT3-ITD

mutations, we next examined the ability of N51- and N73-FLT3 to recruit Shp2

compared to that of WT-FLT3. Using the Baf3-transduced cell lines, previously

described, cells were starved overnight in IMDM and collected (baseline) or stimulated

with 100ng/ml FL for the indicated amount of time. Total cell lysates were prepared and

used in co-immunoprecipitation assays. One mg of protein was immunoprecipitated with

α-FLT3 and immunoblotted with α-Shp2. These results demonstrate that Shp2 is

recruited to WT-FLT3 in a FL-dependent manner (Figure 3.2A and 3.2B, lanes 1-2) and

this association diminishes over time (Figure 3.2B, lanes 1-4). On the contrary, Shp2 is

strongly and constitutively associated to N51-FLT3 (Figure 3.2A, lanes 3-4) and N73-

FLT3 (Figure 3.2B, lanes 5-8) regardless of FL-stimulation. These findings support our

hypothesis that there is an increased recruitment of Shp2 to FLT3-ITDs.
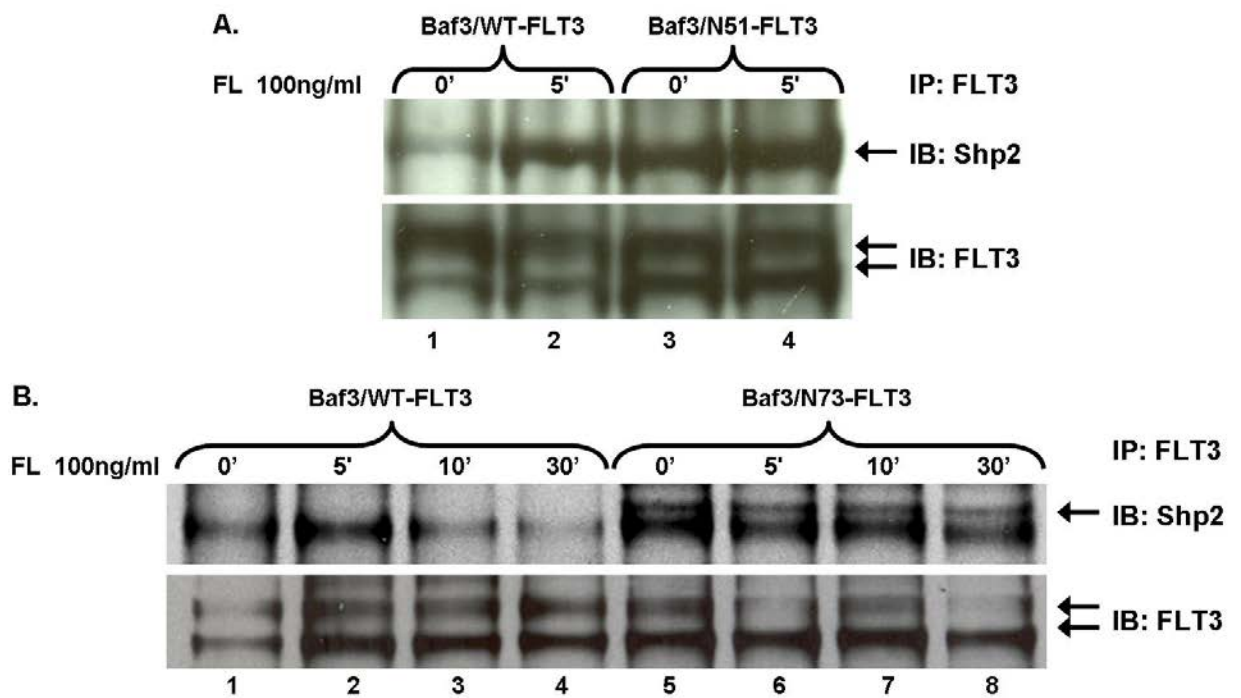
Figure 3.2: Shp2 is constitutively associated to FLT3-ITDs in transduced Baf3 cells

Total cell lysates from Baf3 cells expressing WT-FLT3 (**A, B**), N51-FLT3 (**A**), or N73-FLT3 (**B**) were immunoprecipitated (IP) with α-FLT3 and immunobloted (IB) with α-Shp2.

In addition to the Baf3 cell lines, we also utilized the human AML cell lines HL60 (WT-FLT3 expressing; ITD negative) and MV411 (FLT3-ITD positive). The MV411 cell line serves as a good model as it is derived from a FLT3-ITD+ patient sample, the FLT3-ITD expression is regulated by endogenous genomic promoter elements, and the cell line manifests constitutively active STAT5 (Figure 3.3A). Total cell lysates were prepared from exponentially growing MV411 and HL60 cells and subjected to immunoprecipitation assays. Lysates were immunoprecipitated with α-FLT3 and immunobloted with α-Shp2. A minimal amount of Shp2 was associated with WT-FLT3 in the HL60 cells (Figure 3.3B). However, there was a strong association of Shp2 to FLT3-ITD in the lysates from MV411 cells (Figure 3.3B). Furthermore, we found that Shp2 is constitutively associated with FLT3 in a FLT3-ITD+ primary AML sample (Figure 3.3B, patient # 2797) and to a lesser extent in two FLT3-ITD- primary AML samples (Figure 3.3B, patient #s 2944 and 2945). Collectively, these data provide biochemical evidence using cell lines and primary AML samples that Shp2 is constitutively associated with FLT3-ITD and suggest that Shp2 may play a positive role in mediating FLT3-ITD-induced hyperproliferation.
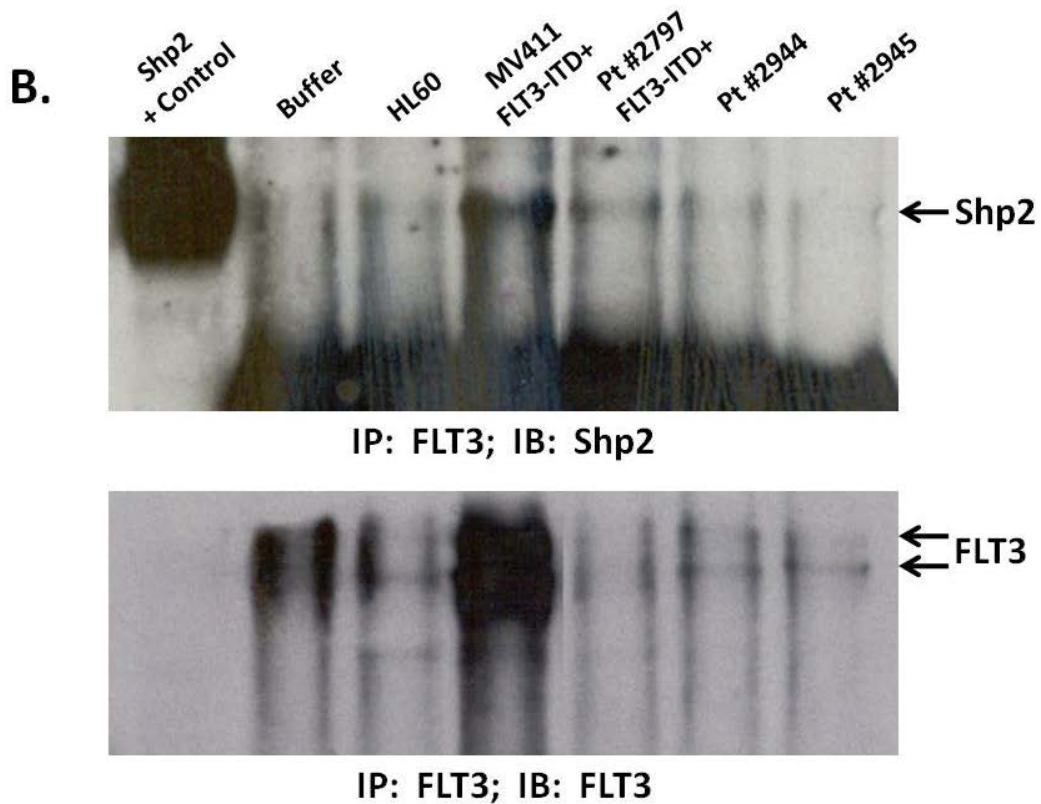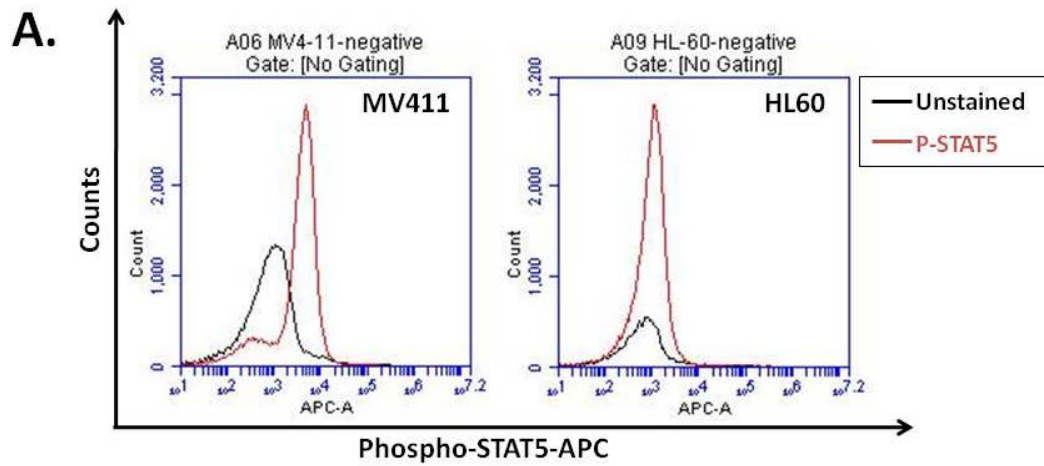
Figure 3.3: Shp2 is constitutively associated to FLT3-ITD in FLT3-ITD+ MV411 cells and in primary AML samples

(**A**) Intracellular staining of phospho-STAT5 in MV411 and HL60 cells assessed by flow cytometry. (**B**) Total cell lysates from MV411 cells (FLT3-ITD+), HL60 cells (FLT3-ITD-), or primary AML cells were immunoprecipitated (IP) with α-FLT3 and immunobloted (IB) with α-Shp2.

Shp2 and STAT5 co-localize in the presence of N51-FLT3

   To further investigate the relationship between Shp2 and FLT3-ITDs we were interested in the potential interaction between Shp2 and STAT5. While Shp2 has been shown to negatively regulate STAT5 by some studies (Yu, Jin et al. 2000; Chen, Wen et al. 2003); it has paradoxically been shown to positively regulate STAT5 by others (Ke, Lesperance et al. 2006; Choudhary, Brandts et al. 2007). In the regulation of the β-casein gene in mammary epithelial cells, Shp2 was shown to interact directly with STAT5. Since we observed a constitutive association of Shp2 to FLT3-ITDs, we hypothesized that Shp2 acts to positively regulate STAT5 in the presence of FLT3-ITDs. To initially address this hypothesis, we examined the potential interaction between STAT5 and Shp2 in FLT3-ITD-expressing cells. Using total cell lysates from WT-FLT3 and N51-FLT3-expressing Baf3 cells, we immunoprecipitated with α-Shp2 (Figure 3.4A) or α-STAT5 (Figure 3.4B) and immunoblotted with α-STAT5 or α-Shp2, respectively. This experiment demonstrated a modest association of Shp2 to STAT5 in the WT-FLT3-expressing Baf3 cells. On the contrary, there was a robust association of Shp2 to STAT5 in the Baf3/N51-FLT3 cell line. The membranes were then stripped and re-blotted with either α-Shp2 or α-STAT5 as a control. These data suggest that the increased recruitment of Shp2 to FLT3-ITDs may subsequently lead to an increased association and/or activation of STAT5 and suggest that Shp2 cooperates with FLT3-ITDs or subsequently with STAT5 to promote hyperproliferation of FLT3-ITD-expressing cells. As a result, we next investigated the effect of reduced Shp2 protein expression on FLT3-ITD-induced hyperproliferation.
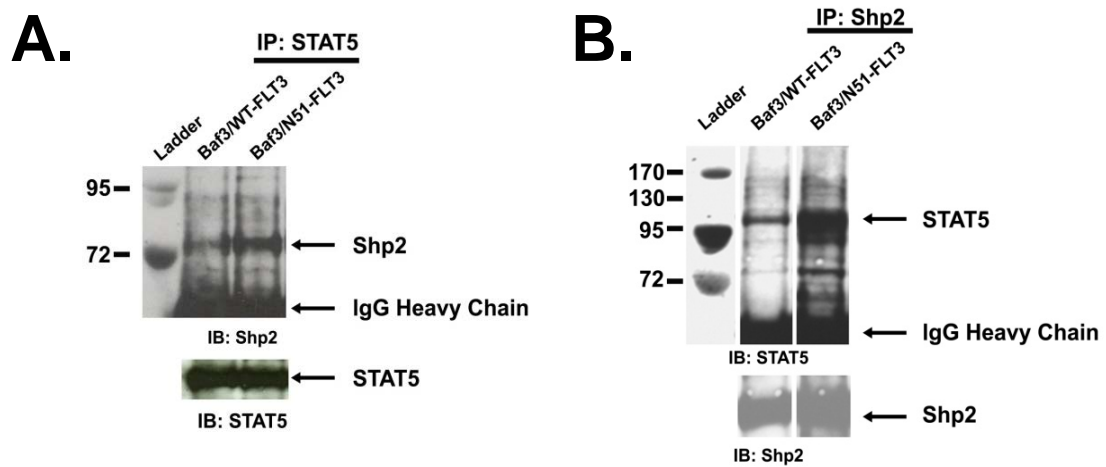
Figure 3.4: Shp2 and STAT5 interaction is increased in N51-FLT3-expressing cells

Total cell lysates from Baf3/WT- and Baf3/N51-FLT3 were immunoprecipitated with either α-Shp2 **(A)** or α-STAT5 **(B)** and immunoblotted with α-STAT5 or α-Shp2, respectively, to examine the interaction between Shp2 and STAT5 in the presence of N51-FLT3 compared to WT-FLT3. Membranes were then stripped and re-probed for either α-Shp2 **(A)** or α-STAT5 **(B)**.

*shRNA targeted to Shp2 significantly reduces hyperproliferation of Baf3 cells
expressing either N51-FLT3 or N73-FLT3*

We hypothesized that reduced Shp2 protein expression would subsequently result
in reduced hyperproliferation induced by N51-FLT3 and N73-FLT3. We transfected the
previously described Baf3 cells with plasmids encoding short hairpin RNA (shRNA)
targeted to Shp2 or a scrambled control (Origene #TR501795) by nucleofection (Amaxa
Nucleofection Kit V) and selected the cells in 1µg/ml puromycin to create stable cell
lines (Figure 3.5). After selection in puromycin, immunoblot demonstrated reduced Shp2
protein expression by at least 50% in cells transfected with shRNA targeted to Shp2 (KD)
compared to scrambled control (SC) in Baf3/WT-FLT3 (Figure 3.6A and 3.6B),
Baf3/N51-FLT3 (Figure 3.6A) and Baf3/N73-FLT3 (Figure 3.6B) cells.

To investigate the functional relevance of reduced Shp2 on activating FLT3-
induced hyperproliferation, cells were starved for 6 hours in IMDM, plated into 96-well
plates in either starvation media (baseline) or stimulated with 50 or 100ng/ml FL and
subjected to thymidine incorporation assays (previously described). Baf3/N51-FLT3
(Figure 3.6C) and Baf3/N73-FLT3 (Figure 3.6D) cells transfected with shRNA-KD
demonstrated significantly reduced proliferation at baseline and in response to FL, in
contrast to that observed with Baf3/N51-FLT3 or Baf3/N73-FLT3 cells transfected with
scrambled shRNA, suggesting a functional role of Shp2 in FLT3-ITD-induced
hyperproliferation. Furthermore, there is a correlation between Shp2 protein expression
and proliferation. When Shp2 protein levels are reduced by only 50% (Figure 3.6A),
proliferation is similar between Baf3/WT-FLT3 cells expressing shRNA-SC and those
expressing shRNA-KD (Figure 3.6C); however when Shp2 protein is more substantially
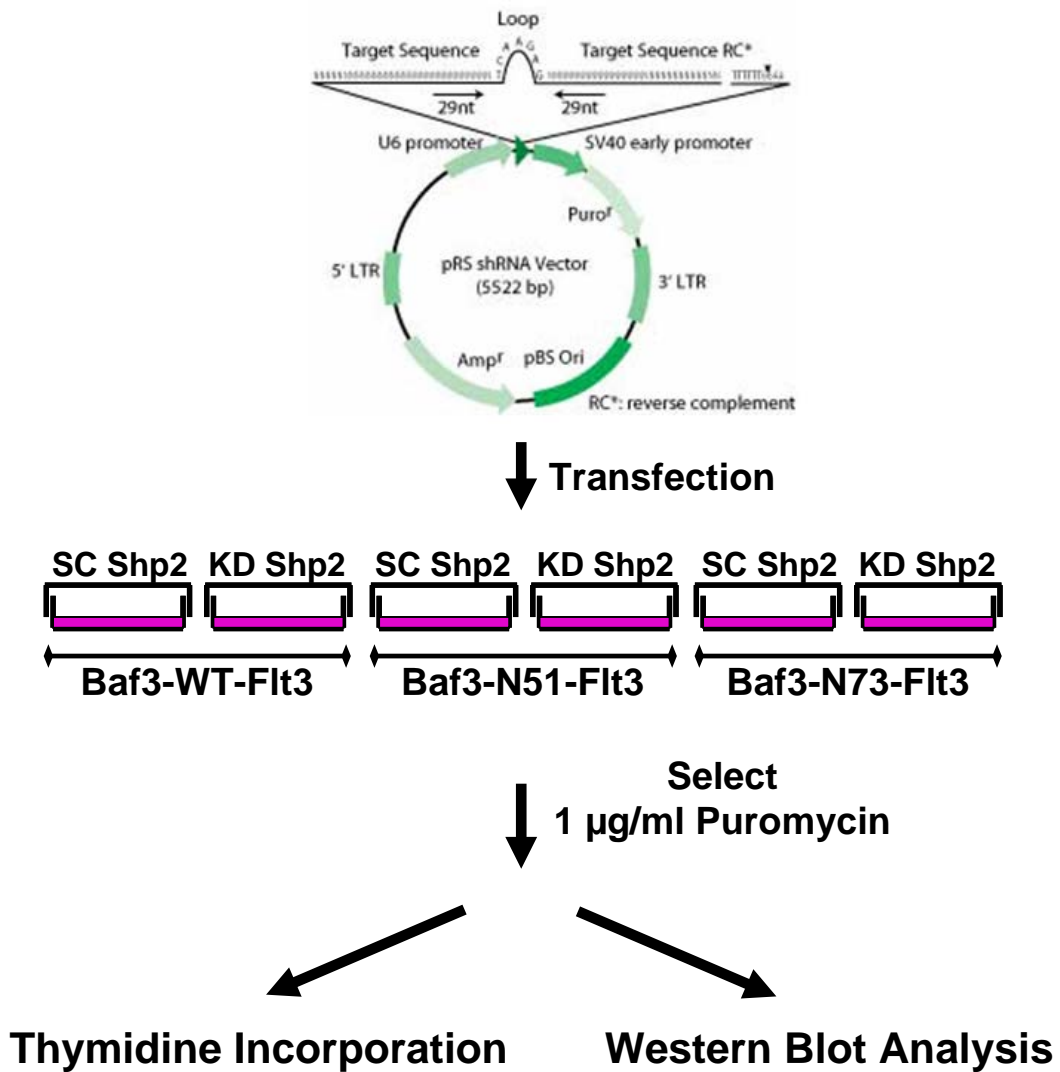
Figure 3.5: shRNA transfection schematic to generate stable cells lines with reduced Shp2 expression

U6 promoter driven shRNA constructs were transfected into Baf3/WT-, N51-, or N73-FLT3 cells, and selected in 1µg/ml puromycin to generate stable cell lines. Selected cells were subsequently used in thymidine incorporation assays as well as immunoblot analysis.

reduced by approximately 70-80% (Figure 3.6B), Baf3/WT-FLT3 cells expressing

shRNA-KD demonstrate a modest decrease in proliferation compared to Baf3/WT-FLT3

cells expressing shRNA-SC at baseline and in response to FL (Figure 3.6D). Since it has

been demonstrated that Shp2 is required for WT-FLT3-induced proliferation (Heiss,

Masson et al. 2006), it is not surprising that there is a modest reduction of WT-FLT3-ITD

induced proliferation with a substantial reduction of Shp2. Cells expressing FLT3-ITDs

however, regardless of the level of Shp2 knockdown, demonstrate reduced proliferation,

suggesting that FLT3-ITD-expressing cells are more sensitive to loss of Shp2 compared

to WT FLT3-expressing cells. This correlation of Shp2 expression with functional

response further supports the hypothesis that Shp2 function contributes to FLT3-ITD-

induced cellular growth. In order to further investigate the Shp2-STAT5 association

exhibited in Figures 3.4A and 3.4B in Baf3/N51-FLT3 cells, we next considered possible

molecular mechanisms.
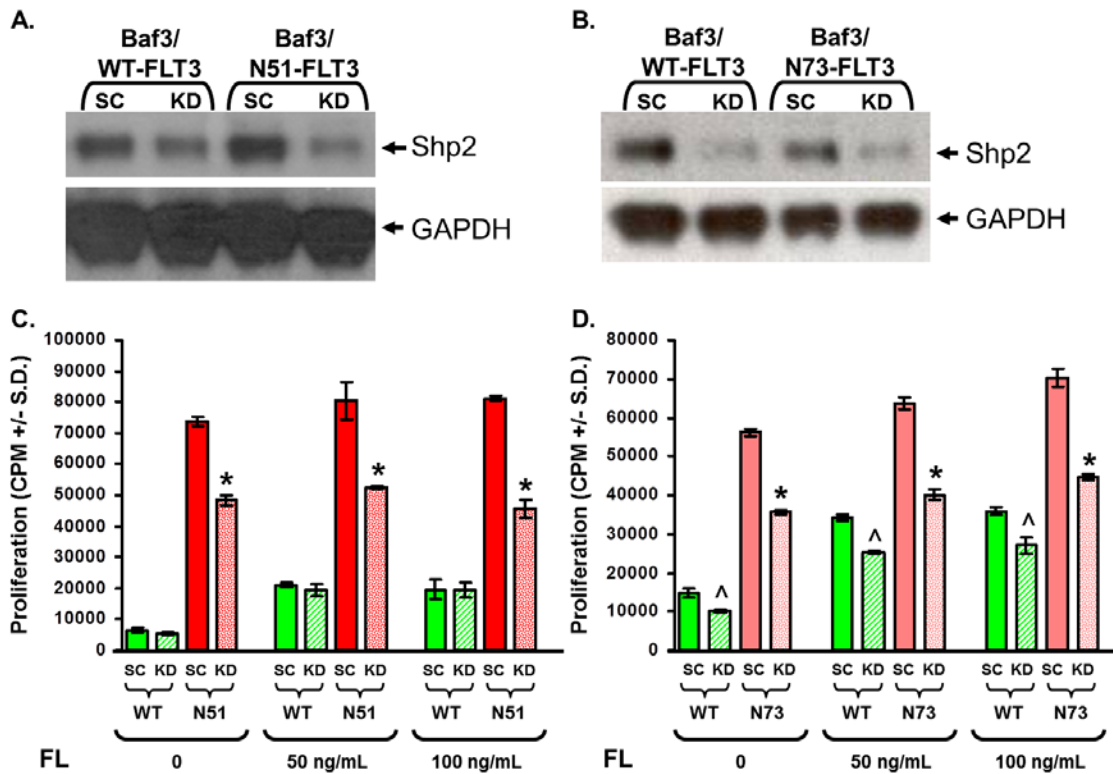
Figure 3.6: Reduced Shp2 protein expression significantly reduces hyperproliferation induced by N51-FLT3 and N73-FLT3 in Baf3 cells

Baf3/WT-FLT3 and Baf3/N51-FLT3 **(A)** and Baf3/WT-FLT3 and Baf3/N73-FLT3 **(B)** cell lines transfected with scrambled shRNA (SC) or shRNA targeting Shp2 (KD) were used in immunoblot analyses and demonstrate at least 50% reduction in Shp2 protein levels in cells transfected with shRNA-KD compared to shRNA-SC **(A, B)** in each respective experiment. Thymidine incorporation assays of Baf3/WT-FLT3 and Baf3/N51-FLT3 **(C)** and Baf3/WT-FLT3 and Baf3/N73-FLT3 **(D)** cell lines transfected with shRNA-SC or shRNA-KD. Representative of two independent experiments (N=4, *$p<0.02$ for N51-KD v. N51-SC, *$p<0.003$ for N73-KD v. N73-SC, and ^$p<0.02$ for WT-KD v. WT-SC by unpaired, two-tailed T-test).

Shp2 and phospho-STAT5 co-localize in the nuclei of MV411 cells

To investigate the interaction between Shp2 and STAT5 we used the human, FLT3-ITD-positive AML patient-derived cell line, MV411 and the human, FLT3-ITD-negative myeloid leukemia patient-derived cell line, HL60. The utilization of MV411 cells is useful and applicable because not only were the cells derived from a human FLT3-ITD+ patient sample, but the FLT3-ITD is driven by endogenous promoter elements. MV411 cells also have a strong hyperactivation of STAT5 compared to FLT3-ITD- HL60 cells (Figure 3.3A) consistent with other reported FLT3-ITD-expressing cells. Even though Shp2 is traditionally thought to be a cytosolic signaling molecule, it has been found in the nucleus of some AML samples (Xu, Yu et al. 2005), yet the role of nuclear-associated Shp2 in leukemogenesis has not been investigated. We therefore examined cytoplasmic and nuclear extracts from both MV411 and HL60 cells. Similar to previous studies, we found that MV411 cells had an increased level of phospho-STAT5 and total-STAT5 in the nuclear fraction compared to the levels of STAT5 in HL60 cells (Figure 3.7A). Interestingly, cytoplasmic and nuclear associated phospho-Shp2 was much higher in MV411 cells than in HL60 cells despite the fact that total-Shp2 protein levels were similar in both cytoplasmic and nuclear fractions of MV411 and HL60 cells (Figure 3.7A). Considering that the nuclear fraction of MV411 cells is enriched in phospho-Shp2, we were next interested in examining the cellular localization and potential association of Shp2 and STAT5.

To examine the physiologic, cellular localization of Shp2 and STAT5, I collaborated with Dr. Xingjun Li in our lab to perform the following *in situ* immunofluorescence studies to compare the nuclear distribution of Shp2 and the potential

co-localization of p-STAT5 in MV411 and HL60 cells. Our results demonstrate that

Shp2 and DAPI co-localize indicating that Shp2 is in the nucleus of both MV411 and

HL60 cells (Figure 3.7B); however the distribution of Shp2 is much more clumped

together in MV411 cells compared to a smooth distribution exhibited in HL60 cells.

Consistent with many previous studies, p-STAT5 was much more intense in FLT3-ITD-

positive MV411 cells compared to weak p-STAT5 signal in HL60 cells (Figure 3.7B).

Remarkably, upon merging the images, there is a robust co-localization of Shp2 and p-

STAT5 in the nucleus of MV411 cells (Figure 3.7B) which is absent in HL60 cells. This

Shp2-STAT5 nuclear co-localization in MV411 cells suggests that Shp2 may participate

with (or in a complex with) STAT5 in the nucleus and may activate STAT5

transcriptional targets promoting cellular transformation and leukemogenesis.
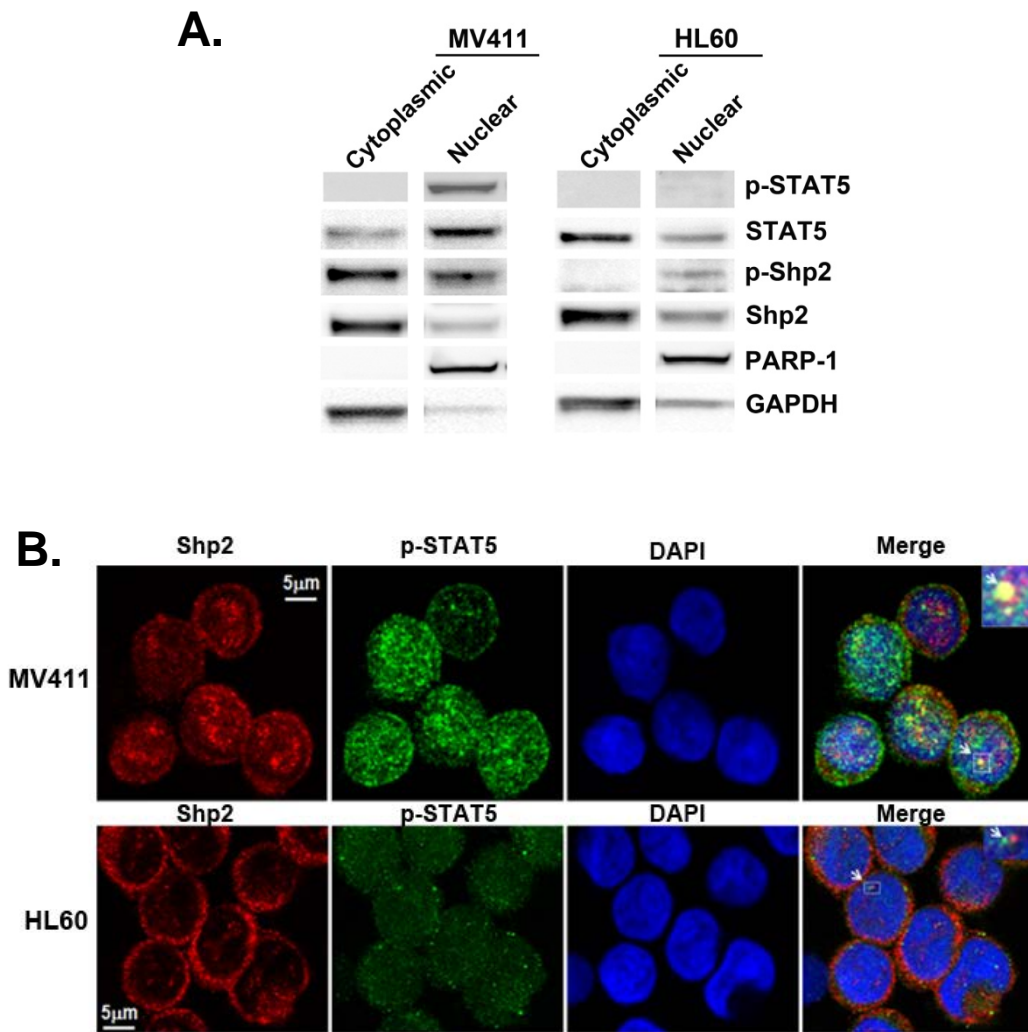
Figure 3.7: Shp2 and phospho-STAT5 co-localize in the nuclei of MV411 cells

Nuclear and cytoplasmic proteins were isolated from MV411 and HL-60 cells and assessed for phospho-STAT5 and phospho-Shp2 by immunoblot analysis **(A)**. Immunostaining for Shp2 and phospho-STAT5 was performed in MV411 and HL60 cells and cells were imaged using confocal microscopy **(B)**.

FLT3-ITD-expressing hematopoietic cells demonstrate increased association of the

shp2-STAT5 complex at the BCL2L1 promoter

Considering the nuclear co-localization of Shp2 and STAT5 in MV411 cells both

biochemically and by immunofluorescence, we next hypothesized that Shp2 may be

working in a complex with STAT5 to activate STAT5 transcriptional targets know to be

implicated in leukemogenesis. We decided to examine the *BCL2L1* promoter which

regulates the expression of Bcl-X_L. Pro-survival protein Bcl-X_L is an applicable target to

investigate because its expression has been implicated in leukemogenesis (Beverly and

Varmus 2009; Mizukawa, Wei et al. 2011), upregulated in hematopoietic progenitors

expressing constitutive active STAT5 (Schuringa, Chung et al. 2004), and downregulated

in hematopoietic progenitors expressing knockdown of Shp2 expression (Li, Modi et al.

2011). The human *BCL2L1* promoter region has two functional interferon-γ activation

sites (GAS, consensus sequence $TTCN^2-N^4GAA$) which are located upstream of the Bcl-

X_L start codon (Figure 3.8A, -321 to -329 and -335 and -344 highlighted in red, atg

underlined), and bind STAT5 to regulate the *BCL2L1* promoter. To examine the

hypothesis that Shp2 is co-localized and participates with STAT5 at the endogenous

promoter *BCL2L1*, we performed chromatin immunoprecipitation (ChIP) assays. As

expected and as a positive control we found increased amplification of the *BCL2L1*

promoter region upon immunoprecipitation with α-STAT5 in the MV411 cells compared

to the HL60 cells (Figure 3.8B). Immunoprecipitation with α-Shp2 consistently yielded

increased levels of the amplified *BCL2L1* promoter region in MV411 cells compared to

HL60 cells (Figure 3.8B) suggesting that Shp2 is functioning in a complex binding the

GAS consensus sequence. To verify the identity of the predicted amplified *BCL2L1*

promoter region, we subcloned amplified PCR products immunoprecipitated with either α-STAT5 or α-Shp2 into TOPO vectors and sequenced them (data not shown). Together the immunofluorescence and ChIP data support the novel finding that Shp2 co-localizes with STAT5 in the nucleus of FLT3-ITD-expressing hematopoietic cells and contributes to the activation of pro-leukemic gene expression.

A.

```
TGCCTTTGCCTAAGGCGGATTTGAATGTAGGTGGTGCGGGGGAGCGGGAGTGGGGCGGGGGGG
                -344            -335    -329        -321
ACTGCCCAGGGAGTGACTTTCCGAGGAAGGCATTTCGGAGAAGACGGGGGTAGAAAAG
```
→

```
GCTGGTGGGAGATTCAGAGTCCACTGGTGCTTTCGATTTGACTTAAGTGAAGTATCTTGGAACC
```
←

```
TAGACCCAGACCTTCGTAAGACCCACAAAGAAACCAGTTCTGGTACCTGGAGGGGGAATGGAAT

TTTTAGGGTAAATGGCATGCATATTAATTATTTTTTTTTCCTGAAGCTCTTTCTCTCCCTTCAG

AATCTTATCTTGGCTTTGGATCTTAGAAGAGAATCACTAACCAGAGACGAGACTCAGTGAGTG

AGCAGGTGTTTTGGACAATGGACTGGTTGAGCCCATCCCTATTATAAAA ATGTCTCAGAGCA
```

B.
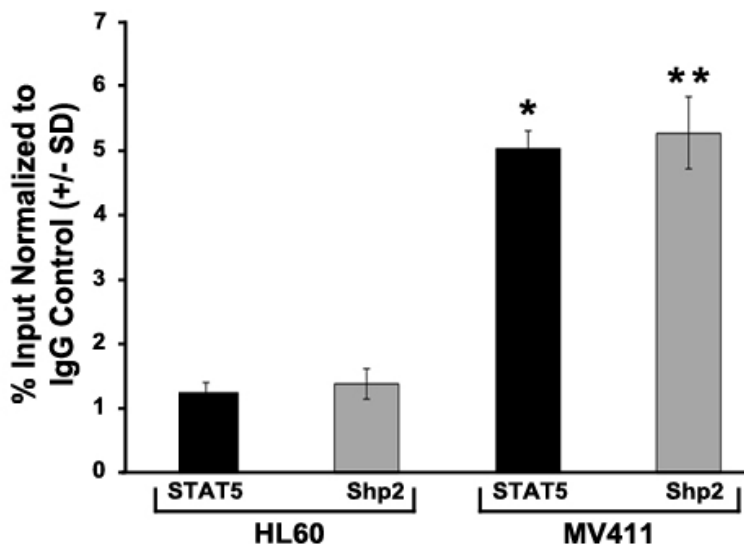
Figure 3.8: FLT3-ITD-expressing hematopoietic cells demonstrate increased association of the Shp2-STAT5 complex at the Bcl-X$_L$ promoter

Schematic diagram demonstrating the human *BCL2L1* promoter with two functional interferon-γ activation sites (GAS sites, consensus sequence TTCN2-N4GAA) at -344 to -335 and -329 to – 321 upstream of the BclXL translation start codon highlighted in red with arrows indicating the primers used to amplify the region **(A)**. For ChIP assays, isolated lysates from HL60 or MV411 cells were immunoprecipitated with either anti-STAT5 or anti-Shp2 followed by quantitative PCR using of purified DNA fragments using primers specific for the human *BCL2L1* promoter **(B)**. The immunoprecipitated fragments were expressed as a percentage of the total chromatin used in the sample. Representative of 3 independent experiments, n=3, *$p<0.005$ for fragments pulled down by STAT5 from MV411 v. HL60 cells and **$p<0.0005$ for fragments pulled down by Shp2 from MV411 v. HL60 cells. Unpaired, two-tailed, T-test used for statistics.

Conclusions

FLT3-ITD mutations confer a poor prognosis in AML patients, yet the molecular mechanisms of these mutations and their contributions to the disease phenotype remains poorly understood. Baf3 cells expressing the FLT3-ITDs, N51-FLT3 and N73-FLT3, both exhibit ligand-independent hyperproliferation, while WT-FLT3 expressing cells are FL-dependent. In addition to their hyperproliferative phenotype, the FLT3-ITD-expressing cells also constitutively activate the transcription factor STAT5. These studies support what has been previously demonstrated (Kiyoi, Ohno et al. 2002; Mizuki, Schwable et al. 2003; Chung, Morrone et al. 2005; Kato, Iwama et al. 2005; Rocnik, Okabe et al. 2006; Choudhary, Brandts et al. 2007) and provide evidence that this model recapitulates what has been observed by others and can be utilized to investigate the role of Shp2 in FLT3-ITD-induced STAT5 hyperactivation and hyperproliferation.

In addition to these confirmatory studies, we have gone on to investigate the role of Shp2 in this system. Since Y599 of WT-FLT3 has been shown to recruit Shp2, and FLT3-ITDs commonly contain a duplicated Y599, we hypothesized that Shp2 is constitutively associated with FLT3-ITDs and the additional and constitutive association of Shp2 participates in the hyperproliferation induced by these FLT3-ITDs. Immunoprecipitation assays demonstrated a constitutive association of Shp2 and FLT3 in N51-FLT3 and N73-ITD-expressisng Baf3 cells as well as in FLT3-ITD-positive MV411 cells. This is contrary to the ligand-dependent Shp2 association demonstrated in WT-FLT3 expressing Baf3 cells. Furthermore, we have demonstrated that reduction of Shp2 protein expression by shRNA targeted to Shp2 significantly reduces the hyperproliferation induced by N51-FLT3 and N73-FLT3.

Shp2 has been shown to participate in the enhancement of cellular signaling (Neel, Gu et al. 2003; Chan and Feng 2007), however, a specific mechanism of how Shp2 may act to promote leukemogenesis in the setting of FLT3-ITD and constitutive active STAT5 has not been elucidated. While previous studies have demonstrated that Shp2 has been shown to be nuclear associated in AML samples (Xu, Yu et al. 2005), the role of Shp2 in the nuclear fraction of AML cells has not been examined. Since the C-SH2 domain has been demonstrated to be important in the activation of STAT5 in mammary epithelial cells (Chughtai, Schimchowitsch et al. 2002), we hypothesized that in the context of FLT3-ITD+ AML, Shp2 may function in a similar fashion, working with STAT5, to enhance pro-leukemic signals as a novel molecular mechanism for Shp2. In support of our hypothesis, we demonstrated that Shp2 is co-localized with STAT5 in the nucleus of FLT3-ITD-bearing hematopoietic cells and present innovative ChIP data suggesting Shp2 is located in the protein complex located at the *BCL2L1* promoter responsible for the transcription of pro-survival gene Bcl-X_L. To the best of our knowledge, this is the first time Shp2 has been found to function at a STAT5-responsive promoter sequence and suggests a new, novel role of Shp2 in the setting of leukemogenesis.

Taken together, these results demonstrate a novel role of Shp2 functioning at the promoter element of STAT5 target gene Bcl-X_L, and suggest that targeting Shp2 may provide a novel therapeutic option for treating FLT3-ITD-positive AML patients.

CHAPTER FOUR

GENETIC DISRUPTION OF SHP2 INHIBITS FLT3-ITD-INDUCED

HYPERPROLIFERATION AND PERMITS LONG TERM SURVIVAL OF ANIMALS

TRANSPLANTED WITH N51-FLT3-ITD-EXPRESSING CELLS

Introduction

To understand the molecular mechanism of FLT3-ITD-induced leukemogenesis, cell lines bear substantial limitations. Studies using heterologous cell lines provide useful mechanistic and functional information; however, their use is limited as cell lines are commonly transformed and may not entirely reflect the signaling mechanisms of primary leukemic cells. Therefore, in addition to using cell lines, we have utilized a retroviral transduction method to introduce FLT3-ITD constructs into primary murine bone marrow cells, complimenting and validating our findings using the FLT3-ITD-expressing Baf3 cells. These primary cell studies will provide a working model of FLT3-ITD-induced leukemogenesis, but moreover, set up the foundation to use an *in vivo* mouse model system. Based on our initial studies in the Baf3 and MV411 cells, we hypothesized the genetic disruption of Shp2 in primary murine bone marrow cells would reduce FLT3-ITD-induced hyperproliferation, STAT5 hyperactivation, and leukemia progression *in vivo*.

For our *in vitro* studies, we used a murine retroviral transduction system to infect primary C57BL/6 low density mononuclear cells (LDMNCs) with empty vector (pMSCV), WT-FLT3, or N51-FLT3. One of the main benefits of this system is the retroviral vector is bicistronic expressing our gene of interest, FLT3, as well as enhanced green fluorescent protein (EGFP). This allows us to use flow cytometry to enrich for

EGFP+, FLT3-expressing cells. Sorted, EGFP+ cells can subsequently be used for *in vitro* experiments to complement our BaF3 studies, as well as set up the working model using primary cells and eventually *in vivo* studies.

We are interested in the role of Shp2 in the bone marrow in the presence of FLT3-ITD-induced leukemic progression and leukemogenesis. In order to understand how Shp2 functions in the context of FLT3-ITDs, we must first consider its role in normal hematopoiesis. Shp2 has been shown to be important for normal embryonic stem cell differentiation (Chan, Johnson et al. 2003); when Shp2 is not fully functional, there is a block in normal ES cell differentiation which retains the ES cells in the undifferentiated, stem cell compartment. Shp2 is also essential for hematopoietic stem cell (HSC) self-renewal, as Shp2+/- HSC have reduced self-renewal in serial transplants (Chan, Li et al. 2006). Therefore, Shp2 is important in stem cell differentiation and self-renewal which leads us to question what happens in the absence of Shp2 when another oncogene, such as N51-FLT3 is also present in the bone marrow?

Homozygous knock out of murine Shp2 results in embryonic lethality during mid-gestation (Saxton, Henkemeyer et al. 1997). Therefore, these Shp2 knockout mice cannot be studied. To combat this problem however, Gen-Sheng Feng and his lab developed a conditional Shp2 knockout animal (Zhang, Chapeau et al. 2004). Two loxP sites were introduced in introns flanking exon 4 of the Shp2 allele. Cre-induced recombination results in deletion of exon 4, insertion of a frameshift mutation and generation of a stop codon rendering the Shp2 protein non-functional (Zhang, Chapeau et al. 2004). These animals can be subsequently bred to other transgenic animals which express promoter-specific Cre recombinase. For example, Zhang and colleagues crossed Shp2$^{flox/flox}$ mice

with CaMKIIα-Cre transgenic animals in order to study the role of Shp2 knockout in adult brain tissue (Zhang, Chapeau et al. 2004).

We had the opportunity to use this Shp2$^{flox/flox}$ mouse model in order to investigate the role of Shp2 in N51-FLT3-induced leukemogenesis. In order to knock out Shp2 in the bone marrow, we crossed Gen-Sheng Feng's Shp2$^{flox/flox}$ animals with Mx1-Cre-positive (Mx1-Cre+) transgenic animals (Kuhn, Schwenk et al. 1995) to generate Mx1-Cre+;Shp2$^{flox/flox}$ and Mx1-Cre-;Shp2$^{flox/flox}$ animals. Upon intraperitoneal injection of polyI/polyC, Cre recombinase is activated and Shp2 is deleted in the hematopoietic compartment of Mx1-Cre+ animals. Mx1-Cre is expressed in hematopoietic tissues, liver, spleen, and duodenum; but is also expressed, to a lesser degree in other tissues such as heart, lung, and kidney (Kuhn, Schwenk et al. 1995). Using LDMNCs from polyI/polyC treated Mx1-Cre+;Shp2$^{flox/flox}$ and Mx1-Cre-;Shp2$^{flox/flox}$ animals, we are able to test the effects of loss of Shp2 on N51-FLT3-induced hyperproliferation and hyperactivation of STAT5 *in vitro*.

As mentioned, the activation of STAT5 is one of the most obvious and aberrantly activated signals in FLT3-ITD signaling; therefore; we are interested in how FLT3-ITDs can work with activated STAT5 to induce leukemogenesis. Interestingly, Moore and colleagues demonstrated that expressing either N51-FLT3 or a constitutively active mutant of STAT5 in human cord blood CD34+ cells both increase the self-renewal capabilities of these cells (Schuringa, Chung et al. 2004; Chung, Morrone et al. 2005). Even though these examples are in human cord blood, these data suggest that FLT3-ITD and/or hyperactive STAT5 contribute to increased HSC self-renewal, which may contribute to the pathogenesis and progression of leukemia.

In addition to *in vitro* experiments, we chose to test the role of Shp2 in FLT3-ITD-induced leukemia *in vivo*. It was previously reported that male, BALB/c, 5-fluorouracil (5FU)-treated bone marrow cells infected with N51-FLT3 transplanted into lethally irradiated female BALB/c recipient mice succumb to myeloproliferative disorder (MPD) quite rapidly with an average latency between 40 and 60 days (Rocnik, Okabe et al. 2006). However, our Shp2$^{flox/flox}$ animals are backcrossed onto a C57BL/6 background; therefore, we first needed to test if N51-FLT3 was able to induce MPD in the C57BL/6 genetic background in order to set up the model system.

Once we established a N51-FLT3-induced MPD model in the C57Bl/6 background, we next investigated the effect of Shp2 deletion *in vivo* by transplanting lethally irradiated recipients with N51-FLT3-transduced bone marrow low density mononuclear cells (LDMNCs) from Mx1-Cre+;Shp2$^{flox/flox}$ or Mx1-Cre-;Shp2$^{flox/flox}$ animals. After allowing the cells to engraft, polyI/polyC was used to induce Cre-recombination, deleting Shp2 in the bone marrow. Using this model, we have been able to test the effects of loss of Shp2 on N51-FLT3-induced leukemogenesis *in vivo*. Since bone marrow Shp2-/- cells have decreased self-renewal, but N51-FLT3- and constitutively activated STAT5-expressing cord blood cells have increased self-renewal, we were able to answer the question of whether or not Shp2 deletion reduces HSC function even in the presence of oncogenic N51-FLT3. We therefore hypothesize that hematopoietic-specific loss of Shp2 in the presence of N51-FLT3 will result in either an increase in latency to or prevention of N51-FLT3-induced malignancy all together.

Results

N51-FLT3 Induces Hyperproliferation of Primary Murine Low Density Bone Marrow Cells

To examine the effect of FLT3-ITDs on cellular proliferation and signaling, we utilized murine bone marrow LDMNCs transduced with N51-FLT3. We hypothesized that primary murine bone marrow progenitors expressing N51-FLT3 would be hyperproliferative and have hyperactivated signaling molecules compared to primary murine bone marrow progenitors expressing WT-FLT3. Murine LDMNCs were isolated by Ficoll gradient and transduced with retroviral supernatants containing pMSCV, pMSCV-WT-FLT3, and pMSCV-N51-FLT3. The pMSCV plasmids are bicistronic expressing the indicated FLT3 cDNA in addition to enhanced green fluorescent protein (EGFP). Transduced cells were sorted for EGFP expression (Figure 4.1A), and were subsequently used for proliferation and biochemical studies.

Thymidine incorporation assays were used to measure proliferation of the transduced cells (Figure 4.1B). Sorted EGFP+ cells were cultured overnight followed by starvation in 0.2% BSA in IMDM for 5 hours. Cells were then counted and plated into thymidine incorporation assays in the absence (baseline) or presence of 100 ng/ml FL, as previously described. These studies demonstrate that cells transduced with MSCV, or WT-FLT3 are fairly quiescent at baseline conditions and proliferate in response to FL-stimulation. Likely MSCV is responsive to FL because of low levels of endogenous FLT3 expression in the LDMNc. Cells transduced with N51-FLT3 however, displayed constitutive hyperproliferation at baseline similar to that observed with Baf3/N51-FLT3 and Baf3/N73-FLT3 and are slightly more proliferative upon FL-stimulation compared to

WT-FLT3. Baf3/N51-FLT3 cells are likely modestly induced by FL, because FL-stimulation elicits activation of endogenous WT FLT3 receptors resulting in increased proliferation.

A portion of EGFP-positive sorted cells were cultured into macrophage progenitors and used to make total protein lysates to examine FLT3 levels. Briefly, macrophage progenitors were starved overnight in serum-free IMDM and collected (baseline) or stimulated with 100ng/ml FL for 5 minutes. Total protein lysates were analyzed by immunoblot analysis and demonstrated similar FLT3 protein expression in both WT-FLT3 and N51-FLT3 transduced murine progenitors (Figure 4.1C). This suggests that the hyperproliferation exhibited by N51-FLT3 is due to the mutation itself and not merely due to overexpression of FLT3.
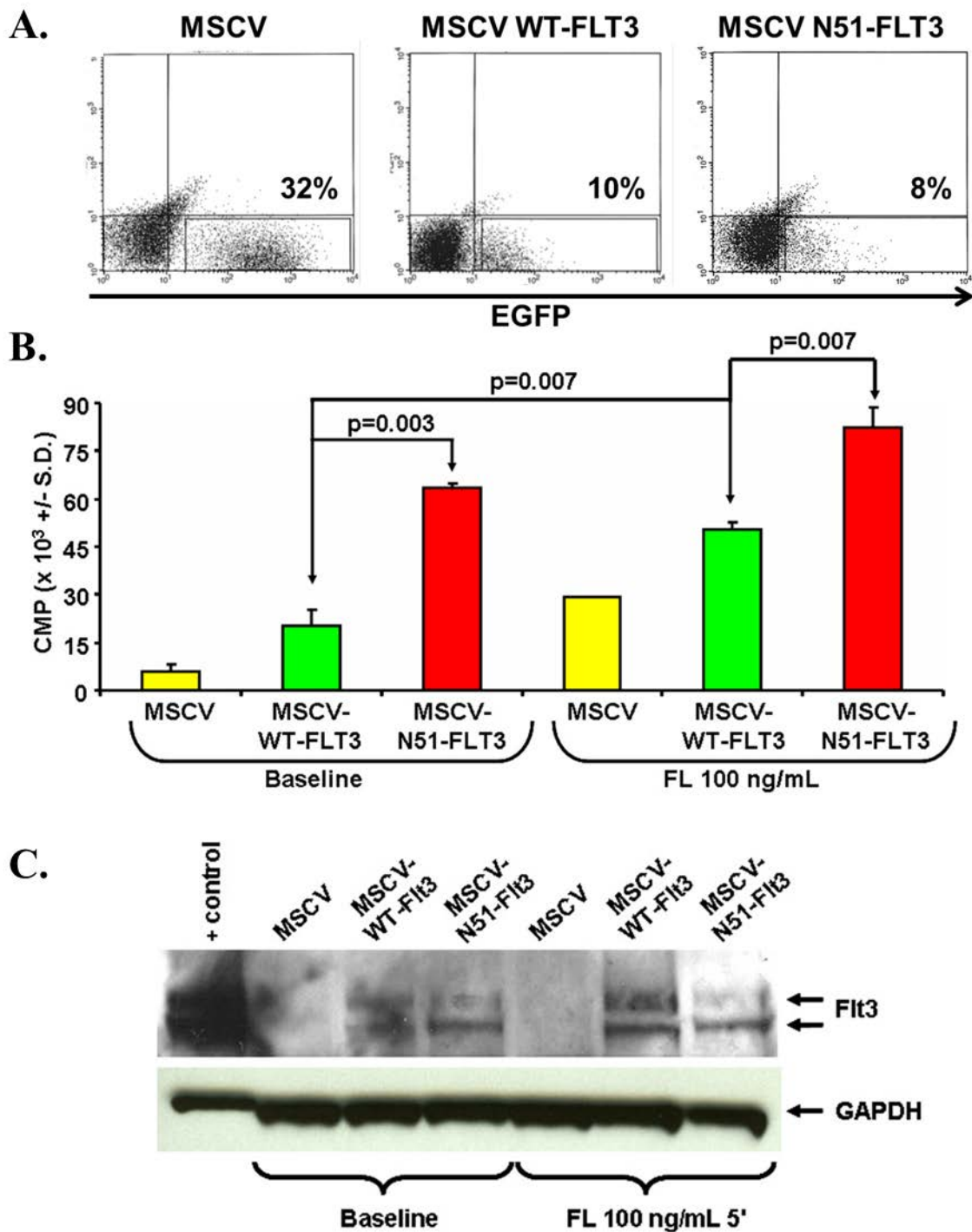
Figure 4.1: N51-FLT3 induces hyperproliferation in murine low density mononuclear cells

(A) FACS analysis was used to sort and collect murine LDMNCs transduced with MSCV (empty vector), WT-FLT3, or N51-FLT3. **(B)** Representative data of 3 independent experiments; ^{3}H thymidine incorporation of MSCV-, WT-FLT3-, and N51-FLT3-transduced LDMNCs; n = 3; statistics generated by unpaired, two-tailed, T-test. **(C)** FLT3 protein expression in WT- and N51-FLT3 expressing cells as demonstrated by western blot analysis.

N51-FLT3 exhibits hyperactivation of STAT5

We illustrated that N51-FLT3 induced a hyperproliferative phenotype in primary

murine bone marrow cells, similar to that observed in the Baf3 cells. We next

investigated the activation of signaling molecules STAT5 and Erk in primary murine

N51-FLT3-expressing cells. Sorted WT-FLT3- and N51-FLT3-transduced primary bone

marrow cells were cultured in M-CSF (50ng/ml)-containing media for one week to

generate macrophage progenitors. Cells were starved overnight in IMDM and then total

cell lysates were prepared at baseline or after FL-stimulation (100ng/ml) for 5, 10, or 30

minutes. Immunoblot analysis (Figure 4.2) revealed similar FLT3 expression in both

WT-FLT3 and N51-FLT3 transduced cells. Interestingly, the unglycosylated, immature

form of FLT3 (lower band) is the predominant form in the N51-FLT3-expressing cells

compared to the glycosylated, mature form (upper band) in the WT-FLT3-containing

cells (Figure 3.2). This observation has been reported previously, and is thought to be

due to retention of immature, relatively unglycosylated FLT3-ITD in the endoplasmic

reticulum and/or golgi apparatus (Schmidt-Arras, Bohmer et al. 2005; Koch, Jacobi et al.

2008). Consistent with this, through collaboration with Dr. XingJun Li, we have shown

preliminary data that there is co-localization between FLT3 and golgi, as well as Shp2

and golgi in FLT3-ITD+ cells compared to FLT3-ITD- cells (data not shown), therefore

one possible mechanism is that Shp2 interacts with FLT3-ITD in the golgi. As

anticipated, STAT5 was constitutively activated by N51-FLT3 independent of FL-

stimulation while STAT5 activation was undetectable in WT-FLT3-transduced cells

(Figure 4.2). We observed Erk activation to be robustly induced by FL in both WT- and

N51-FLT3 expressing cells. At the 5-minute time point however, phospho-Erk appeared

64

higher in the WT-FLT3-expressing cells. We have seen this phenomenon on several

occasions and suspect that the mature, membrane-bound FLT3 (which is more heavily

expressed in WT-FLT3-expressing cells than N51-FLT3-expressing cells) signals more

efficiently to Erk, which is commonly an out-put of traditional Shp2 activity, while the

immature, endoplasmic reticulum or golgi-bound FLT3 (predominant in N51-FLT3-

expressing cells) signals primarily to STAT5, which is consistent with the findings of

others (Choudhary, Olsen et al. 2009; Schmidt-Arras, Bohmer et al. 2009). Phospho-

STAT5 participates in the activation of transcriptional targets, especially pro-leukemic

proteins such as Bcl-X$_L$ and Cyclin-D1 which are often upregulated in cancer.

Collectively, these findings indicate that we are able to induce FL-independent

hyperproliferation and STAT5 hyperphosphorylation using the retroviral vector, MSCV-

N51-FLT3, permitting us to examine the contribution of various molecular mechanisms

to FLT3-ITD-induced leukemogenesis.
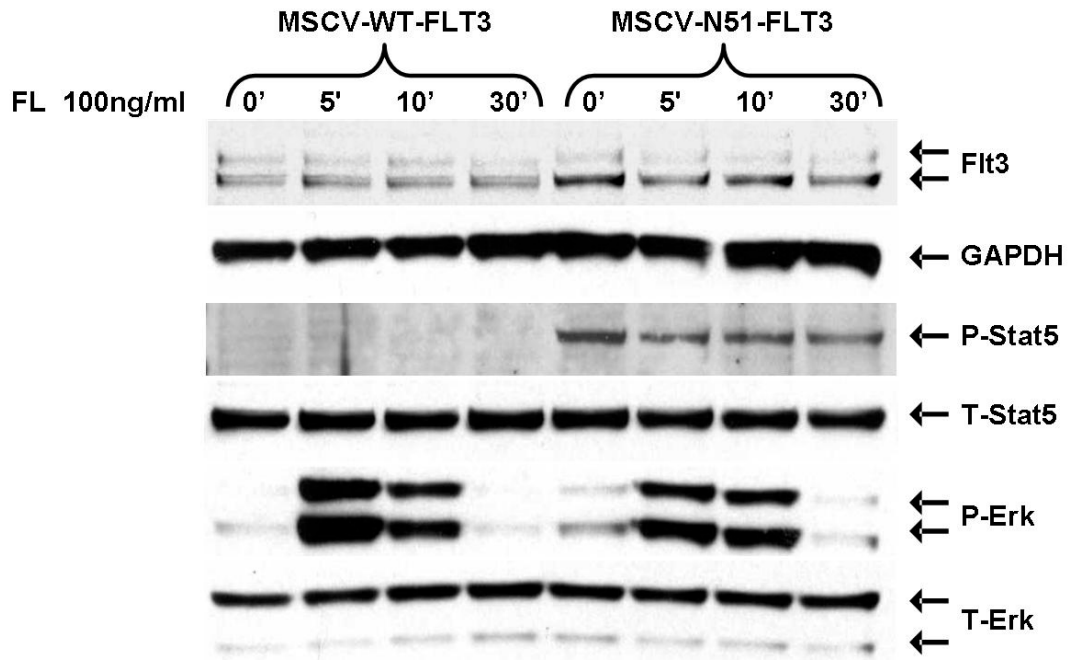
Figure 4.2: Western blot analysis of primary bone marrow transduced with WT- or N51-FLT3

Whole cell lysates from WT-FLT3- and N51-FLT3-transduced macrophage progenitors were subjected to immunoblot analysis and probed with α-FLT3, α-GAPDH, α-phospho-STAT5 (P-STAT5), α-total-STAT5 (T-STAT5), α-phospho-Erk (P-Erk), or α-total-Erk (T-Erk) antibodies.

Conditional Shp2 knockout mouse model

As mentioned previously, Gen-Sheng Feng and his lab created a Shp2$^{flox/flox}$ mouse model which he graciously shared with us. Shp2$^{flox/flox}$ animals were crossed with Mx1-Cre+ animals to result in heterozygous Shp2$^{flox/+}$;Mx1-Cre+ and Shp2$^{flox/+}$;Mx1-Cre- progeny. Heterozygous animals were subsequently mated to yield Shp2$^{flox/flox}$;Mx1-Cre+ and Shp2$^{flox/flox}$;Mx1-Cre- animals. To induce Cre recombinase expression, 300μg of polyI/polyC was injected intraperitoneally on days 1, 3, and 5 into 4-6 week old animals. Two to six weeks post polyI/polyC treatment, LDMNCs were isolated and transduced with either WT-FLT3 or N51-FLT3, sorted, and used in thymidine incorporation assays or by FACS analysis of phospho-STAT5 (Figure 4.3).
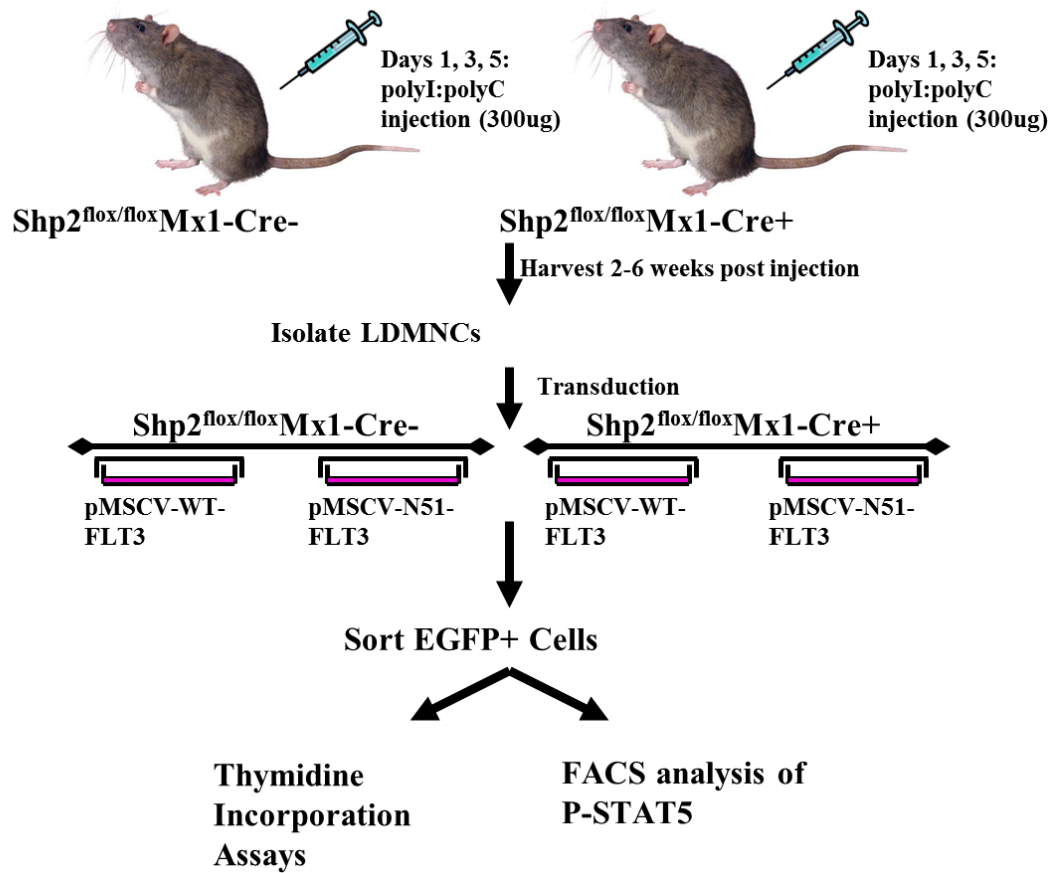
Figure 4.3: Schematic representation of Shp2$^{flox/flox}$; Mx1-Cre+ and Shp2$^{flox/flox}$; Mx1-Cre- animals and their use for *in vitro* functional and biochemical studies

To measure Shp2 recombination and generation of the recombined Shp2-null allele, we performed the following experiment. Two to six weeks post polyI/polyC treatment, Shp2$^{flox/flox}$;Mx1-Cre+ and Shp2$^{flox/flox}$;Mx1-Cre- mice were sacrificed and tissues harvested. Genomic DNA was extracted from tail and bone marrow samples of the polyI/polyC-treated Shp2$^{flox/flox}$;Mx1-Cre- and Shp2$^{flox/flox}$;Mx1-Cre+ mice and total protein lysates were produced from a portion of the bone marrow of the same mice. Using primers that amplify the WT-Shp2 allele, Shp2-floxed, and recombined Shp2 (Shp2-null) allele, PCR amplification is shown in Figure 4.4. DNA from tail and bone marrow (BM) from polyI/polyC-treated Shp2$^{flox/flox}$;Mx1-Cre- animals as well as DNA derived from the tail of polyI/polyC-treated Shp2$^{flox/flox}$;Mx1-Cre+ animals contains only the Shp2-floxed allele and do not have any detectable Shp2-null allele. However, DNA from the BM of Shp2$^{flox/flox}$;Mx1-Cre+ animals demonstrates a clear recombination of the Shp2-Flox allele, yielding the Shp2-null allele (Figure 4.4A). Similarly there was a significant reduction in Shp2 protein expression in total protein lysates from the BM of polyI/polyC-treated Shp2$^{flox/flox}$;Mx1-Cre+ animals compared to that of polyI/polyC-treated Shp2$^{flox/flox}$;Mx1-Cre- mice (Figure 4.4B). Recombination of Shp2 at the DNA level as well as reduction of Shp2 protein levels indicates that in this system, polyI/poyC treatment is sufficient to reduce Shp2 DNA and protein in the BM of Shp2$^{flox/flox}$;Mx1-Cre+ animals suggesting that this animal model is suitable to test the loss of Shp2 on N51-FLT3-induced hyperproliferation and hyperactivation of STAT5.

A.

| kB | Ladder | Shp2^flox/flox; Mx1Cre - | | Shp2^flox/flox; Mx1Cre + | |
| | | Tail | Bone Marrow | Tail | Bone Marrow |

Flox Allele

Null Allele

B. Bone Marrow

Mx1Cre -   Mx1Cre +

← Shp2

← GAPDH
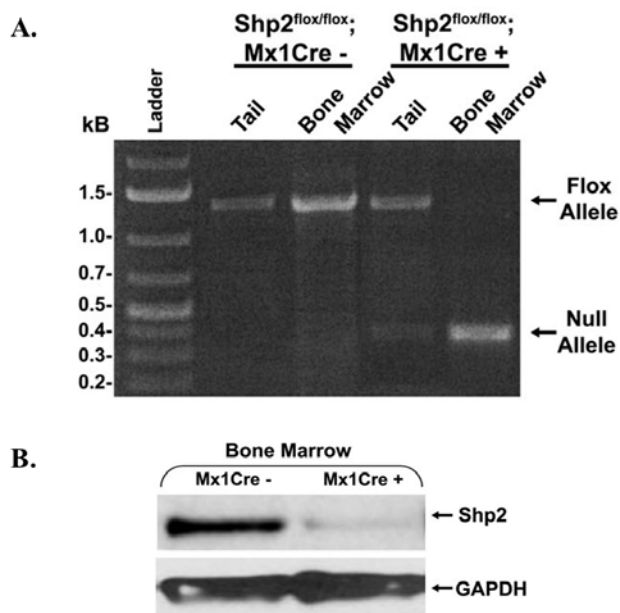
Figure 4.4: Shp2 DNA recombination and protein deletion after PolyI/polyC treatment

(A) Polymerase chain reaction (PCR) amplifying the floxed Shp2 allele as well as the recombined, null allele of DNA from tail and bone marrow cells from polyI/polyC treated Shp2^flox/flox;Mx1-Cre- (Mx1 Cre-) and Shp2^flox/flox;Mx1-Cre+ (Mx1 Cre+) animals. **(B)** Immunoblot analysis of Shp2 protein levels of the bone marrow from Shp2^flox/flox;Mx1-Cre- (Mx1Cre-), or Shp2^flox/flox;Mx1-Cre+ (Mx1Cre+) mice.

After demonstrating successful recombination by polyI/polyC treatment, LDMNCs of polyI/polyC-treated Shp2^flox/flox;Mx1-Cre- and Shp2^flox/flox;Mx1-Cre+ cells were isolated and transduced with either WT-FLT3 or N51-FLT3. Transduced cells were then sorted on EGFP expression and collected. Transduction efficiencies are similar between the 4 cell types (Figure 4.5A). Additionally, a small portion of EGFP+ cells were lysed and total cell protein lysates were made and subjected to immunoblot analysis. The 4 sorted cell populations demonstrated similar total FLT3 expression, as well as total Erk (control) expression (Figure 4.5B). This suggests that WT-FLT3- or N51-FLT3-expressing Shp2^flox/flox;Mx1-Cre- and WT-FLT3- or N51-FLT3-expressing Shp2^flox/flox;Mx1-Cre+ cells can be transduced to express similar levels of FLT3, and can therefore be subsequently compared to one another to understand the effects of loss of Shp2 on N51-FLT3-induced transformation.

A.

Shp2^flox/flox;Mx1Cre −

pMSCV-WT-FLT3   31.5%

pMSCV-N51-FLT3   30.9%

Shp2^flox/flox;Mx1Cre +

pMSCV-WT-FLT3   34.7%

pMSCV-N51-FLT3   28.0%

EGFP

B.

Mx1 Cre-   Mx1 Cre+

WT-FLT3   N51-FLT3   WT-FLT3   N51-FLT3

← FLT3

← T-Erk
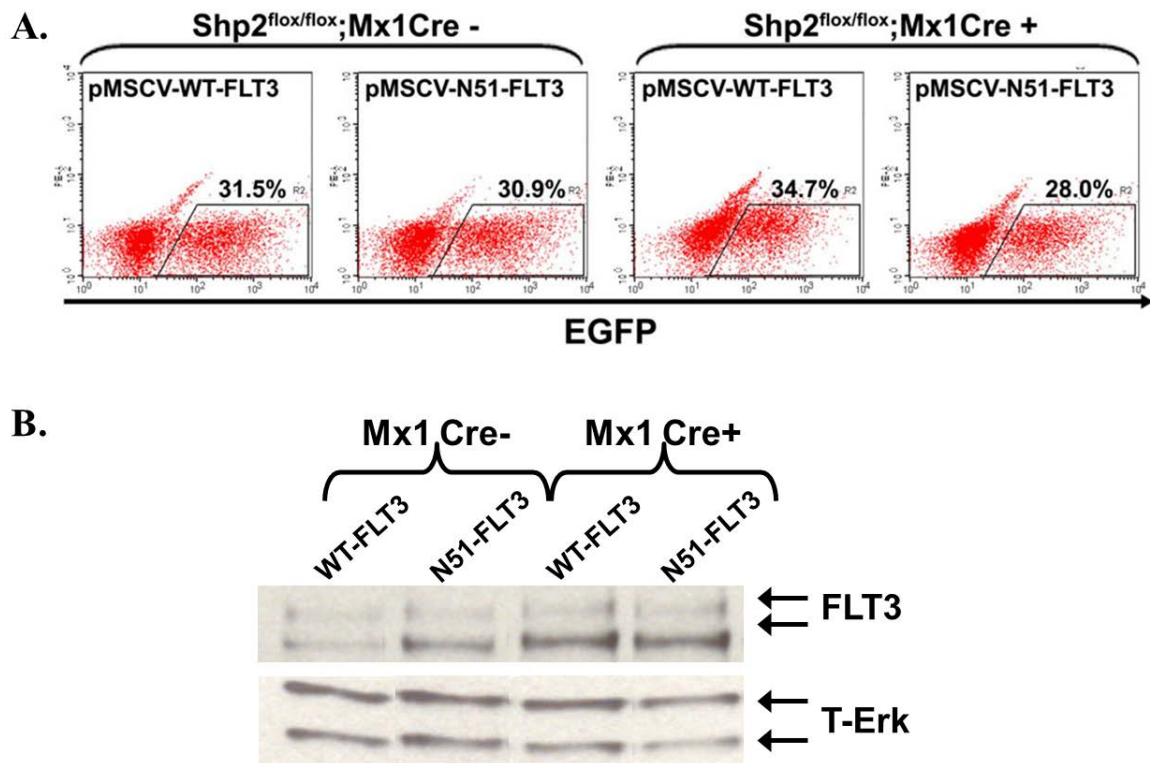
Figure 4.5: Transduction efficiency and FLT3 expression of WT-FLT3 or N51-FLT3 transduced Shp2^flox/flox;Mx1-Cre- or Shp2^flox/flox;Mx1-Cre+ cells

(**A**) WT-FLT3- or N51-FLT3-transduced Shp2^flox/flox;Mx1-Cre- and Shp2^flox/flox;Mx1-Cre+ were sorted using FACS. (**B**) Equal amounts of protein lysates from WT-FLT3 or N51-FLT3 expressing Shp2^flox/flox;Mx1-Cre- cells and WT-FLT3 or N51-FLT3 expressing Shp2^flox/flox;Mx1-Cre+ cells were subjected to SDS-Page gel electrophoresis and probed with α-FLT3 or α-T-Erk.

Genetic knockout of Shp2 in vitro results in reduced hyperproliferation induced by N51-FLT3

In order to investigate the loss of Shp2 on N51-FLT3-induced cellular hyperproliferation, polyI/polyC-treated Shp2$^{flox/flox}$;Mx1-Cre+ and Shp2$^{flox/flox}$;Mx1-Cre- LDMNCs were transduced with either WT-FLT3 or N51-FLT3 retroviral supernatant and EGFP+ cells sorted and collected. EGFP+ cells were then cultured overnight in prestimulation media. The following day, cells were starved in 0.2% BSA-IMDM for 4-5 hours, as previously described, and plated into thymidine incorporation assays in the absence (baseline) or presence of 100ng/ml FL. WT-FLT3-expressing Shp2$^{flox/flox}$;Mx1-Cre- cells proliferate upon FL stimulation and their proliferation is similar to that compared to polyI/polyC-treated Shp2$^{flox/flox}$;Mx1-Cre+ cells (Figure 4.6). N51-FLT3-expressing Shp2$^{flox/flox}$;Mx1-Cre- cells are hyperproliferative at baseline and upon FL-stimulation (Figure 4.6). However, this hyperproliferation is significantly decreased at baseline and upon FL-stimulation in N51-FLT3-expressing polyI/polyC-treated Shp2$^{flox/flox}$;Mx1-Cre+ cells. These data suggest that without Shp2, the ability for N51-FLT3 to induce cellular hyperproliferation is compromised and that Shp2 in part contributes to the hyperproliferative phenotype exhibited by N51-FLT3-expressing cells.
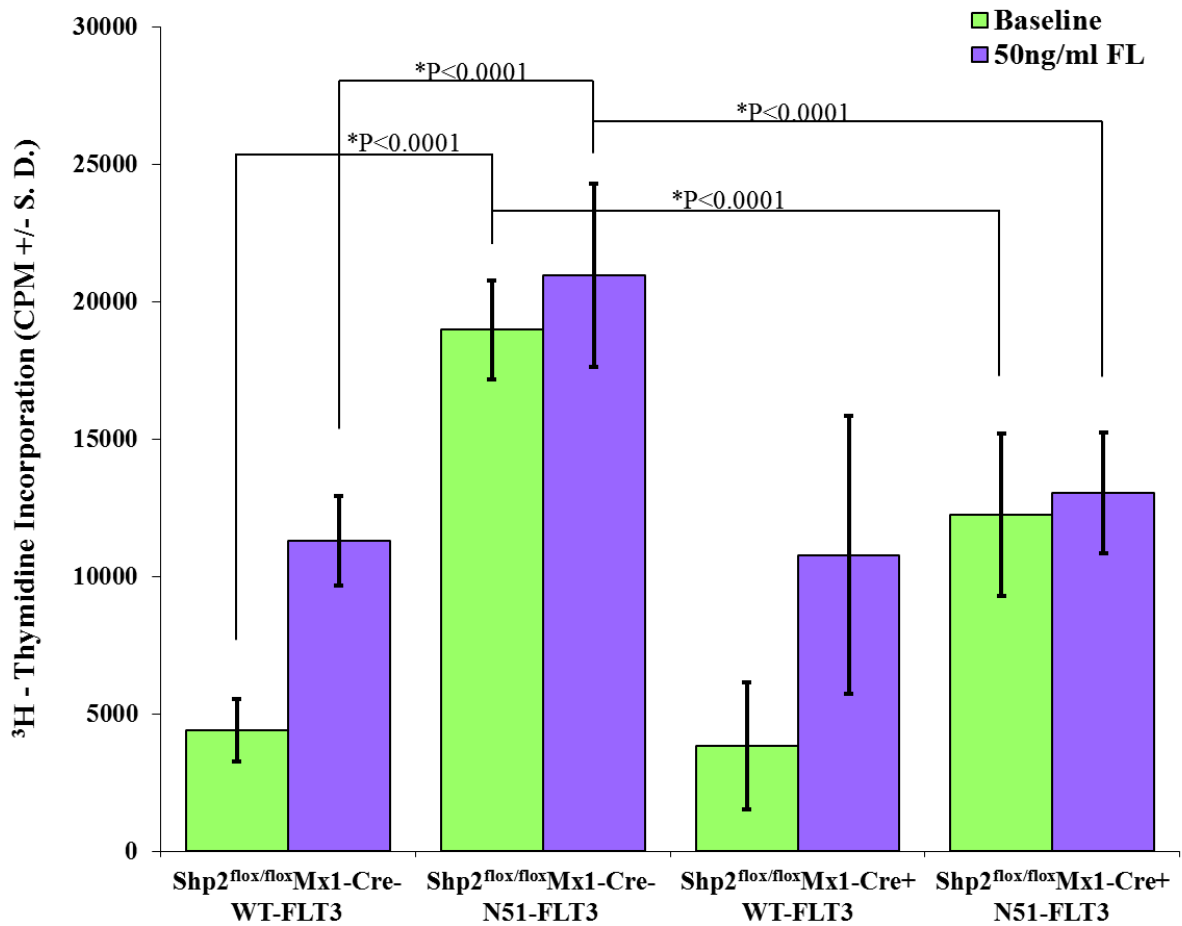
Figure 4.6: Loss of Shp2 significantly reduces N51-FLT3 hyperproliferation *in vitro*

^{3}H-tritiated thymidine incorporation assays comparing WT-FLT3- or N51-FLT3-expressing Shp2$^{flox/flox}$;Mx1-Cre- (WT levels of Shp2) to WT-FLT3- or N51-FLT3-expressing Shp2$^{flox/flox}$;Mx1-Cre+ (Shp2 knockout cells) at baseline and in response to FL-stimulation are shown. Data presented is the combination of 2 independent experiments (n = 4 in 2 independent experiments). Statistical analysis performed using random effects ANOVA.

In vitro knockout of Shp2 results in reduced N51-FLT3-induced activation of STAT5

As previously stated, aberrant activation of STAT5 is one of the hallmarks of FLT3-ITD-induced signaling. In order to examine N51-FLT3-induced hyperactivation of STAT5 in the absence of Shp2, we made total cell protein lysates from WT-FLT3- or N51-FLT3-transduced polyI/polyC-treated Shp2$^{flox/flox}$;Mx1-Cre- or Shp2$^{flox/flox}$;Mx1-Cre+ cells and subjected them to immunoblot analysis. Similar to previous experiments with primary cells, STAT5 activation is undetectable in WT-FLT3-expressing cells regardless of the Shp2 level (Figure 4.7). N51-FLT3-expressing cells demonstrate high levels of phospho-STAT5 with WT Shp2 levels (Shp2$^{flox/flox}$;Mx1-Cre- cell extracts), but levels are reduced by 1.78 fold when Shp2 is deleted (polyI/polyC-treated Shp2$^{flox/flox}$;Mx1-Cre+ cell extracts) (Figure 4.7). When blotting for total Shp2 levels, we observed a significant reduction in both the WT-FLT3- and N51-FLT3-transduced Shp2$^{flox/flox}$;Mx1-Cre+ cell extracts; however, we noted that the degree of Shp2 reduction was different between WT-FLT3-expressing Cre+ cell extracts and N51-FLT3-expressing Cre+ cell extracts (Figure 4.7). We speculate that the rapidly proliferating N51-FLT3-expressing cells, especially those with residual Shp2 protein, are able to proliferate quite quickly, outgrowing some of the Shp2-/- cells. Ultimately the reduction in Shp2 is much more significant in WT-FLT3-expressing cell lysates. However, it is notable that only a 20% (1.2-fold) reduction of Shp2 results in a 46% (1.78-fold) reduction in P-STAT5, indicating that even a modest reduction of Shp2 levels significantly reduces phospho-STAT5 levels in the N51-FLT3-expressing cells.

	WT-FLT3		N51-FLT3	
Mx1-Cre:	−	+	−	+
P-STAT5 Relative	0.03	0.01	1	0.56
T-STAT5 Relative	1.23	1.19	1	1.21
T-SHP2 Relative	0.61	0.15	1	0.83
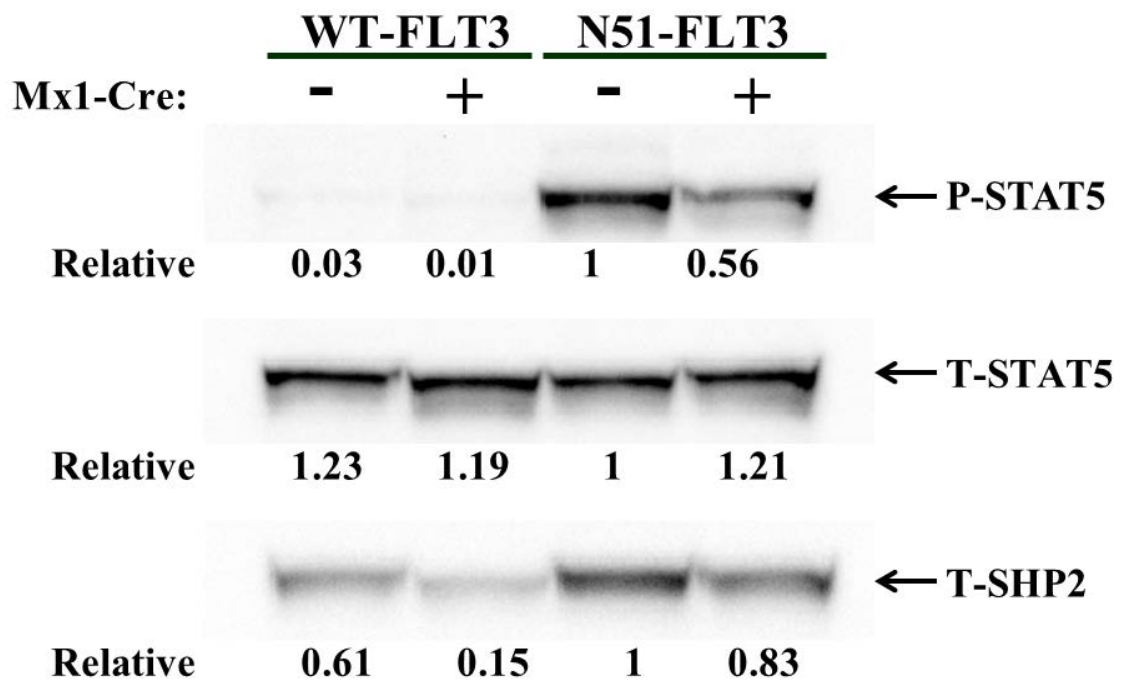
Figure 4.7: Genetic disruption of Shp2 results in a significant reduction of P-STAT5 induced by N51-FLT3 measured by immunoblot analysis

Sorted, EGFP+ WT-FLT3- or N51-FLT3 expressing Shp2$^{flox/flox}$;Mx1-Cre- and Shp2$^{flox/flox}$;Mx1-Cre+ cells were cultured overnight in prestimulation media (containing 100ng/ml SCF, TPO, and G-CSF). The following morning total cell lysates were prepared and run on SDS-Page gels. Membranes were probed with α-phospho STAT5 (P-STAT5), α-total STAT5 (T-STAT5), and α-total Shp2 (T-Shp2). Relative quantity was measured using the BIO-RAD Chemidoc imager and is indicated as the percent expression compared to N51-FLT3, Shp2$^{flox/flox}$;Mx1-Cre- samples.

To test the P-STAT5 levels by a second means, WT-FLT3- or N51-FLT3-expressing Cre- or Cre+ cells were stained intracellularly with α-P-STAT5-APC or APC mouse IgG1 isotype and analyzed by flow cytometry. Figure 4.8A displays the scatterplots from FACS analysis of the four cell populations. Both WT-FLT3-expressing Shp2$^{flox/flox}$;Mx1-Cre- and Shp2$^{flox/flox}$;Mx1-Cre+ demonstrate negligible amounts of P-STAT5 as detected by flow cytometry, similar to that observed using immunoblot. As expected, N51-FLT3-expressing Shp2$^{flox/flox}$;Mx1-Cre- cells highly activated STAT5, with 44% of the cells positive for P-STAT5 staining (Figure 4.8A). However, upon Shp2 deletion in the N51-FLT3-expressing Shp2$^{flox/flox}$;Mx1-Cre+ cells, there was a 1.7-fold reduction of STAT5 activation (26%), very similar to that observed using immunoblotting. This flow cytometry data in the N51-FLT3-expressing cells is highlighted in the histogram in Figure 4.8B, where there is an obvious shift to the left in P-STAT5 immunofluorescence levels when Shp2 protein expression is reduced. This data nicely complements the immunoblot data in Figure 4.7, as the changes in P-STAT5 percentages are nearly identical between the two types of experiments, providing further data that N51-FLT3-expressing cells rely heavily on Shp2 to activate STAT5.

Overall, the Shp2$^{flox/flox}$;Mx1-Cre mouse model provides a useful model system *in vitro* where we are able to use Shp2-null bone marrow cells to demonstrate that reduced Shp2 levels result in a significant reduction in N51-FLT3-induced cellular hyperproliferation and STAT5 activation, which nicely correlates with the data presented in Chapter Three using Baf3 cells and shRNAs targeted to Shp2. To further investigate this role of Shp2 on N51-FLT3-induced MPD, we will next use the mouse model *in vivo*

to knock out Shp2 in a N51-FLT3-transplant recipient mouse to determine if the loss of

Shp2 in the bone marrow will prevent N51-FLT3-induced MPD.
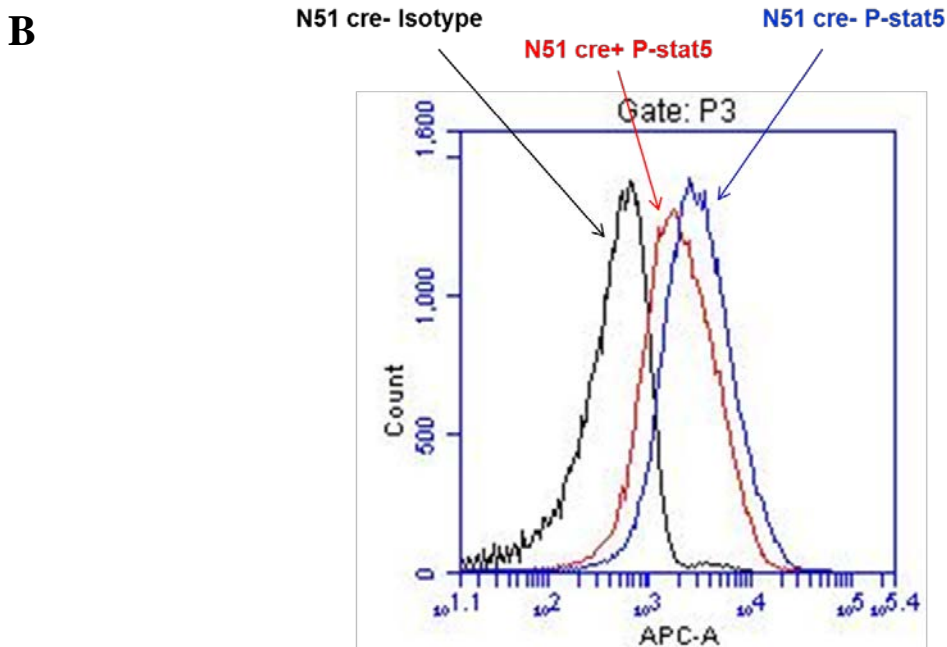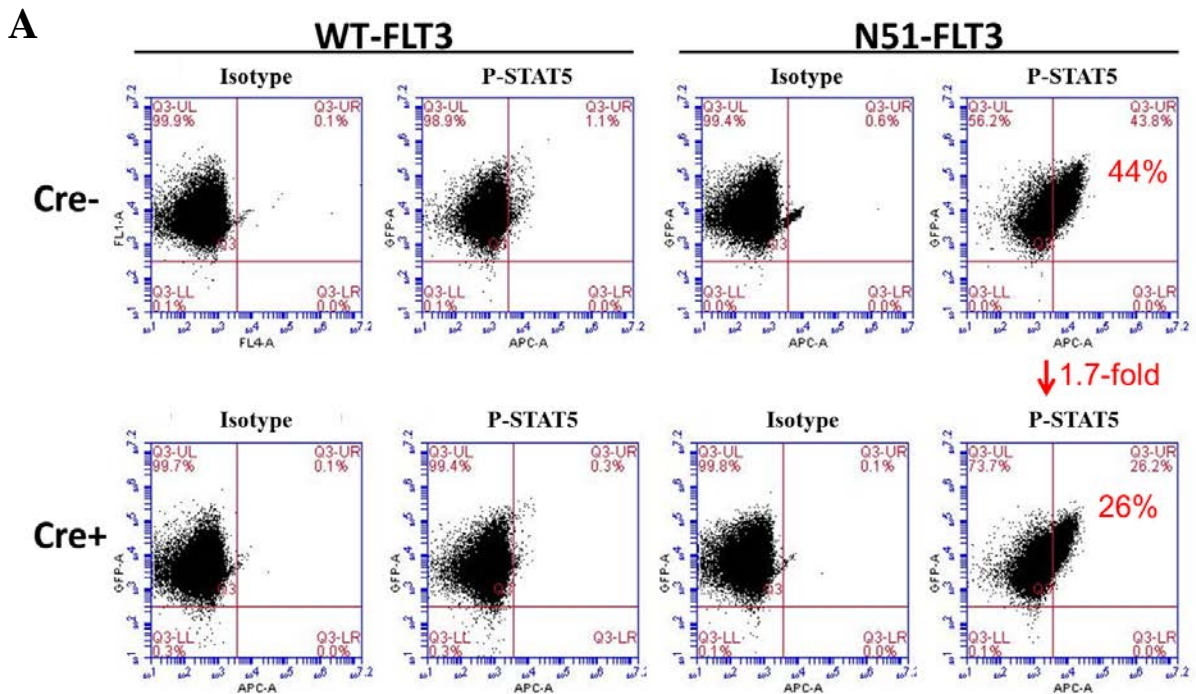
Figure 4.8: Genetic disruption of Shp2 results in a significant reduction of P-STAT5 induced by N51-FLT3 as measured by flow cytometry

A portion of the previously described sorted, EGFP+ WT-FLT3- or N51-FLT3-transduced Cre- or Cre+ cells were stained with α-P-STAT5-APC or the corresponding isotype. Cells were analyzed by FACS and the P-STAT5-APC positive populations measured. Data is presented in scatterplots **(A)** and summarized in histogram **(B).**

Establishing a FLT3-ITD+ C57BL/6 mouse model

We have demonstrated that loss of Shp2 significantly reduces the proliferation and the aberrant activation of STAT5 induced by N51-FLT3 *in vitro* using both cell line and primary cell models. In order to test the leukemic potential of N51-FLT3 in the absence of Shp2 *in vivo*, we proposed to transplant lethally irradiated recipient mice with WT-FLT3 or N51-FLT3-transduced Shp2$^{flox/flox}$;Mx1-Cre- or Shp2$^{flox/flox}$;Mx1-Cre+ LDMNCs followed by treatment with polyI/polyC to delete Shp2 expression. These recipient animals would provide a useful model system to test the effects of Shp2 knockout on the leukemic potential of N51-FLT3 *in vivo*.

Given that previous transplant models of N51-FLT3-induced MPD in vivo utilized BalbC mice (Kelly, Liu et al. 2002), we needed to establish an effective model on the murine, C57Bl/6 background. In order to investigate N51-FLT3-induced MPD on a C57BL/6 background, we set up our *in vivo* experiment as depicted in Figure 4.9. Briefly, 3 Shp2$^{flox/flox}$;Mx1-Cre- C57BL/6 mice (CD45.2 positive) were injected with 150 mg/kg 5-fluorouracil (5-FU) to enrich for primitive progenitors and hematopoietic stem cells (HSCs). Three days later, mice were euthanized and LDMNCs were isolated and plated into prestimulation media overnight. After two rounds of retroviral transductions, cells were sorted on EGFP positivity and resuspended in 0.05% endotoxin-free BSA-IMDM at a concentration of 1 million EGFP+ cells plus 100,000 supporting low density mononuclear supporting splenocytes in 300μl volume. The splenocytes contain more mature progenitors which act to supplement the recipient animals' immune system while the immature, stem cell and progenitor donor cells have time to engraft and fully reconstitute the bone marrow. Cells were administered via tail vein injection into 7

lethally irradiated F1 (C57/BoyJ F1) recipients (CD45.1/CD45.2 double positive). The

advantage of transplanting C57BL/6 mice into F1 recipients is that the donor, C57BL/6

animals are single positive for CD45.2, while the F1 recipients are CD45.1/CD45.2

double positive, therefore we are able to use flow cytometry to determine the percentage

of cells that came from the donor animals and the percentage of cells from the recipient

host.

5-FU (150 mg/kg)

Shp2$^{flox/flox}$ MxCre-

72 hrs post 5-FU
Isolate Bone
Marrow LDMNCs

pMSCV-
N51-FLT3

Sort EGFP+ Cells

Transplant 1 million GFP+ cells
100,000 supporting
spleenocytes

1100 cGy

7 F1 animals

Follow Monthly
cbcs and chimerism
(CD45.1/CD45.2 host:CD45.2 donor)
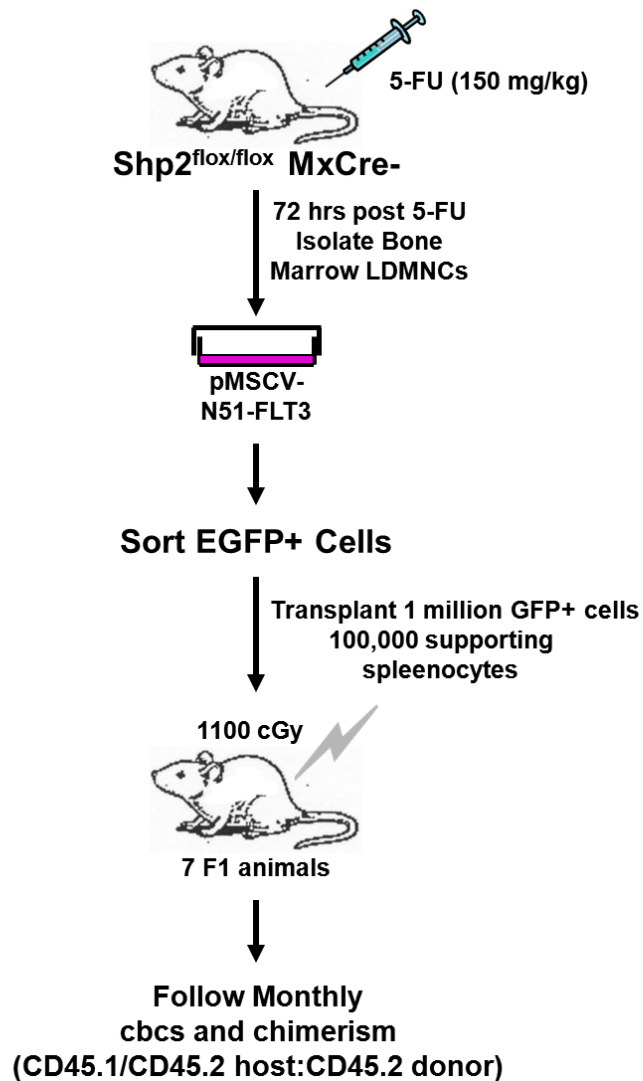
Figure 4.9: Schematic representation N51-FLT3-induced MPD *in vivo* on a C57Bl/6
background

Tail vein bleeds were performed at 5 and 10 weeks post-transplant. Using the peripheral blood, complete blood counts (cbc) were assessed to determine the number of white blood cells. The samples were then subjected to red blood cell lysis buffer to remove the majority of erythrocytes followed by staining with α-CD45.1-phycoerythrin (PE) and α-CD45.2-allophycocyanin (APC). Flow cytometry was used to analyze the percentage of blood cells which were EGFP-positive, suggesting that they were N51-FLT3-expressing donor cells and to analyze the percentage of blood cells which were donor-derived (CD45.2-APC+), or residual recipient cells (CD45.1-PE/CD45.2-APC double positive). Figure 4.10A demonstrates the average percentage of EGFP+ cells, average number of white blood cells (WBCs, measured in thousands), and the average percentage of donor-derived CD45.2-APC+ cells. We observed an obvious trend that the EGFP+ and CD45.2+ donor-derived cell populations increased between 5 and 10 weeks post-transplant (Figure 4.10A). While the average number of white blood cells increased slightly, the increase was less apparent. However, consistent with increasing EGFP+ cells, we found that several of the N51-FLT3-transplanted recipients developed MPD between 10-14 weeks post-transplant as demonstrated by the survival curve of this cohort of animals (Figure 4.11). A spleen from a representative N51-FLT3-transplant recipient is shown demonstrating splenomegaly with a length of approximately twice that of a wild type mouse (Figure 4.10B). Upon hematoxalin and eosin (H&E) staining of cross sections of the spleens, we observed significant disruption of the splenic architecture by N51-FLT3 indicative of MPD (Figure 4.10C). This pilot study demonstrated that N51-FLT3-induced MPD in C57BL/6 animals is feasible, permitting us to proceed with

studies in the Shp2$^{flox/flox}$;Mx1Cre+ mouse model of MPD to test the effect of Shp2 loss on N51-FLT3-induced leukemogenesis.
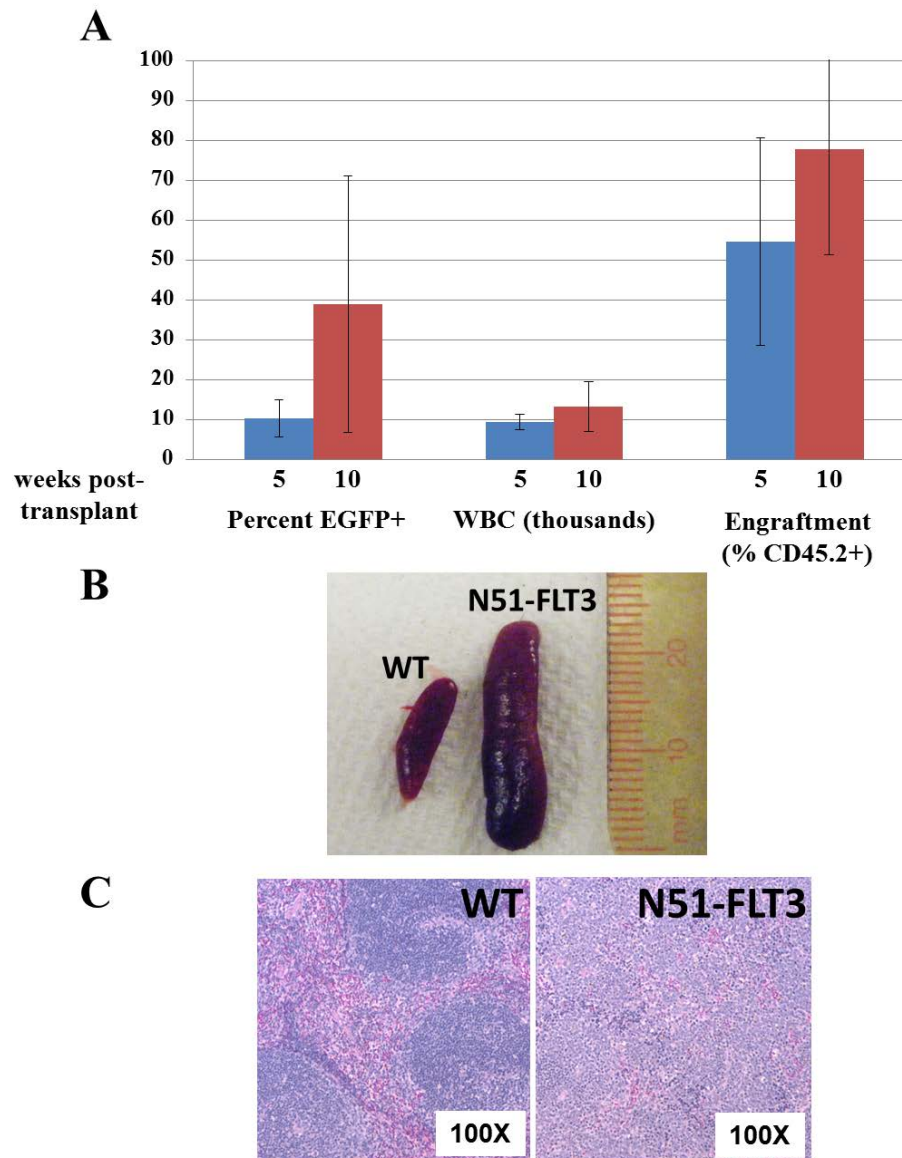
Figure 4.10: N51-FLT3-induced MPD on a C57Bl/6 background

(A) Percent EGFP+, white blood cells number (thousands), and percent donor cells (CD45.2+) are displayed as the average of the transplant recipients 5 weeks (7 animals) and 10 weeks (6 animals) post-transplant. Whole spleen **(B)** and H&E staining of a cross section **(C)** of a wildtype mouse compared to a representative N51-FLT3-transplant recipient.
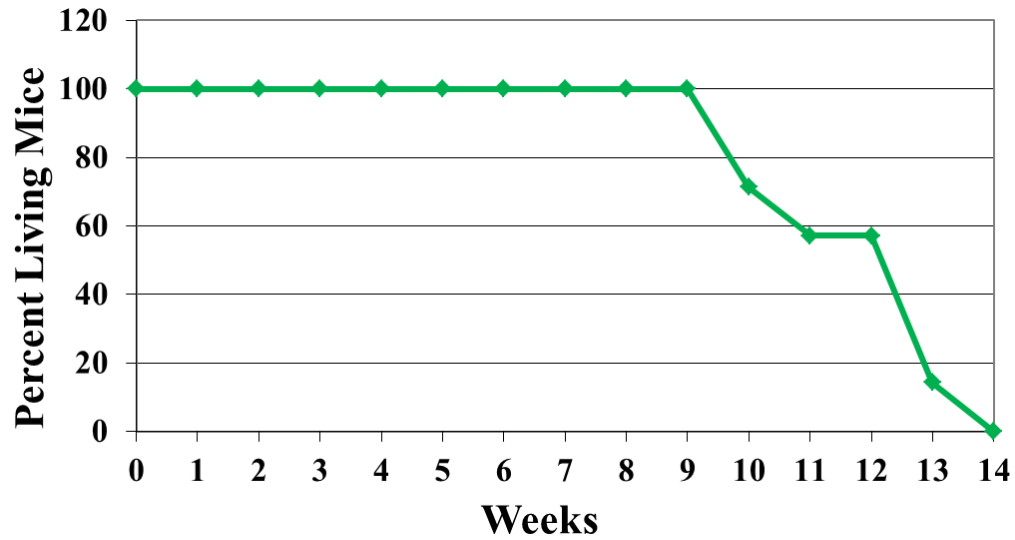
Figure 4.11: Survival curve of N51-FLT3-transplant recipients on C57Bl/6 background

Shp2$^{flox/flox}$;Mx1-Cre- cells transduced with N51-FLT3 and transplanted into lethally irradiated recipients. Survival curve represents the percent living animals at a given time point post-transplant, n = 7.

Loss of Shp2 expression in a N51-FLT3+ mouse model

In setting up the N51-FLT3-transduced, Shp2$^{flox/flox}$;Mx1-Cre+ animal transplant model in order to test the loss of Shp2 on N51-FLT3-induced leukemogenesis, we encountered a serious challenge. Unfortunately, 5-FU treatment of Shp2$^{flox/flox}$;Mx1-Cre+ animals resulted in substantial cell death of bone marrow cells, presumably because Shp2-decficnet cells are less quiescent than wild type controls (Chan, Li et al. 2006; Chan, Cheung et al. 2011; Zhu, Ji et al. 2011). Therefore, 5-FU treatment of Shp2$^{flox/flox}$ Mx1-Cre+ animals resulted in significantly reduced cell numbers; insufficient for retroviral transduction and subsequent transplantation of Shp2$^{flox/flox}$;Mx1-Cre+ cells into

83

recipient animals which presented us with a serious problem in our proposed transplant study.

To speculate on this problem, we have found that there is breakthrough Mx1 promoter-directed Cre expression even without polyI/polyC treatment which contributes to low levels of Shp2 recombination and a baseline reduced Shp2 expression. Therefore, baseline reduced Shp2 levels may have caused the bone marrow cells in the Shp2$^{flox/flox}$;Mx1-Cre+ animals to be much more sensitive to 5-FU treatment compared to the Shp2$^{flox/flox}$;Mx1-Cre- animals. Furthermore, the 5-FU treatment itself may have induced a cytokine release resulting in unwanted enhanced Mx1 promoter-directed Cre expression in the Shp2$^{flox/flox}$;Mx1-Cre+ animals, leading to further reduction in Shp2 expression which resulted in death of bone marrow cells. To overcome this problem, we utilized a lineage depletion kit from StemCell Technologies to isolate the most immature and stem cell-like progenitors from the bone marrow LDMNCs from both the Shp2$^{flox/flox}$;Mx1-Cre- Shp2$^{flox/flox}$;Mx1-Cre+ animals for all subsequent experiments.
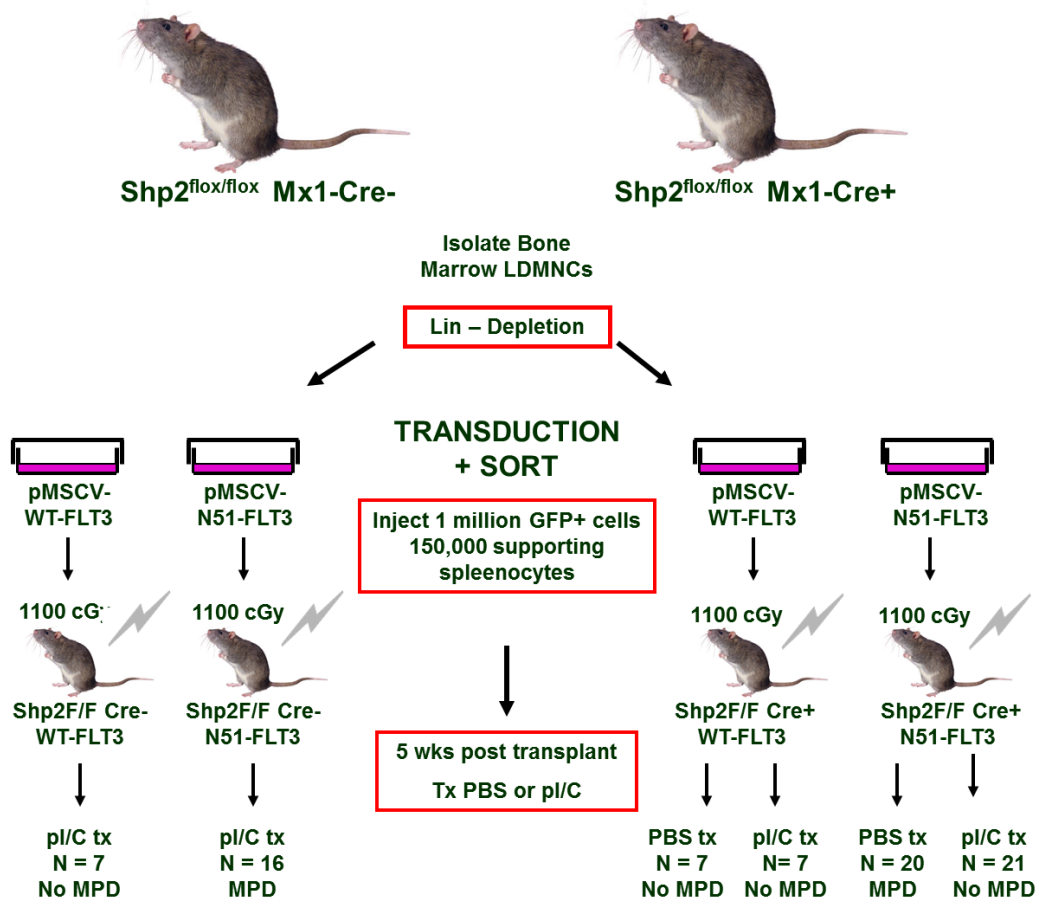
Figure 4.12: Schematic representation of WT-FLT3- or N51-FLT3-transduced-Shp2$^{flox/flox}$;Mx1-Cre- and Shp2$^{flox/flox}$;Mx1-Cre+ transplants

General outline of the experimental design is shown beginning with harvesting the bone marrow LDMNCs, transduction, transplant, monitoring, and division into polyI/polyC or PBS treatment groups. Diagram represents the combination of animals used in 3 independent experiments with expected outcomes indicated.

The overall scheme of the transplant experiments is highlighted in Figure 4.12. Shp2$^{flox/flox}$;Mx1-Cre- and Shp2$^{flox/flox}$;Mx1-Cre+ animals were sacrificed and bone marrow LDMNCs isolated and subjected to lineage depletion. A small amount of cells (both pre and post lineage depletion) were stained with a cocktail of lineage markers including Gr-1, Mac-1, B220, Ter119, CD-3, and CD-8. Prior to lineage depletion, 3.6% of Cre- and 5.8% of Cre+ cells were lineage negative, after lineage negative isolation, Cre- cells were 54% and Cre+ cell were 65.6% lineage negative (Figure 4.13A). These lineage-negative LDMNCs were transduced with either pMSCV-WT-FLT3 or pMSCV-N51-FLT3 retroviral supernatants on days 3 and 4, and then plated into prestimulation media until sorted on EGFP expression. Shp2$^{flox/flox}$;Mx1-Cre- cells had similar transduction efficiencies of either 41.3% EGFP+ in Cre-, WT-FLT3-expressing cells or 47% EGFP+ in Cre-, N51-FLT3-expressing cells (Figure 4.13B). On the other hand, the transduction efficiencies of the Cre+ cells were significantly lower, 15% for Cre+, WT-FLT3 and 21% EGFP+ for Cre+, N51-FLT3 (Figure 4.13B). Interestingly, we often observed a similar difference in transduction efficiencies between Cre- and Cre+ cells. We suspect that breakthrough Cre expression leads to a slight reduction in Shp2 levels and these cells do not divide as rapidly, therefore are not transduced as easily as the Cre-cells. On the day of the transplant, 2 wild type F1 animals were sacrificed and spleen-derived LDMNCs were isolated by ficoll gradient to provide radioprotective cells. After the transduced cells were sorted, 1 million EGFP+ cells and 150,000 supporting splenocytes were mixed in 300μl total volume of 0.2% endotoxin-free BSM-IMDM and administered via tail vein injection. Combining three independent experiments, we

transplanted the following animals followed by treatment with either phosphate buffered

saline (PBS) or polyI/polyC:

Table 4.1: Number of transplant recipients, and treatment received post-transplant

Genotype	Number of Animals
Shp2$^{flox/flox}$Mx1-Cre- WT-FLT3	7 (polyI/polyC treated)
Shp2$^{flox/flox}$Mx1-Cre- N51-FLT3	16 polyI/polyC treated)
Shp2$^{flox/flox}$Mx1-Cre+ WT-FLT3	7 (PBS treated)
	7 (polyI/polyC treated)
Shp2$^{flox/flox}$Mx1-Cre+ N51-FLT3	20 (PBS treated)
	21 (polyI/polyC treated)
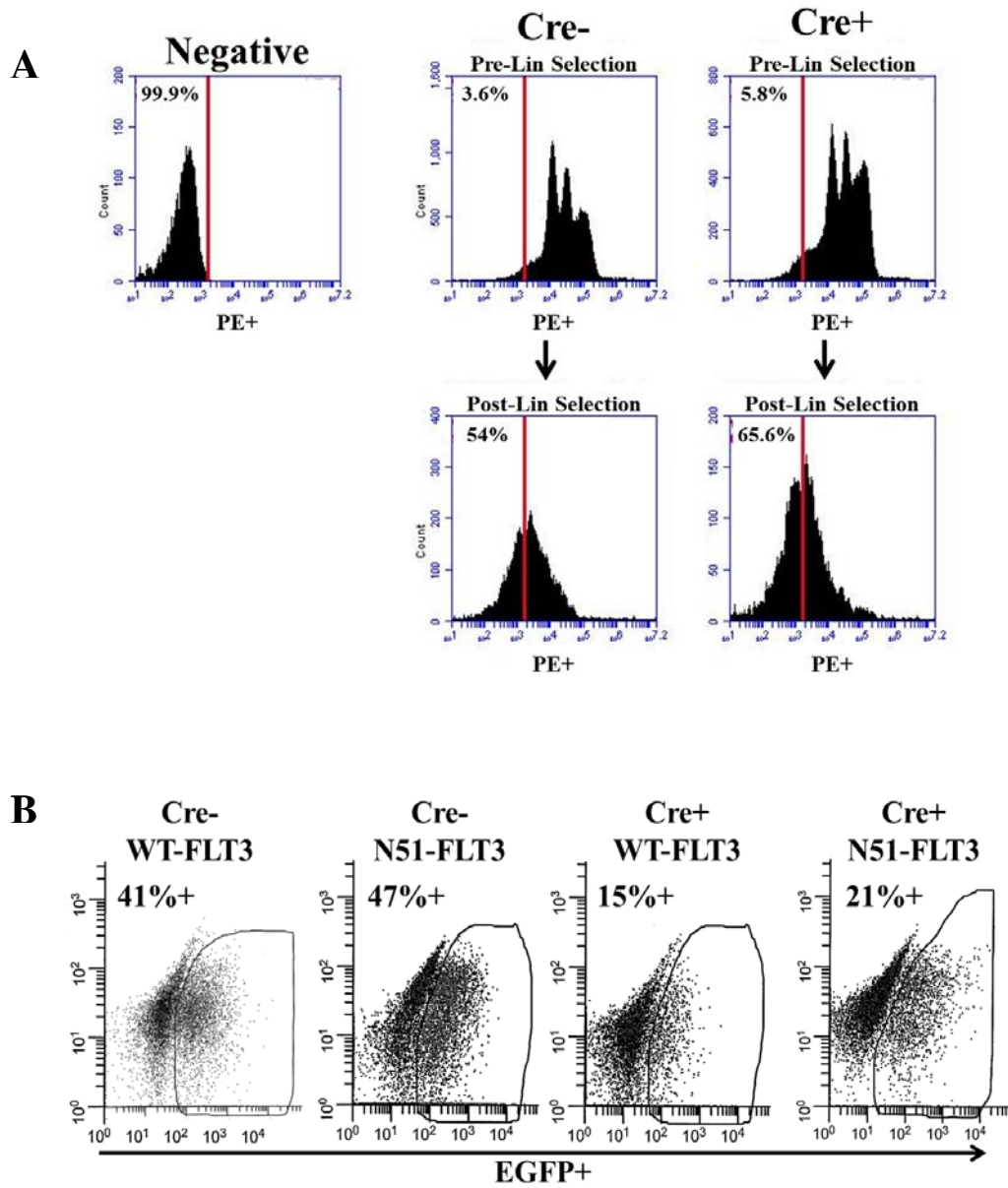
Figure 4.13: Lineage depletion of bone marrow LDMNCs and sorting by fluorescence activated cell sorting (FACS)

(A) Flow cytometry analysis demonstrating the enrichment in lineage negative populations of LDMNCs before and after Lineage depletion. **(B)** FACS of transduced Shp2$^{flox/flox}$;Mx1-Cre- and Shp2$^{flox/flox}$;Mx1-Cre+ bone marrow Lin- cells with either WT-FLT3 or N51-FLT3.

Animals transplanted with N51-FLT3-transduced cells demonstrate MPD and increased mortality compared to those transplanted with WT-FLT3-transduced cells

We initially compared the survival of animals transplanted with N51-FLT3-transduced cells to that of WT-FLT3-transduced cells, and found that similar to transplants utilizing bone marrow from 5-FU-treated Shp2$^{flox/flox}$;Mx1Cre- animals, animals transplanted with N51-FLT3-transduced Shp2$^{flox/flox}$;Mx1Cre- Lin- cells succumbed to MPD (Figure 4.14). These animals were treated with polyI/polyC during the 5th week post-transplant.

The Kaplan Meier curve demonstrated that the Cre-, WT-FLT3 recipients had an overall much longer survival compared to N51-FLT3 recipients (Figure 4.14). While there were a couple of deaths in the WT-FLT3 transplant recipient group, we examined their spleen and bone marrow by H&E staining and consultation with pathologist, Dr. George Sandusky, Department of Pathology at Indiana University School of Medicine, and have concluded that these animals did not die of MPD or a leukemic phenotype. This data supports the idea that the presence of N51-FLT3 is truly leukemogenic in nature and WT-FLT3 alone is not sufficient to cause MPD in this mouse model.
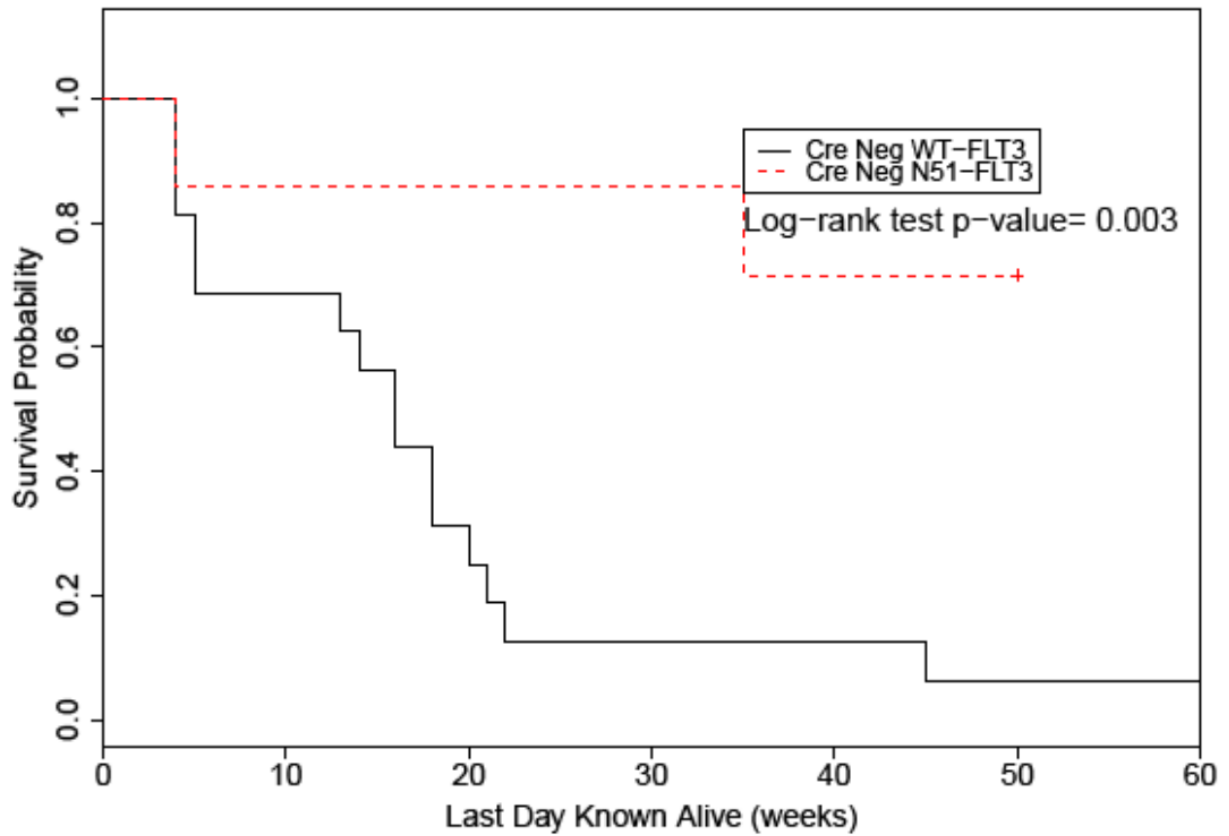
Figure 4.14: Overall Survival of animals transplanted with WT-FLT3- and N51-FLT3-transduced Shp2$^{flox/flox}$;Mx1Cre- Lin- cells

Overall survival of Shp2$^{flox/flox}$;Mx1-Cre- WT-FLT3 or N51-FLT3 transplant recipient mice. Kaplan Meier estimation was calculated using 'last day known alive (weeks)'. n = 7 for Cre-, WT-FLT3; n = 16 for Cre-, N51-FLT3; statistics generated by log-rank test.

Loss of Shp2 expression does not increase the overall survival of animals transplanted with N51-FLT3-transduced cells

We were next interested to specifically determine if genetic reduction of Shp2 would reduce the latency to or the severity of N51-FLT3-induced malignancy *in vivo*. To perform these studies, four to six weeks after transplant, peripheral blood was evaluated from animals transplanted with N51-FLT3-transduced Shp2$^{flox/flox}$;Mx1-Cre+ cells with complete blood counts for white blood cell counts and with flow cytometry for EGFP-positive populations and CD45.2-APC-positive donor-derived populations. Based on these data, animals were divided into 2 groups: those to receive polyI/polyC, which we expect to induce Cre-recombinase expression and result in reduced Shp2 expression in the bone marrow, and those to receive PBS, which should maintain normal levels of Shp2 expression. The average chimerism (% 45.2+), EGFP expression, and white blood cell counts in the two N51-FLT3, Shp2$^{flox/flox}$;Mx1-Cre+ groups prior to receiving polyI/polyC to induce Shp2 recombination or PBS as a vehicle control are displayed in Figure 4.15A-C, respectively. Chimerism, EGFP, and white blood cell counts were similar comparing the two groups prior to treatment. During week 5 post-transplant, animals were treated with either 300µg of polyI/polyC (150µl of 2mg/ml polyI/polyC) or 150µl PBS as a control every other day for a total of 3 treatments. Animals were monitored over time with subsequent tail bleeds to monitor white blood cell counts, chimerism, EGFP expression, and progression to MPD. Upon death, animals were harvested, spleens weighed, and femurs and spleens sent to pathology for H&E staining to examine the tissues for evidence of malignancy. We hypothesized that the polyI/polyC-treated N51-FLT3, Shp2$^{flox/flox}$;Mx1-Cre+ transplant recipients would either

fail to develop MPD or have an increased latency to disease compared to PBS-treated

N51-FLT3, Shp2$^{\text{flox/flox}}$;Mx1-Cre+ transplants.

The overall survival of the PBS-treated vs. polyI/polyC-treated Cre+ N51-FLT3

animals is shown in Figure 4.15D. We hypothesized that loss of Shp2 in the presence of

N51-FLT3 would either increase the latency to disease, or prevent MPD entirely. As

expected, a several polyI/polyC treated Cre+ N51-FLT3 animals did demonstrate

prolonged survival, however, a few polyI/polyC-treated Cre+ N51-FLT3 animals died

even earlier than PBS-treated Cre+ N51-FLT3 animals, therefore there is no significant

difference in the overall survival of PBS-treated animals transplanted with Cre+ N51-

FLT3 compared to polyI/polyC-treated animals transplanted with Cre+ N51-FLT3

(Figure 4.15D).
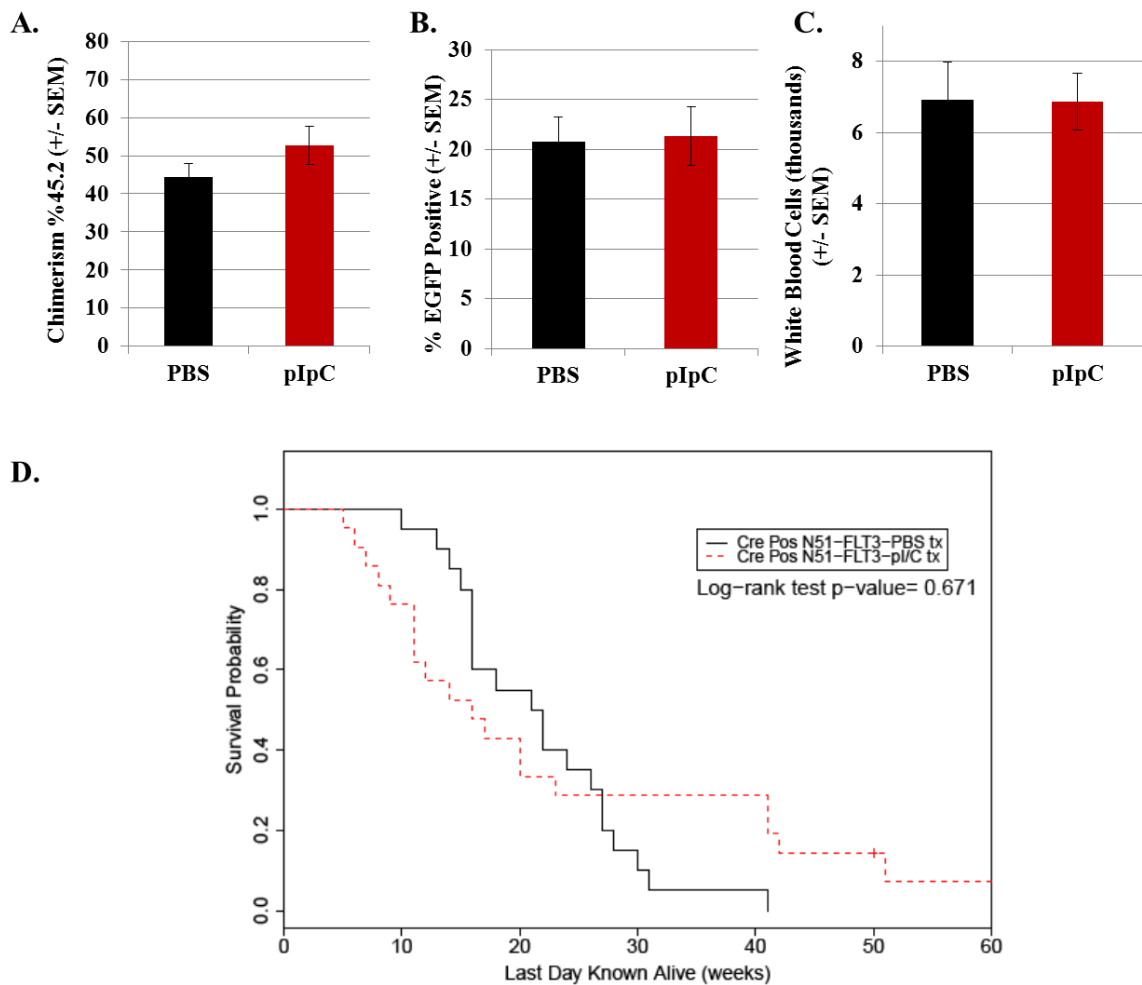
Figure 4.15: Overall Survival of PBS-treated Cre+ N51-FLT3 vs pI/pC-treated Cre+ N51-FLT3 transplanted animals

(A) Average chimerism (CD45.2%+), **(B)** percent EGFP+, and **(C)** white blood cell counts 4 weeks post-transplant of N51-FLT3-transduced Shp2$^{flox/flox}$;Mx1Cre+ cells into lethally irradiated recipients (baseline), n = 21 for PBS group and n = 20 for polyI/polyC group. **(D)** Kaplan Meier curve represents overall survival of PBS-treated Cre+ N51-FLT3 (n = 18) vs. polyI/polyC-treated Cre+ N51-FLT3 (n = 17) transplanted animals with pathological diagnosis at time of death.

In order to fully understand why the polyI/polyC-treated animals experience early lethality, we examined the spleen and bone marrow histopathology and discovered that many of the polyI/polyC-treated animals transplanted with N51-FLT3-transduced Shp2$^{flox/flox}$;Cre+ cells experienced early death due to profound bone marrow failure, examined with and confirmed by Dr. George Sandusky (Figure 4.16). Compared to a wildtype bone marrow specimen (demonstrating a heterogeneous population of bone marrow cells with scant adipose pockets), a representative bone marrow failure specimen is shown and demonstrates severe hypocellularity and excessive adipose (Figure 4.16). The remaining bone marrow cells appeared stromal and fibroblast-like. Normal splenic architecture is shown in the wildtype spleen sample with obvious white and red pulp. The spleen from the representative bone marrow failure specimen does have some visible red and white pulp, with evidence of extramedullary hematopoiesis (EMH). EMH is a general term referring to hematopoiesis which occurs outside the bone marrow, and in these mice the splenic EMH is working to repopulate the animal's hematopoietic system due to the deficiencies of the bone marrow. Therefore, it seems that if Shp2 is knocked out too soon, or too completely, the animals succumb to bone marrow failure and death. However, we noted that some polyI/polyC-treated animals demonstrated prolonged survival compared to the PBS-treated Cre+ N51-FLT3 animals, therefore we next investigated the malignancy-specific survival.
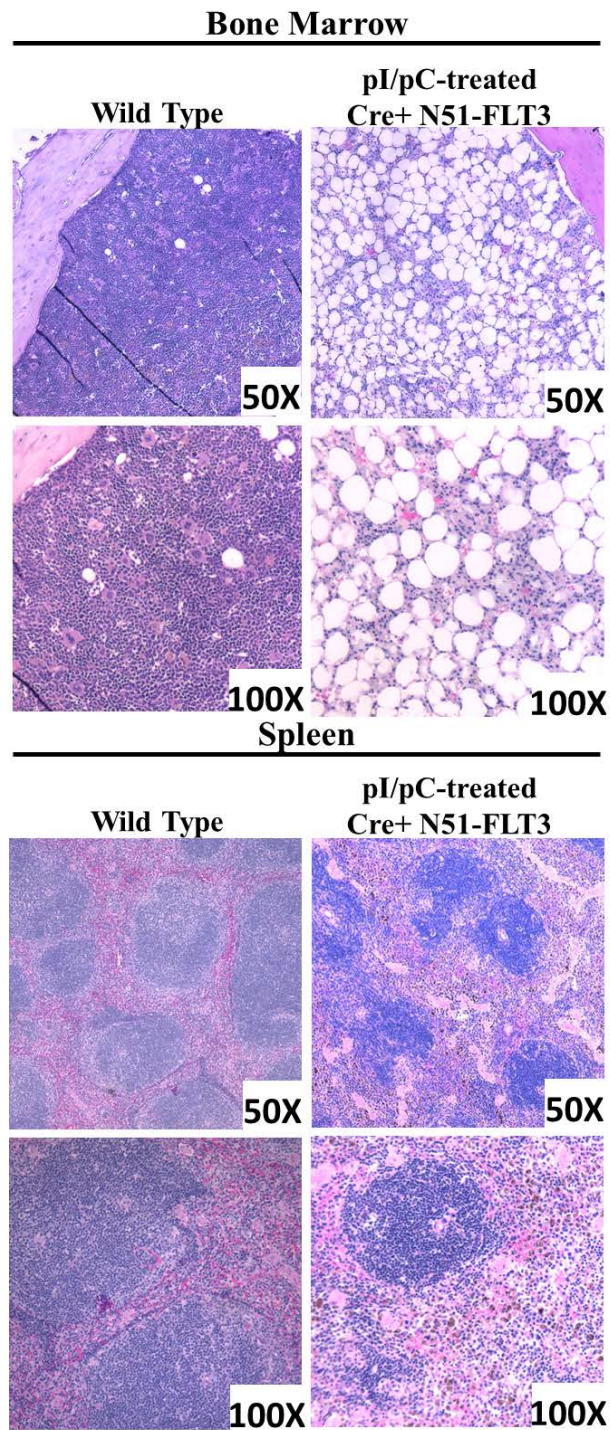
Figure 4.16: H&E staining of a polyI/polyC-treated Cre+ N51-FLT3 animal with bone marrow failure

Bone marrow and spleen tissues from a wildtype mouse and from a representative polyI/polyC-treated Cre+ N51-FLT3 animal that died of bone marrow failure were sectioned and stained with H&E, shown at 50X and 100X magnification.

Loss of Shp2 increases the latency to and reduces the severity of malignancy in

animals transplanted with N51-FLT3-transduced cells

Although there was not a statistically significant difference in the overall survival

of PBS-treated Cre+ N51-FLT3 treated animals vs. polyI/polyC-treated Cre+ N51-FLT3

animals, we were interested to determine if genetic disruption of Shp2 was able to

decrease the severity of or increase the latency to death specifically caused by

malignancy. Therefore, we consulted with Dr. George Sandusky, to review the

histopathology of animals at the time of death. For animals succumbing to malignancy,

we found MPD (Figure 4.17*i* and *ii*), lymphoproliferative disorder (Figure 4.17*iii*), as

well as a mixed myelo- and lymphoproliferative disorder (not shown). Although several

of the polyI/polyC-treated Cre+ N51-FLT3 animals did eventually develop leukemic

disease, the average spleen weight of animals that died of confirmed leukemia were

significantly smaller in the polyI/polyC-treated Cre+ N51-FLT3 group than the PBS-

treated Cre+ N51-FLT3 group (Figure 4.18A), implying a less severe and more indolent

disease. Futhermore, when evaluating survival in animals who specifically succumbed to

malignancy, the Kaplan Meier survival curve for malignancy-specific survival of PBS-

treated Cre+ N51-FLT3 animals vs. polyI/polyC-treated Cre+ N51-FLT3 animals

demonstrated a significantly prolonged survival in the polyI/polyC-treated Cre+ N51-

FLT3 animals compared to the PBS-treated Cre+ N51-FLT3 animals (Figure 4.18B).

These data suggest that in our *in vivo* model of N51-FLT3-induced MPD, the absence of

Shp2 results in an increased latency to and decreased severity of malignant disease.
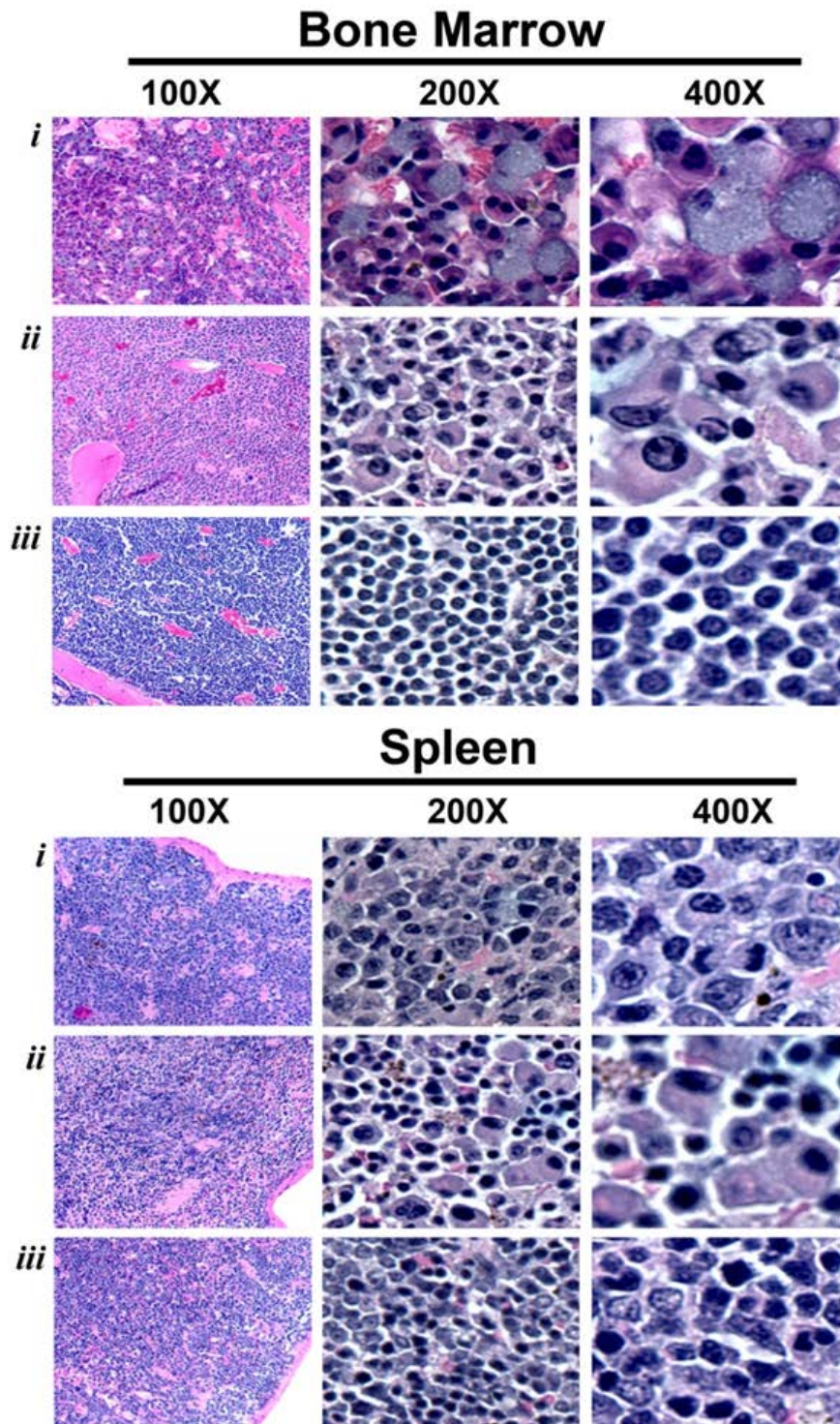
Figure 4.17: H&E staining of a representative N51-FLT3-induced hematologic malignancies

Bone marrow and spleen sections from animals that died of myeloproliferative disease (*i* and *ii*) or lymphoproliferative disease (*iii*) were sectioned and stained with H&E, shown at 100X, 200X, and 400X magnification.
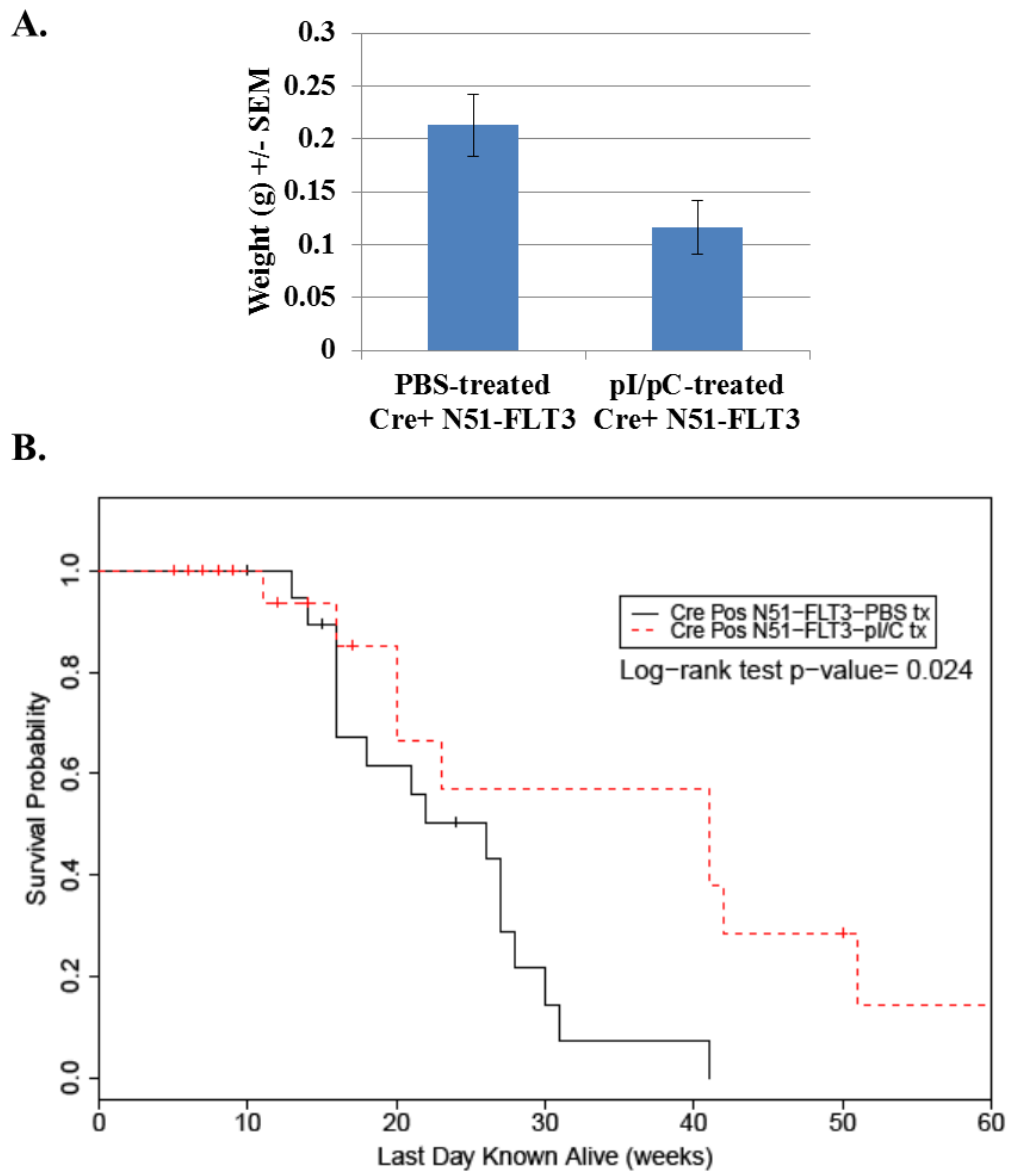
Figure 4.18: Malignancy-specific survival of PBS-treated Cre+ N51-FLT3 vs pI/pC-treated Cre+ N51-FLT3 transplanted animals

(A) Average spleen sizes of PBS-treated N51-FLT3, Shp2$^{flox/flox}$;Mx1-Cre+ animals (n = 16) compared to polyI/polyC-treated N51-FLT3, Shp2$^{flox/flox}$;Mx1-Cre+ animals (n = 10) that succumbed to malignancy, $p<0.05$, statistics performed using unpaired, two-tailed student's *t* test. (B) Kaplan-Meier analysis of malignancy specific survival of mice transplanted with N51-FLT3-transduced Shp2$^{flox/flox}$;Mx1Cre+ cells comparing PBS-treated mice (control) to polyI:polyC-treated mice (genetic deletion of Shp2), n=16 in the PBS group and n=10 in the polyI;polyC group, $p=0.024$ by log-rank test.

98

Loss of Shp2 reduces the long term hematopoietic stem cell repopulating activity of

N51-FLT3-transduced bone marrow cells

Since we experienced a high proportion of polyI/polyC-treated Cre+ N51-FLT3

animals that died from bone marrow failure, we examined the chimerism and EGFP+

populations in the animals in the PBS-treated vs. the polyI/polyC-treated animals

transplanted with N51-FLT3-transduced Shp2$^{flox/flox}$;Mx1Cre+ cells. Comparing the

average percentages of polyI/polyC-treated N51-FLT3-Cre+ cells to PBS-treated N51-

FLT3-Cre+ cells over time, there was a general decrease in the chimerism (percent donor

cells) post-treatment in the polyI/polyC-treated N51-FLT3-Cre+ animals from 52.7%

before polyI/polyC injection to 25.9% (10-13 weeks), to 19.8% (17-20 weeks) (Figures

4.19A and 4.19B). The chimerism of PBS-treated N51-FLT3-Cre+ animals however

remained relatively constant around 40-45% donor cells over the same time frame. We

noticed significant variation in the PBS-treated animals, likely due to breakthrough Cre

expression in some animals; therefore we present the data in bar graph form (Figure

4.19A) as well as in scatter plots to demonstrate this variability (Figure 4.19B).

Examining the EGFP percentages over time, again there was a significant decrease in the

percent EGFP+ cells after polyI/polyC treatment of the N51-FLT3-Cre+ transplanted

animals (Figures 4.20A and 4.20B) from 21.3% EGFP+ at baseline (before polyI/polyC

treatment), to a mere 2.4% (10-13 weeks), to 1.9% EGFP+ (17-20 weeks). Similar to the

chimerism, the EGFP expression of PBS-treated N51-FLT3-Cre+ animals remains

relatively constant at approximately 20% after PBS treatment with a slight dip in EGFP

expression between weeks 10-13 (11.7%). Again to demonstrate the variability between

the PBS-treated animals the data is presented in bar graphs (Figure 4.20A) and in scatter

plots (Figure 4.20B). These data suggest that after Shp2 is knocked out in the bone marrow of the polyI/polyC-treated N51-FLT3-Cre+ transplanted animals, the transplanted cells have a significantly reduced capacity to repopulate the recipient host. Furthermore, while chimerism is significantly lower, the EGFP expression is reduced to even lower percentages, suggesting that the remaining CD45.2+ donor cells have silenced N51-FLT3.
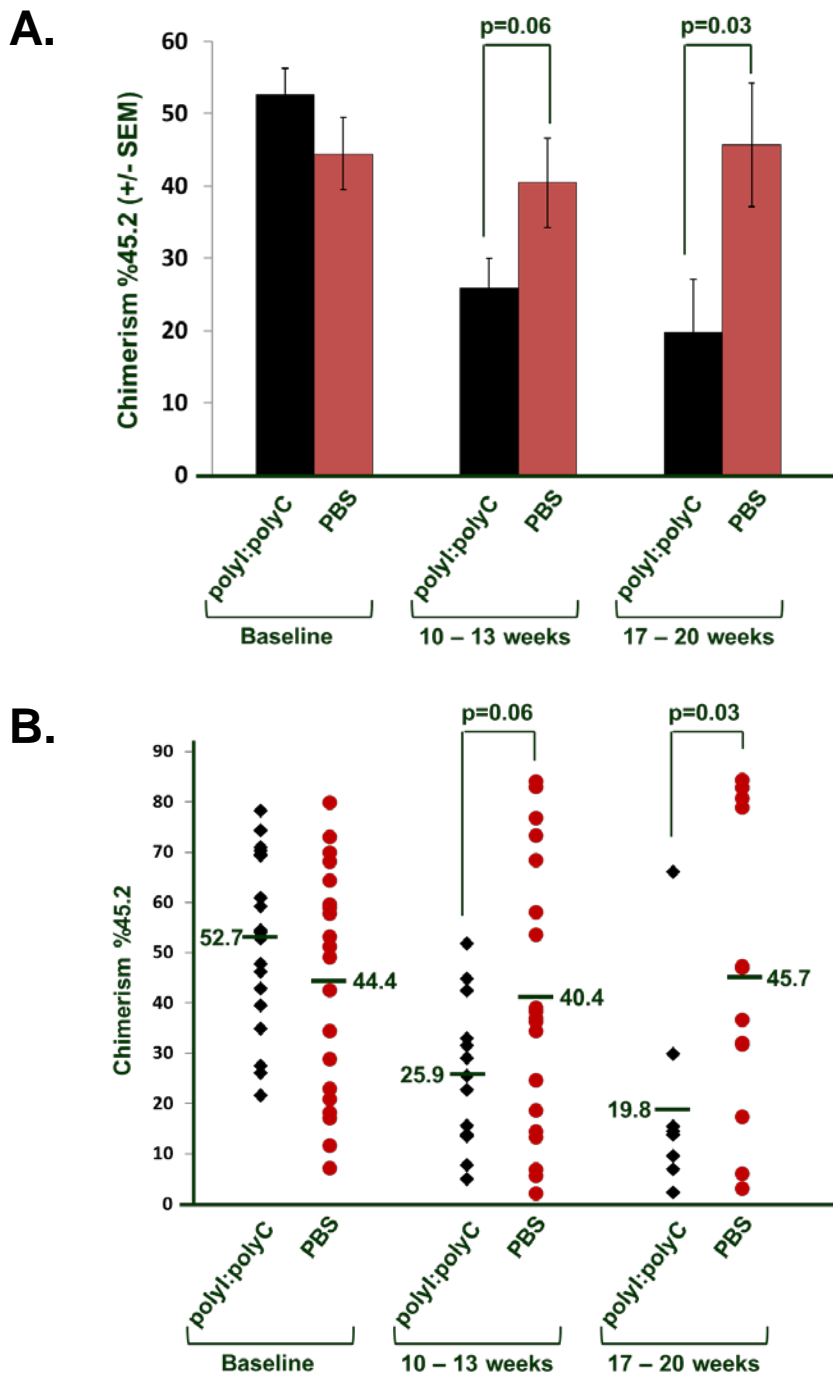
Figure 4.19: Chimerism of polyI/polyC-treated vs. PBS-treated N51-FLT3, Shp2$^{flox/flox}$;Mx1-Cre+ transplants

(A) Chimerism (percent CD45.2+) shown as a bar graph displayed as the average chimerism at baseline (4 weeks post-transplant prior to polyI/polyC treatment), 10-13, and 17-20 weeks post-transplant +/- the standard error of the mean. **(B)** Chimerism (percent CD45.2+) shown as a scatter plot with the average at baseline (4 weeks post-transplant prior to polyI/polyC treatment), 10-13, and 17-20 weeks post-transplant. Statistics generated using unpaired, two-tailed, student's *t* test.
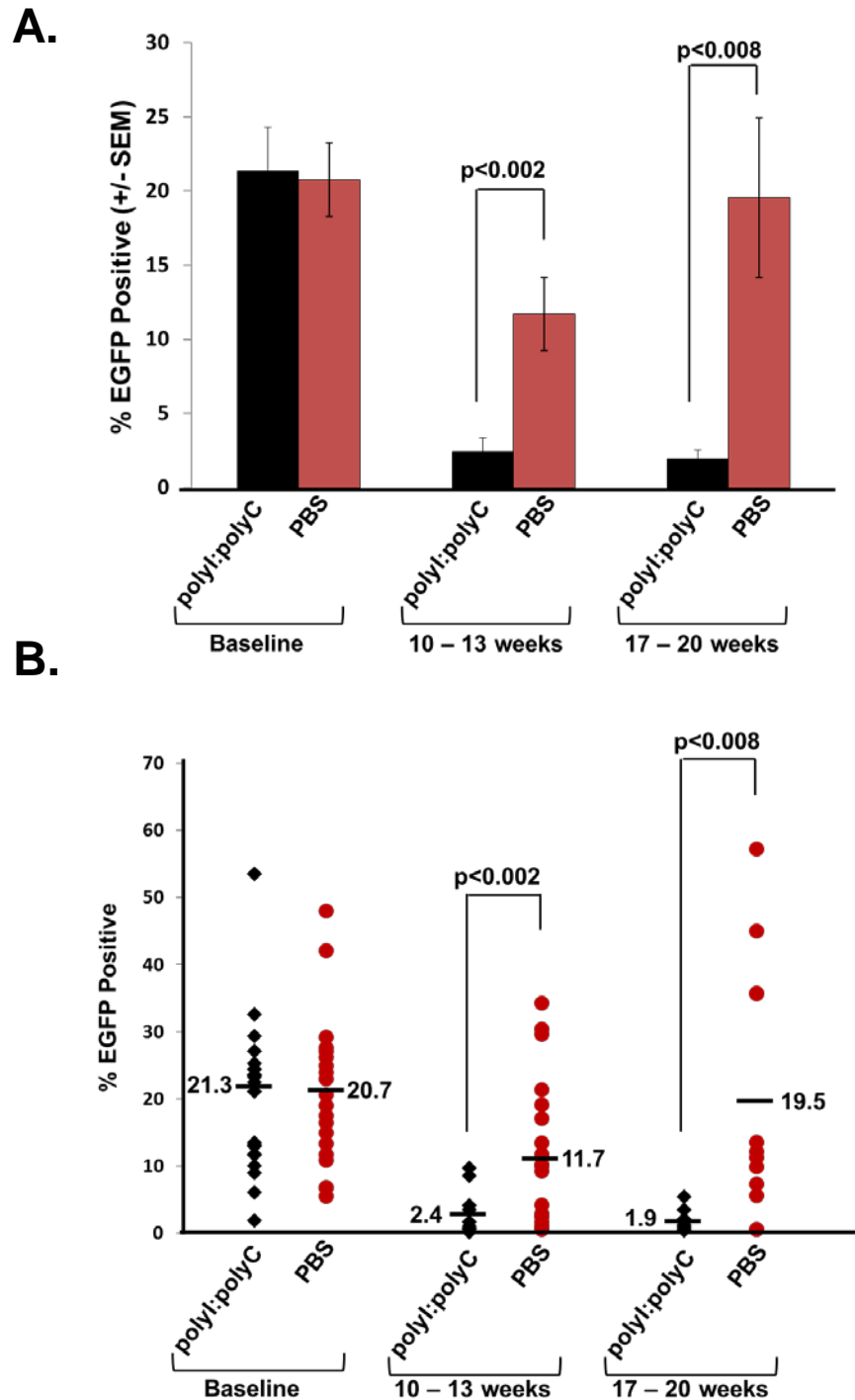
Figure 4.20: EGFP levels of polyI/polyC-treated vs. PBS-treated N51-FLT3, Shp2$^{flox/flox}$Mx1-Cre+ transplants

(A) EGFP+ shown as a bar graph displayed as the average at baseline (4 weeks post-transplant prior to polyI/polyC treatment), 10-13, and 17-20 weeks post-transplant +/- the standard error of the mean. **(B)** EGFP+ shown as a scatter plot with the average at baseline (4 weeks post-transplant prior to polyI/polyC treatment), 10-13, and 17-20 weeks post-transplant. Statistics generated using unpaired, two-tailed, student's *t* test.

In addition to percent chimerism and percent EGFP, we have also used the percent chimerism to calculate the hematopoietic stem cell (HSC) repopulating units (RU). This is important because when we transplant mixtures of cells, it can be difficult to interpret differences in raw percentages. Converting the data into repopulating allows us to calculate the actual differences in the numbers of long term engrafted stem cells in the recipient animals. Repopulating units are calculated by dividing the percent donor cells by 100 minus percent donor cells and multiplying by the number of competitors X 10^5. The formula is shown below:

$$RU = \frac{Competitors\ (1 \times 10^5)\ X\ \%\ donor}{100 - \%donor}$$

An example: $$RU = \frac{1.5\ (we\ used\ 1.5 \times 105\ splenocytes)\ X\ 45\%}{55\%}$$

$$RU = 1.23$$

Repopulating units calculated from mice 4-6 months after transplant represent the long-term hematopoietic stem cells (HSCs). The repopulating units of polyI/polyC-treated N51-FLT3-Cre+ transplanted animals was 1.5 prior to polyI/polyC treatment and decreased significantly to 0.4 by the 10-13 week time point as demonstrated in bar a bar graph (Figure 4.21A) and in a scatter plot to demonstrate animal-variability (Figure 4.21B). This reduction was maintained to the 17-20 week time point, also having 0.4 repopulating units. On the contrary, the repopulating units of PBS-treated N51-FLT3-Cre+ transplanted animals started at 1.2 and increased significantly to 2.1 by the 17-20 week time point. There is a statistically significant difference at the latest time point (17-20 weeks) which represents a higher stem cell function in the PBS-treated N51-FLT3-
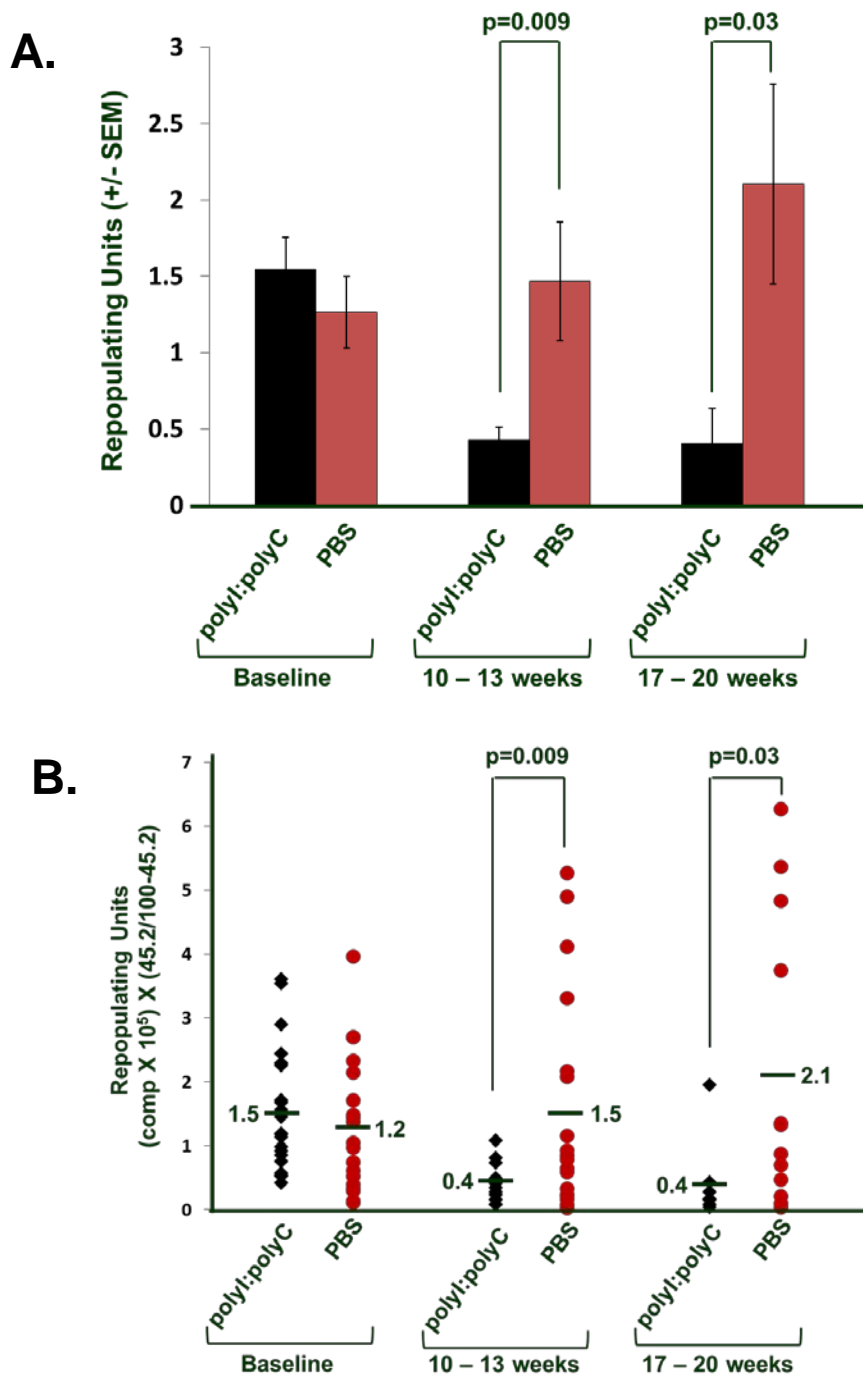
Figure 4.21: Average repopulating units of N51-FLT3, Shp2$^{flox/flox}$Mx1-Cre+ animals

(A) Repopulating units (RU) shown as a bar graph displayed as the average at baseline (4 weeks post-transplant prior to polyI/polyC treatment), 10-13, and 17-20 weeks post-transplant +/- the standard error of the mean. **(B)** Repopulating units (RU) shown as a scatter plot with the average at baseline (4 weeks post-transplant prior to polyI/polyC treatment), 10-13, and 17-20 weeks post-transplant. Statistics generated using unpaired, two-tailed, student's *t* test.

Cre+ transplanted animals than in the polyI/polyC-treated N51-FLT3-Cre+ transplanted animals.

Overall, these findings demonstrate that polyI/polyC-treatment to reduce Shp2 expression significantly decreases the chimerism, EGFP expression, and repopulating units, or stem cell function of N51-FLT3-Cre+ transplanted animals. Importantly, these findings indicate that even in the presence of N51-FLT3, Shp2 is required for stem cell function and sustained hematopoiesis. Furthermore, these data suggest that lack of Shp2 expression confers a functional defect to the ability of hematopoietic stem cells to repopulate the recipient host, even when expressing oncogenic N51-FLT3, and indicate that the increased latency to and attenuated severity of the malignancy in the polyI/polyC-treated animals is due to a reduced competitive advantage of the N51-FLT3 cells lacking Shp2 expression, leading to reduced repopulating activity and reduced establishment of malignancy.

N51-FLT3 transplants are more sensitive to loss of Shp2 than WT-FLT3 transplant recipient

Given that loss of Shp2 results in reduced HSC/hematopoietic progenitor function, and self-renewal (Chan, Johnson et al. 2003; Chan, Li et al. 2006; Chan, Cheung et al. 2011; Zhu, Ji et al. 2011), and given that expression of FLT3-ITD, or constitutive active STAT5 in CD34+ HSCs results in enhanced self-renewal (Schuringa, Chung et al. 2004; Chung, Morrone et al. 2005), we were surprised to observe the early and profound bone marrow failure in the polyI/polyC-treated mice transplanted with N51-FLT3-Cre+ transduced cells. This led us to hypothesize that the N51-FLT3-transduced cells were particularly sensitive to loss of Shp2 expression. To examine this hypothesis, we directly compared the repopulating ability of polyI/polyC-treated mice transplanted Shp2$^{flox/flox}$;Mx1Cre+ cells transduced with WT-FLT3 to that of N51-FLT3. We expected one of two outcomes. Either the loss of Shp2 would result in bone marrow failure-induced death equally between polyI/polyC-treated WT-FLT3, Shp2$^{flox/flox}$;Mx1Cre+ and polyI/polyC-treated N51-FLT3, Shp2$^{flox/flox}$;Mx1Cre+ transplanted animals or that polyI/polyC-treated WT-FLT3, Shp2$^{flox/flox}$;Mx1Cre+ transplanted animals would be less susceptible to the loss of Shp2, suggesting that N51-FLT3 is particularly sensitive to loss of Shp2.

We compared the overall survival of polyI/polyC-treated animals transplanted with WT-FLT3-transduced Shp2$^{flox/flox}$;Mx1Cre+ cells to polyI/polyC-treated animals transplanted with N51-FLT3-transduced Shp2$^{flox/flox}$;Mx1Cre+ cells (Figure 4.22). Generally, the polyI/polyC-treated Cre+ WT-FLT3 transplanted mice had an increased survival compared to the polyI/polyC-treated Cre+ N51-FLT3 animals. While there was

one early death (6 weeks post-treatment) in the polyI/polyC-treated Cre+ WT-FLT3

transplanted animals, this death was not due bone marrow failure or malignancy, as

determined by pathology. In contrast, in the polyI/polyC-treated Cre+ N51-FLT3

transplanted animals, the first two deaths (9 and 11 weeks post-treatment) were caused by

bone marrow failure, while other animals lived significantly longer but did eventually

succumb to malignancy. Although these are preliminary findings, our data suggest that

the N51-FLT3 transplanted animals are more dependent on Shp2 than their WT-FLT3

transplanted counterparts, implying that there is an inherent difference between WT-

FLT3 and N51-FLT3 and that N51-FLT3 requires certain levels or functions of Shp2 that

are not essential to WT-FLT3.
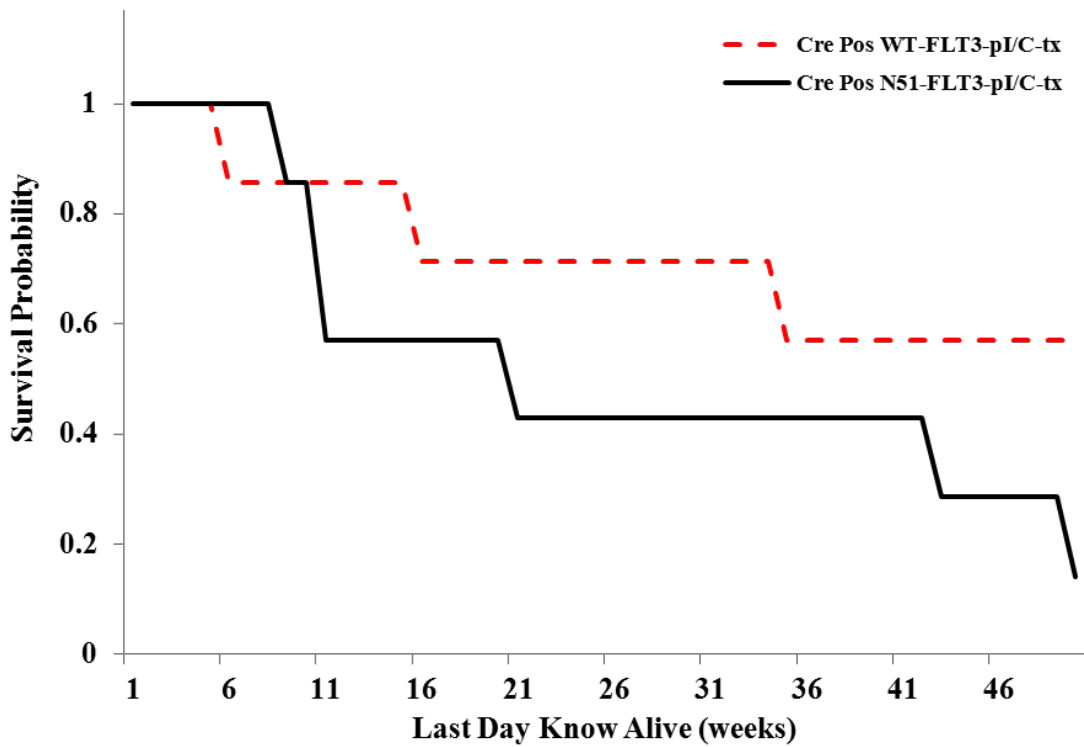
Figure 4.22: Overall survival of polyI/polyC-treated animals transplanted with WT-FLT3- vs. N51-FLT3-transduced Shp2$^{flox/flox}$;Mx1Cre+ cells

Kaplan-Meier analysis of polyI/polyC-treated animals transplanted with WT-FLT3- vs. N51-FLT3-transduced Shp2$^{flox/flox}$;Mx1-Cre+ cells; n = 7 in each group.

To investigate the potential differences between the HSC compartments in polyI/polyC-treated animals transplanted with WT-FLT3- vs. N51-FLT3-transduced Shp2$^{flox/flox}$;Mx1Cre+ cells we next examined average EGFP+ populations, average chimerism, and average repopulating units as shown in Figures 4.23, 4.24, and 4.25, respectively. Interestingly, at baseline, EGFP expression was stronger in the N51-FLT3-transplanted animals compared to the WT-FLT3-transplanted animals. While EGFP populations decreased over time in both polyI/polyC-treated Cre+ WT-FLT3 transplanted animals as well as in polyI/polyC-treated Cre+ N51-FLT3 transplanted animals, the reduction from baseline in the N51-FLT3-transplanted animals was more substantial than in the WT-FLT3-transplanted animals and dropped to nearly zero by 24 weeks post-treatment (Figure 4.23).
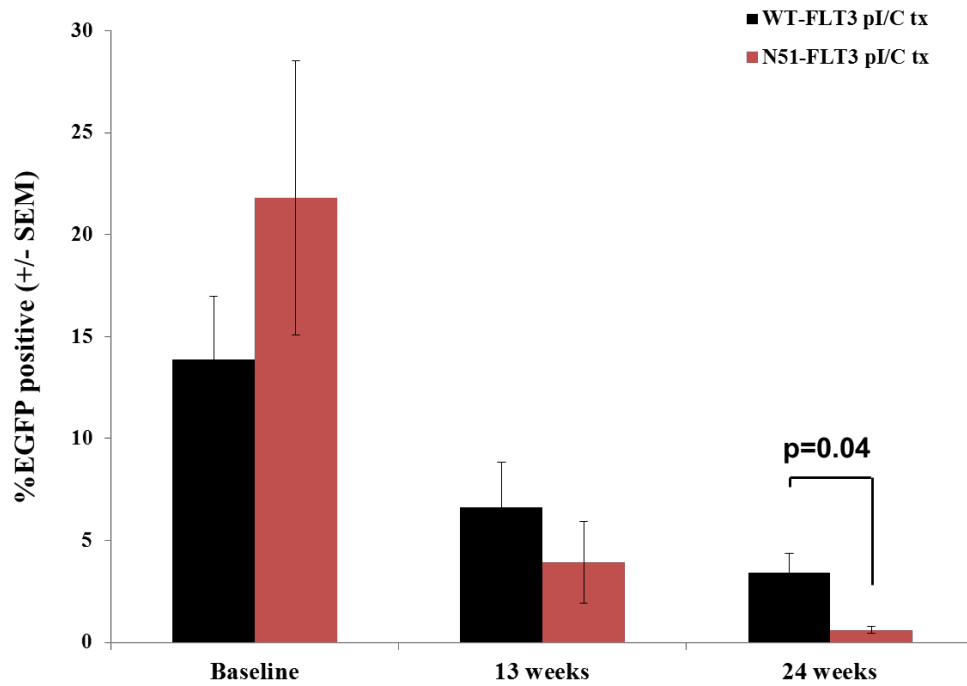
Figure 4.23: Percent EGFP positive populations of polyI/polyC-treated WT-FLT3 vs. polyI/polyC-treated N51-FLT3 transplant recipients

Percent EGFP+ populations are shown as the average at each time point, baseline (4 weeks post-transplant; right before polyI/polyC treatment), 13 weeks, and 24 weeks post-transplant. n = 7 in each group, statistics performed using unpaired, two-tailed student's *t* test.

Comparing the chimerism of the two groups, the average chimerism of polyI/polyC-treated Cre+ WT-FLT3 transplanted animals displayed a minor decrease after polyI/polyC treatment (between baseline and 13 weeks), but then remained constant to the 24 week time point (Figure 4.24). The chimerism of polyI/polyC-treated Cre+ N51-FLT3 transplanted animals, however, decreased sharply after polyI/polyC-treatment (between baseline and 13 weeks) and chimerism continued to decrease to significantly lower levels than the polyI/polyC-treated Cre+ WT-FLT3 transplanted animals by 24 weeks post-transplant (Figure 4.24).

We next converted chimerism to repopulating units (RU) and observed a trend toward increased RU in the N51-FLT3-transplanted animals at baseline compared to the WT-FLT3-transplanted animals. However, similar to that observed with EGFP expression, the RU of the N51-FLT3-transplanted animals dropped drastically after polyI/polyC-treatment (baseline to 13 weeks) and continued to drop to significantly lower levels than the WT-FLT3-transplanted animals by 24 weeks post-treatment (Figure 4.25).

Again, although this is a preliminary study with few animals, these data support our second hypothesis that there is an inherent difference between WT-FLT3 and N51-FLT3 transplant recipients in the absence of Shp2. WT-FLT3 transplants have a greater capacity to tolerate the loss of Shp2, whereas N51-FLT3 recipient animals depend on Shp2 to a greater extent, which is evident by the significant difference in survival, percent EGFP+, percent chimerism, and repopulating units when Shp2 is knocked out of the bone marrow of animals transplanted with N51-FLT3 compared to animals transplanted with WT-FLT3. Overall, this suggests that while Shp2 is inherently important for normal

hematopoiesis and engraftment, in the presence of oncogenic N51-FLT3, Shp2 is even more important for stem cell function and hematopoiesis.
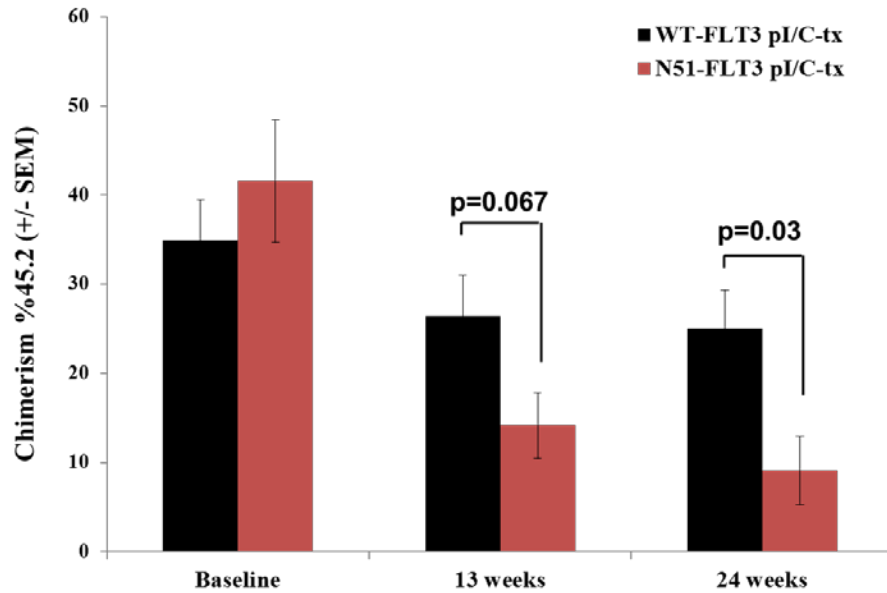
Figure 4.24: Chimerism of polyI/polyC-treated WT-FLT3 vs. polyI/polyC-treated N51-FLT3 transplant recipients

Chimerism (%CD45.2 positive populations) is shown as the average at each time point, baseline (4 weeks post-transplant, before polyI/polyC treatment), 13 weeks, and 24 weeks post-transplant. n = 7 in each group; statistics performed using unpaired, two-tailed student's t test.
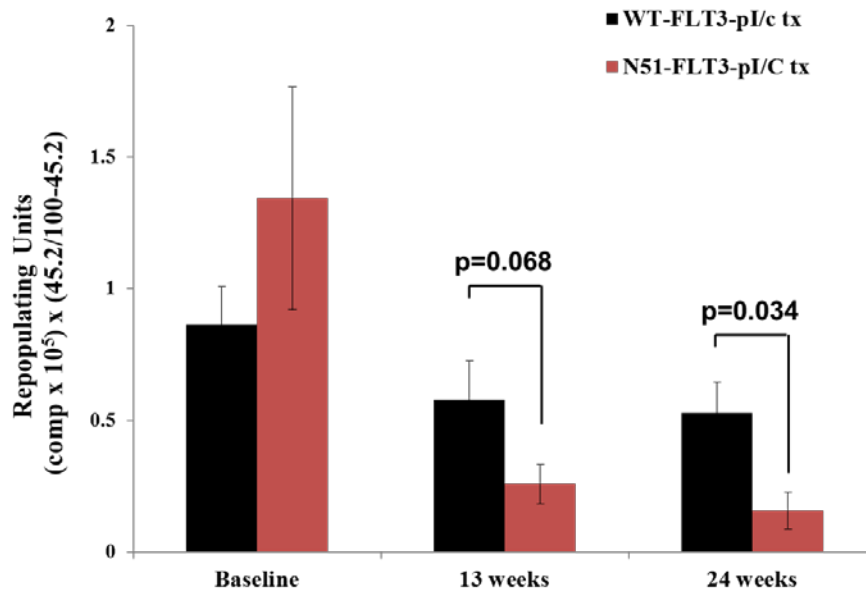
Figure 4.25: Repopulating units of polyI/polyC-treated WT-FLT3 vs. polyI/polyC-treated N51-FLT3 transplant recipients

Repopulating unites are calculated by the formula (competitors x 10^5) x (%45.2/[100-%45.2]) and are represented as the average at each time point; baseline (4 weeks post-transplant, before polyI/polyC treatment), 13 weeks, and 24 weeks post-transplant. n = 7 in each group, statistics performed using unpaired, two-tailed student's t test.

Conclusions

Internal tandem duplication mutations within FLT3 have been a popular focus of AML researchers over the past several years; however, the molecular mechanisms of FLT3-ITDs are still unclear. Our previous data demonstrate that in FLT3-ITD signaling there is constitutive association of Shp2 to the mutant FLT3-ITD receptor. We have further demonstrated that genetic disruption of Shp2 *in vitro* results in reduced N51-FLT3-induced cellular hyperproliferation and hyperactivation of STAT5, supporting the data presented in chapter 3 using Baf3 cell lines expressing WT-FLT3, N51-FLT3, or N73-FLT3 and shRNAs targeted to Shp2.

All of this *in vitro* data established and validated the rationale for proceeding into the Shp2 knock-out mouse model. Our two main conclusions from these *in vivo* studies are the following. First, without Shp2 expression, N51-FLT3-transduced cells induce malignancy *in vivo* with an increased latency and reduced severity compared to N51-FLT3-transduced cells expressing wildtype levels of Shp2. Second, preliminary studies suggested that N51-FLT3-transduced cells are more dependent on Shp2 for engraftment and stem cell function than WT-FLT3-transduced cells. These findings suggest that cells expressing FLT3-ITD are particularly dependent on Shp2 at the stem cell level, which is relevant since AML is a clonal disease of aberrant hematopoietic stem cells. However, even though the polyI/polyC-treated Cre+ N51-FLT3 transplanted animals had an increase in disease latency, they did eventually succumb to malignancy. While targeting Shp2 may be beneficial in treating FLT3-ITD-positive AML patients, it will likely not be sufficient to cure them of disease. Inhibition of Shp2 however, could be used in combination therapy as one target in a cocktail of drugs. It would be interesting to

combine Shp2 inhibition with some of the FLT3 inhibitors, which also are insufficient to cure FLT3-ITD-positive AML as a monotherapy.

The Shp2$^{flox/flox}$;Mx1Cre mouse model is quite challenging to work with because once Shp2 is knocked out, the knock out cells are difficult to culture long term. In our experience, we have transduced them, sorted them, and then used them in experiments short term, but we must always be very conscious of the Shp2 levels when we are taking our final reading for each individual experiment. As an alternative approach, it would be interesting to cross the Shp2$^{flox/flox}$ animals to a Vav-Cre transgenic mouse model (Georgiades, Ogilvy et al. 2002). Vav-Cre is expressed in most hematopoietic cells of all hematopoietic organs (Georgiades, Ogilvy et al. 2002). Since the Vav promoter is not conditionally inducible, when it is endogenously activated, cre recombinase expression will result in recombination of the Shp2 gene and turn "off" its expression. This model may be useful to maintain Shp2 "knocked out" in bone marrow cells; however, since the Vav promoter is activated fairly early in development, it is also possible that the Shp2$^{flox/flox}$;VavCre animals may die *in utero*, as constitutional Shp2 knock out is embryonic lethal. However, if the animals did mature to birth, or even to gestational day 14.5 when fetal liver cells could be obtained, it may provide a complementary model to study the role of Shp2 in the presence of N51-FLT3 in an *in vitro* system. Another possible experimental idea is to use the FLT3-ITD knock-in mouse model (now available from Jackson Laboratories) originally developed in Dr. Gary Gilliland's lab (Lee, Tothova et al. 2007). It would be interesting to cross the Shp2$^{flox/flox}$ mouse with the FLT3-ITD knock-in model to use as another mouse model to test the role of Shp2 on

FLT3-ITD-induced MPD by using the bone marrow cells *in vitro* or the animal models *in vivo*.

While our findings suggest that Shp2 is necessary for engraftment and stem cell function, we still have several *in vivo* options to consider. Due to the high percentage of polyI/polyC-treated Cre+ N51-FLT3 transplanted animals that succumb to bone marrow failure, we have considered a few alternative approaches. First, we could use bone marrow LDMNCs as supporting cells, as opposed to the splenocytes we have used in the past. This experimental modification may be sufficient to supplement the bone marrow just enough to prevent bone marrow-induced death upon the deletion of Shp2 in the presence of N51-FLT3. Another possibility is to use heterozygous $Shp2^{flox/+}$;Mx1Cre+ animals as donor animals. Therefore, after transduction of N51-FLT3, transplantation into lethally irradiated recipients, and treatment with polyI/polyC, recipient animals will only lose 50% of Shp2 in the N51-FL3-transduced cells. We would hypothesize that this partial loss of Shp2 would be insufficient to cause bone marrow failure and death, yet sufficient to increase the latency to N51-FLT3-induced malignancy which would support further investigation of targeting Shp2 as one therapeutic option for FLT3-ITD-positive AML patients.

CHAPTER FIVE

PROTEIN TYROSINE PHOSPHATASE, SHP2, INHIBITOR, II-B08;

A POTENTIAL THERAPEUTIC OF FLT3-ITD-POSITIVE AML

Introduction

Current therapies for treating FLT3-ITD-poisitve AML focus on high dose
chemotherapy. However, these regimes are too harsh for the majority of AML patients.
Those AML patients who are able to sustain such treatments still only have an
approximate long term survival rate of 20%. These poor survival rates offer a vast
opportunity to identify specific molecular targets in an effort to develop better therapies
for the treatment of AML.

We presented solid functional evidence demonstrating that Shp2 contributes to the
cellular hyperproliferation and hyperactivation of STAT5 in FLT3-ITD-expressing cell
lines and murine primary cells. Therefore, we were next interested in identifying a
specific and efficacious Shp2 inhibitor. Genetic approaches are highly informative for
targeting specific genes and their respective proteins, and for understanding molecular
mechanisms. However, identifying a pharmacologic Shp2 inhibitor is a key step in
actually treating FLT3-ITD-positive AML patients. Fortunately, we were able to
collaborate with tyrosine phosphatase biochemist, Dr. Zhong-Yin Zhang at the Indiana
University School of Medicine. He and his lab identified a novel, salicylic acid-based
small molecule inhibitor which is both selective and potent in targeting the phosphatase
domain of Shp2 called Compound 9 or II-B08 (Zhang, He et al.). Through this
collaboration, we were able to use II-B08 to determine its effect on FLT3-ITD-positive
primary cells *in vitro.* We hypothesized that treating N51-FLT3-expressing primary

117

murine bone marrow cells with II-B08 would result in reduced hyperproliferation and hyperactivation of STAT5 compared to DMSO vehicle treatment.
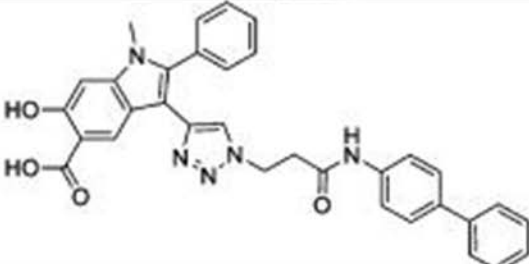
In addition to *in vitro* assays, we also tested II-B08 *in vivo* by taking advantage of a syngeneic transplant system. 32D cells are an IL-3-dependent, murine cell line derived fromC3h/HeJ mice which can be syngeneicly transplanted into C3h/HeJ recipient mice without the complications of irradiation. Therefore, C3h/HeJ recipient mice were transplanted with N51-FLT3-expressing 32D cells in order to create a leukemic mouse model which could be subsequently treated with Shp2 inhibitor, II-B08, in order to evaluate its therapeutic potential. We hypothesized that treating N51-FLT3-syngeneic transplant recipient animals with II-B08 would reduce N51-FLT3-induced elevated white blood cell counts, reduce N51-FLT3 (GFP) expression, and potentially improve the survival of these animals when compared N51-FLT3 syngeneic transplants treated with DMSO.

Results

Identification of Shp2 inhibitor, II-B08

As identified in the publication, the chemical structure of II-B08 is shown in Figure 5.1A. II-B08 is highly potent and selective for Shp2 with an IC_{50} value of 5.5 µM. In addition to its chemical structure, the ribbon structure is shown in Figure 5.1B, which demonstrates the orientation of II-B08 into the phosphatase domain of Shp2. Compared to similar phosphatases, including, SHP1, PTP1B, and HePTP, II-B08 had an approximate 3-fold or better IC_{50} value as shown in Table 5.1 (adapted from (Zhang, He et al.)). During our collaboration with Dr. Zhong-Yin Zhang, we also demonstrated that increasing concentrations of II-B08 resulted in decreased Erk activation and decreased

thymidine incorporation of cells expressing Shp2 gain-of-function mutations (Figures 4

and 5 from (Zhang, He et al.) in which I am a co-author). Using II-B08, we are also able

to pharmacologically interrogate the contribution of Shp2 in FLT3-ITD-expressing cells.
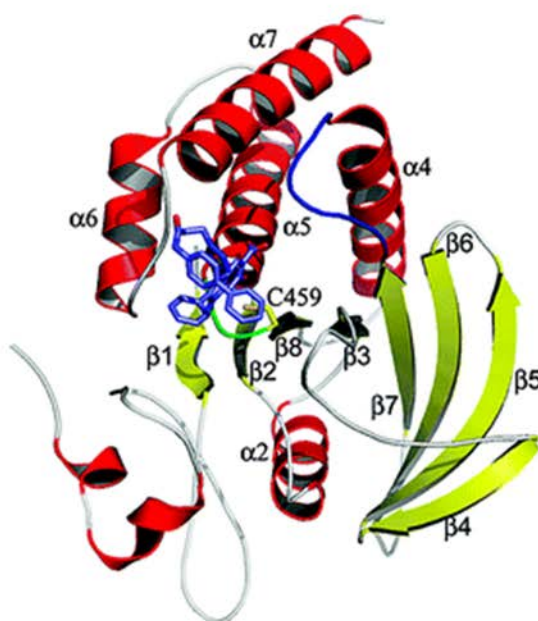
Figure 5.1: The Shp2 inhibitor, II-B08

(A) Chemical structure of II-B08 (Compound 9). **(B)** Ribbon diagram of Shp2 catalytic domain in complex II-B08. The molecule is oriented with the C-terminal end of the β_8 strand toward the viewer. α-Helices and β-strands are colored in red and yellow, respectively. The P-loop is shown in green and the WPD loop in blue. II-B08 is shown in stick-and-bond mode. Figure adapted from (Zhang, He et al.).

PTP	$IC_{50}(\mu M)$
SHP2	5.5 ± 0.4
SHP1	15.7 ± 2.1
PTP1B	14.3 ± 1.5
HePTP	>50
Lyp	25.0 ± 3.6
FAP1	20.3 ± 1.3
CD45	30.0 ± 6
LAR	>50
PTPα	>50
VHR	>50
Cdc14A	>50
LMWPTP	31.1 ± 1.9

[a]All measurements were made using *p*NPP as a substrate at pH 7.0, 25°C, and *I* = 0.15M.

Table 5.1: Selectivity of II-B08 against a panel of protein tyrosine phosphatases (Adapted from (Zhang, He et al.))

Shp2 inhibitor, II-B08, significantly reduces FLT3-ITD-induced hyperproliferation

and activation of STAT5

We hypothesized that hyperproliferation induced by FLT3-ITDs would be significantly reduced by treatment with II-B08. Furthermore, based on our previous biochemical and genetic studies, we hypothesized that N51-FLT3-expressing cells would be more sensitive to Shp2 inhibition compared to WT-FLT3-expressing cells. Proliferation assays were performed using thymidine incorporation assays (previously described). EGFP-positive WT-FLT3- or N51-FLT3-expressing LDMNCs were starved for 4-5 hours and then plated into thymidine incorporation assays with increasing concentrations of II-B08. We observed a dose-dependent, but statistically insignificant decrease in the proliferation of WT-FLT3-expressing cells upon II-B08 treatment (Figure 5.2A). However, N51-FLT3-expressing LDMNCs exhibited a statistically significant, dose-dependent decrease in the hyperproliferation induced by N51-FLT3 with increasing concentrations of II-B08 (Figure 5.2A). This suggests that Shp2 inhibition has a greater effect on N51-FLT3-expressing cells than on WT-FLT3-expressing cells, which is very important in identifying a drug as a potential therapeutic.
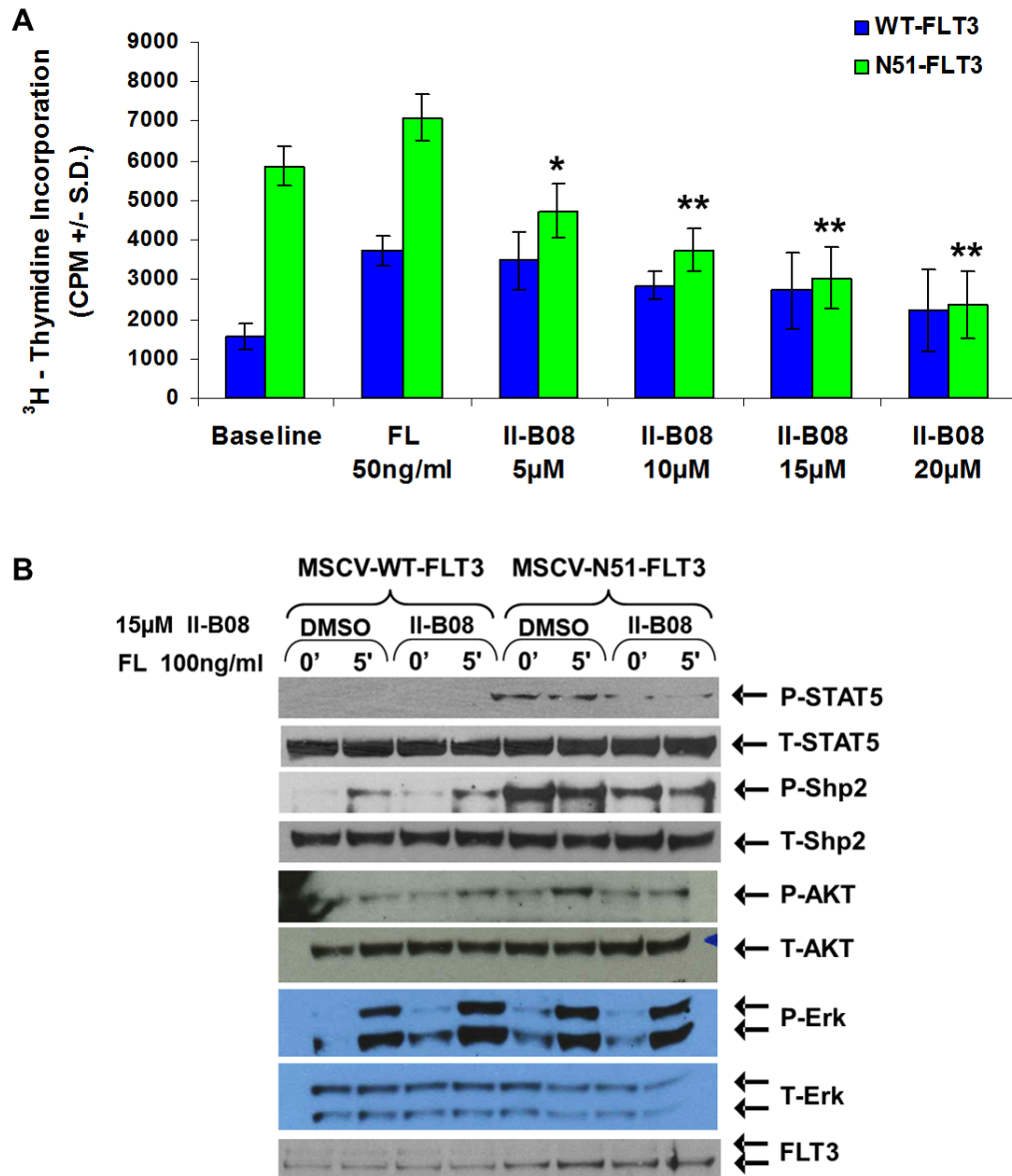
Figure 5.2: II-B08 treatment reduces cellular hyperproliferation induced by N51-FLT3

(A) Thymidine incorporation analysis of bone marrow LDMNCs transduced with either MSCV-WT-FLT3 or MSCV-N51-FLT3 in the absence or presence of increasing concentrations of II-B08; data is representative of two independent experiments combined with n = 4-6 replicates per experiment, *p=0.002 for N51-FLT3, 5µM II-B08 v. N51-FLT1, baseline, **p<0.0001 for N51-FLT3, 10µM, 15µM, and 20µM II-B08 v. N51-FLT3, baseline (unpaired, two-tailed t-test). **(B)** Immunoblot analysis of cells transduced with WT-FLT3 or N51-FLT3 and treated with or without 15µM II-B08 in the absence or presence of FL stimulation. Blots were probed for phospho- and total-STAT5, phospho- and total-Shp2, phospho- and total-AKT, phospho- and total-Erk, and FLT3 protein levels.

123

To investigate the effect of II-B08 on the activation of STAT5, we treated sorted, bone marrow LDMNCs transduced with WT-FLT3 or N51-FLT3 with or without 15µM II-B08, and collected total cell lysates at baseline or after 5 minute stimulation with100ng/ml FL. Total cell lysates were subjected to immunoblot analysis and probed for phospho- and total-STAT5, phospho- and total-Shp2, phospho- and total-AKT, phospho- and total-Erk, and FLT3 (Figure 5.2B). While we do not detect any activation of STAT5 in the WT-FLT3 expressing cells regardless of FL-stimulation or II-B08 treatment, there is a robust activation of STAT5 in the N51-FLT3-expressing cells at baseline and upon FL-stimulation. This activation is abrogated by at least 50% when N51-FLT3-expressing cells are treated with II-B08 (Figure 5.2B). The reduction in phospho-STAT5 in II-B08-treated, N51-FLT3 transduced cells is comparable to the reduction exhibited in phospho-Shp2 levels of II-B08 treated N51-FLT3 transduced cells (Figure 5.2B). Upon examination of AKT, we similarly observed a reduction in AKT activation in II-B08-treated N51-FLT3-expressing cells upon FL-stimulation. Surprisingly, Erk activation was unaffected by II-B08 at this 5 minute time point. Collectively, however, this data suggests that pharmacologic inhibition of Shp2 using II-B08 reduces cellular hyperproliferation, Shp2 hyperphosphorylation, and promiscuous activation of STAT5 induced by N51-FLT3.

II-B08 treatment reduces sustained Ras activation in N51-FT3-expressing cells

It has been well established that Shp2 activates Ras (Feng 1999); therefore we hypothesized that in the presence of FLT3-ITD mutants and a constitutive association of Shp2 to FLT3-ITD, there would subsequently be an increase in Ras activation. As we were surprised to see a lack of effect of II-B08 on phospho-Erk levels in the N51-FLT3-expressing cells, we directly examined FL-stimulated Ras activation in the presence of II-B08. Briefly, cells were starved in 0.2% BSA-IMDM for 4 hours and then treated with the indicated concentration of II-B08, or the maximum equivalent concentration of DMSO for 2 hours, with the indicated period of FL-stimulation (in the presence of II-B08). Cells were immediately lysed, protein extracts were quantified, and subjected to Ras activation assays. Ras was constitutively activated in the N51-FLT3-expressing cells compared to the WT-FLT3-expressing cells; however, upon 5 minutes of FL-stimulation, similar to that observed with Erk activation, there was no detectable change in Ras activation in N51-FLT3- or WT-FLT3-expressing cells (Figure 5.3A). As Shp2 has been shown previously to be critical for sustained activation of the Ras-Erk signaling cascade (Maroun, Naujokas et al. 2000; Shi, Yu et al. 2000), we next examined the effect of II-B08 on Ras-GTP levels following 60 minutes of FL stimulation (Figure 5.3B). Ras-GTP levels were reduced to nearly undetectable levels in the WT-FLT3-expressing cells following 60 minutes FL stimulation, while they remained elevated in the N51-FLT3 expressing cells. Treatment with II-B08 both at 10 and 20 μM significantly reduced FL-stimulated Ras-GTP levels in the N51-FLT3-expressing cells (Figure 5.3B). These findings indicate that reduced proliferation of the N51-FLT3-expressing cells by

treatment of II-B08 is mediated not only by reduced STAT5 activation but is also due to

reduced Shp2 phosphorylation, Akt activation, and Ras activation.
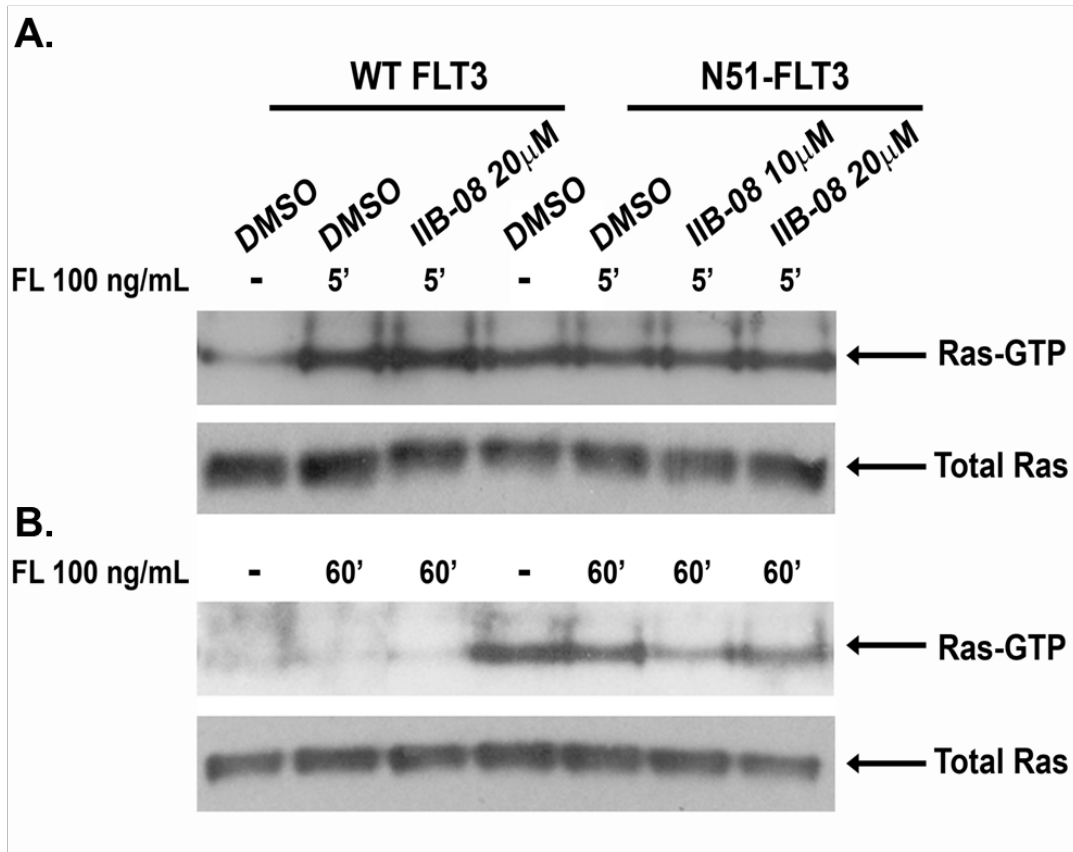
Figure 5.3: II-B08 treatment reduces sustained Ras activation in N51-FLT3-expressing cells

Ras activation assays with sorted, GFP+, WT-FLT3- or N51-FLT3-expressing LDMNCs. Cells were starved for 4 hours and then treated for 2 hours in the indicated concentration of II-B08, or DMSO vehicle with the last 5 (**A**) or 60 (**B**) minutes of 2-hour treatment in the presence of 100ng/ml FL. Treated cells were then lysed, subjected to Ras activation assays, and analyzed by immunoblot analysis. A small amount of total cell lysates were kept separate from the Ras activation assay and subjected directly to immunoblot with α-Ras as a control (**A and B**).

II-B08 treatment increases apoptosis in N51-FLT3-expressing cells

We have demonstrated that N51-FLT3 expressing cells treated with II-B08 have reduced hyperproliferation. We next examined how II-B08 treatment affected apoptosis of N51-FLT3-expressing cells. To address this question, sorted, GFP+, bone marrow LDMNCs transduced with either MSCV-WT-FLT3 or MSCV-N51-FLT3 were plated into 12-well non tissue culture plates in a total volume of 750µl of 2% FBS-IMDM or in the presence of DMSO, 5µM, 15µM, or 30µM II-B08 overnight at 37˚C. Cells were collected and stained with propidium iodide and Annexin-V-APC and subjected to flow cytometry analysis. Propidium iodide-single positive cells are necrotic, annexin-V-APC-single positive cells are considered early apoptotic and double positive cells are in a state of late apoptosis. Figure 5.4 represents the percent increase in apoptosis detected when the II-B08-treated samples were compared to the average apoptosis in DMSO treated cells. Upon treatment with low levels of II-B08, WT-FLT3 and N51-FLT3-expressing cells have a similar level of apoptosis (Figure 5.4). However, when cells are treated with 30 µM II-B08, there is a dramatic, statistically significant increase in the apoptosis of N51-FLT3-expressing cells compared to WT-FLT3-expressing cells (Figure 5.4). In fact as the concentration of II-B08 increases there is a statistically significant, dose dependent increase in the percent apoptotic cells in N51-FLT3-expressing cells which is not exhibited in WT-FLT3-expressing cells.
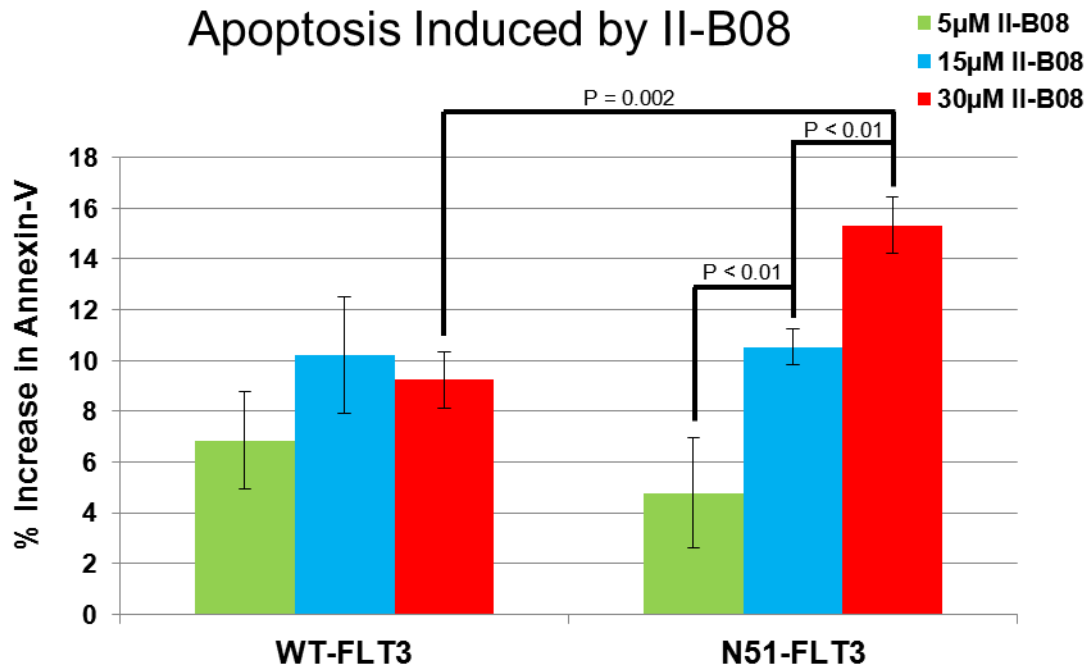
Figure 5.4: Apoptosis induced by II-B08

Annexin-V staining, measuring apoptosis of WT-FLT3 or N51-FLT3 transduced cells. Apoptosis is shown as percent increase in annexin-V staining when cells were treated with 5µM, 15µM, or 30µM II-B08 and compared to DMSO. n = 4. P = 0.002 for 5µM II-B08 WT-FLT3 v. N51-FLT3; P < 0.01 for 5µM II-B08 N51-FLT3 v. 15µM II-B08 N51-FLT3 and for 15µM II-B08 N51-FLT3 v. 30µM II-B08 N51-FLT3 as determined by unpaired, two-tailed, *t*-test.

This data demonstrates that N51-FLT3-expressing cells are more sensitive to the inhibition of Shp2 compared to WT-FLT3-expressing cells and this sensitivity is exhibited by a robust increase in the percent apoptotic cells in N51-FLT3-expressing cells treated with moderate amounts of II-B08. The increase in apoptosis in N51-FLT3 cells, but not in WT-FLT3 cells, supports the use of II-B08 in further investigation including *in vivo* models and as a potential therapeutic agent for FLT3-ITD-positive AML.

Syngeneic 32D-N51-FLT3 transplant recipients develop myeloproliferative disorder
(MPD) and can be used to test II-B08 in vivo

In vitro assays using inhibitors are valuable because they help researchers understand the molecular mechanisms of pharmacologic inhibition. However, in addition to the *in vitro* assays which have been described, we were interested in testing the effects of II-B08 *in vivo*. Therefore, we utilized a syngeneic leukemic mouse model and subsequently treated the animals with II-B08.

To create this mouse model, fellow graduate student, Charles Goodwin, and I collaborated to transduce nascent 32D cells with pMSCV-N51-FLT3-EGFP viral supernatant for two consecutive days. Cells were then sorted on EGFP expression and the EGFP+ cells expanded. After the cells had expanded sufficiently, EGFP expression was re-evaluated using flow cytometry demonstrating robust expression (96% EGFP positive, Figure 5.5). C3h/HeJ recipient animals were transplanted with 2×10^6 32D-N51-FLT3 cells via tail vein injection. Three weeks after transplantation, peripheral blood was collected via tail vein and assessed by complete blood counts (cbc) as well as percent GFP+ cells as shown in Figure 5.5. Animals demonstrated elevated EGFP expression were divided into two groups for treatment with either 100mg/kg of II-B08 or with an equivalent volume of 50% DMSO:PBS.
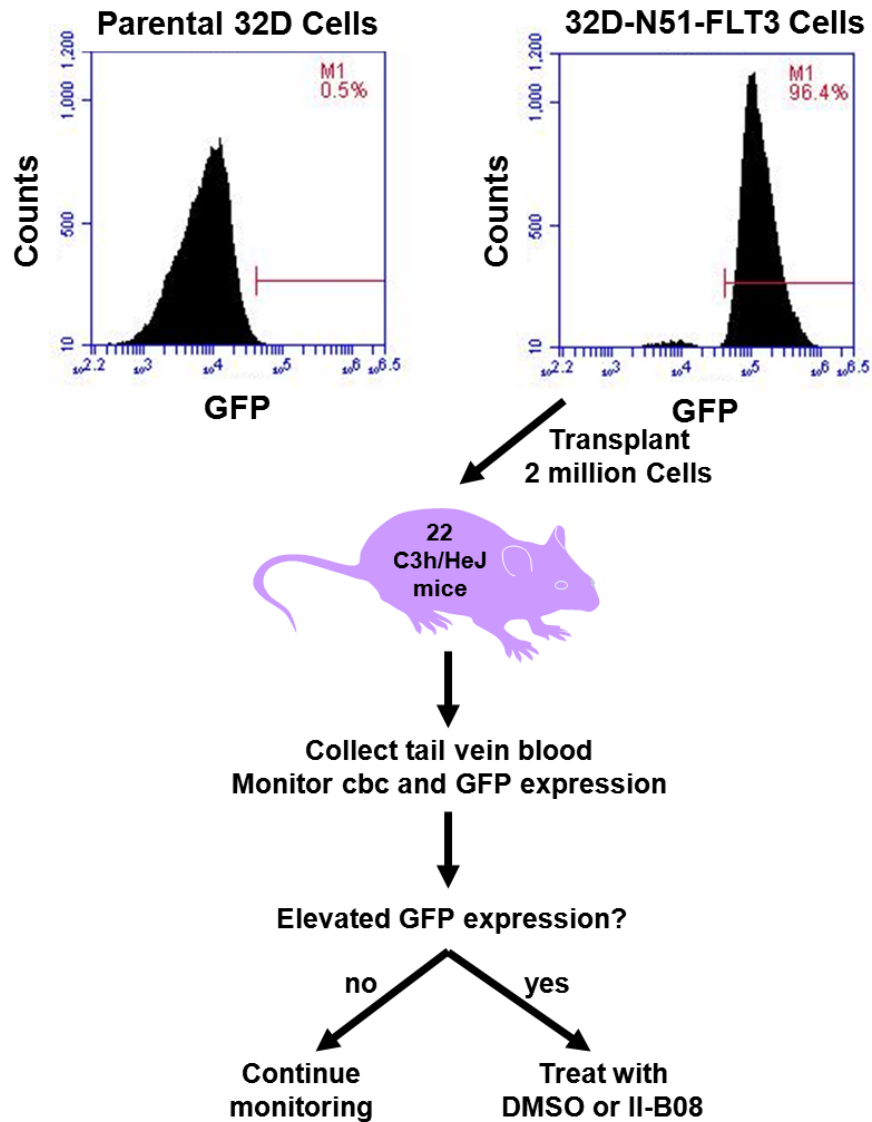
Figure 5.5: Schematic representation of syngeneic transplant

C3h/HeJ female recipients were transplanted with 2×10^6 32D-N51-FLT3 cells. Mice were monitored for white blood cell counts and EGFP expression by the collection of tail vein peripheral blood. When mice exhibited an elevated EGFP level, they were then treated either with 100mg/kg II-B08 or the equivalent volume of vehicle and monitored over time.

Transplantation of N51-FLT3-expressing cells into lethally irradiated recipients has previously been shown to develop lethal myeloproliferative disorder with an average latency of 40 to 50 days (Kelly, Liu et al. 2002). However in this syngeneic 32D-N51-FLT3 transplant system, recipients succumbed to myeloproliferative disorder in approximately half of the recipients, with an average latency of 3-5 weeks. The animals that developed MPD had rapidly increasing GFP percentages and white blood counts, with profound splenomegaly. Figure 5.6 displays an example of one of 32D-N51-FLT3 syngeneic recipient that succumbed to MPD. The percent EGFP increased rapidly between weeks 3 and 5 (Figure 5.6A). There was also marked splenomegaly displayed in the diseased animal (Figure 5.6B and 5.6C). The 1.48gm spleen weighed nearly 10 times the average weight of a WT spleen and measured over 3cm in length (Figure 5.6C). The development of MPD in these syngeneic 32D-N51-FLT3 transplant animals sets up the system as one which will be useful to test II-B08.

To test II-B08 *in vivo*, 22 C3h/HeJ animals were transplanted with 2×10^6 32D-N51-FLT3 cells as shown in Figure 5.5. Of these, 7 animals developed high EGFP levels and were subsequently randomized for treatment with either II-B08 or vehicle. Four animals were placed into the II-B08 treatment group and 3 in the DMSO group. They were each treated with daily intraperitoneal injections of either 100mg/kg II-B08 or the equivalent volume of 50% DMSO:PBS for up to 20 days. The combined survival data is shown by Kaplan Meier analysis (Figure 5.7). While most animals rapidly succumb to MPD regardless of treatment group, there was one II-B08-treated animal (N125) that demonstrated long-term survival (Figure 5.7).
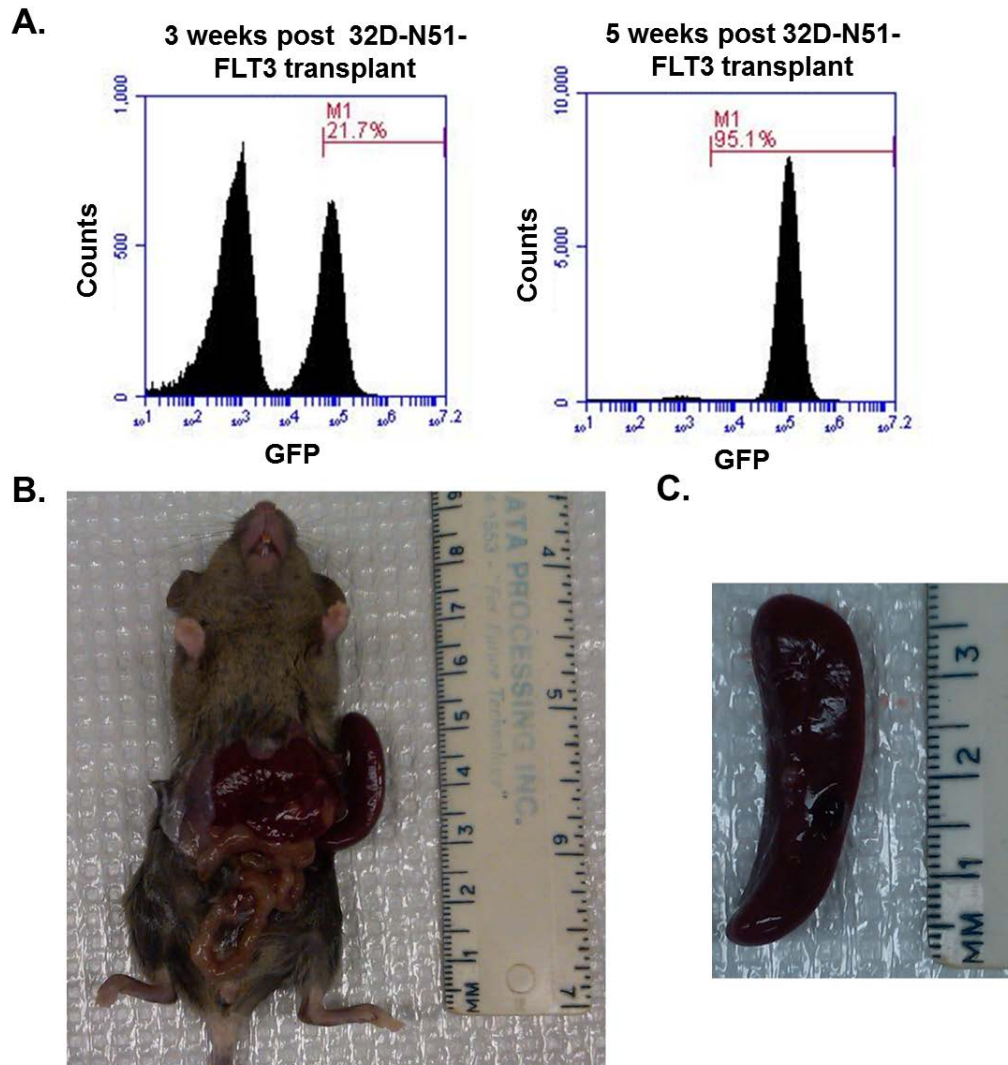
Figure 5.6: N51-FLT3 induces MPD in a syngeneic transplant model

(A) Representative 32D-N51-FLT3-transplanted animal displays EGFP expression of 21.7% and 95.1% at 3 and 5 weeks post-transplant, respectively. **(B)** Splenomegaly and hepatomegaly are apparent after the animal died. **(C)** Spleen is over 3 cm long.
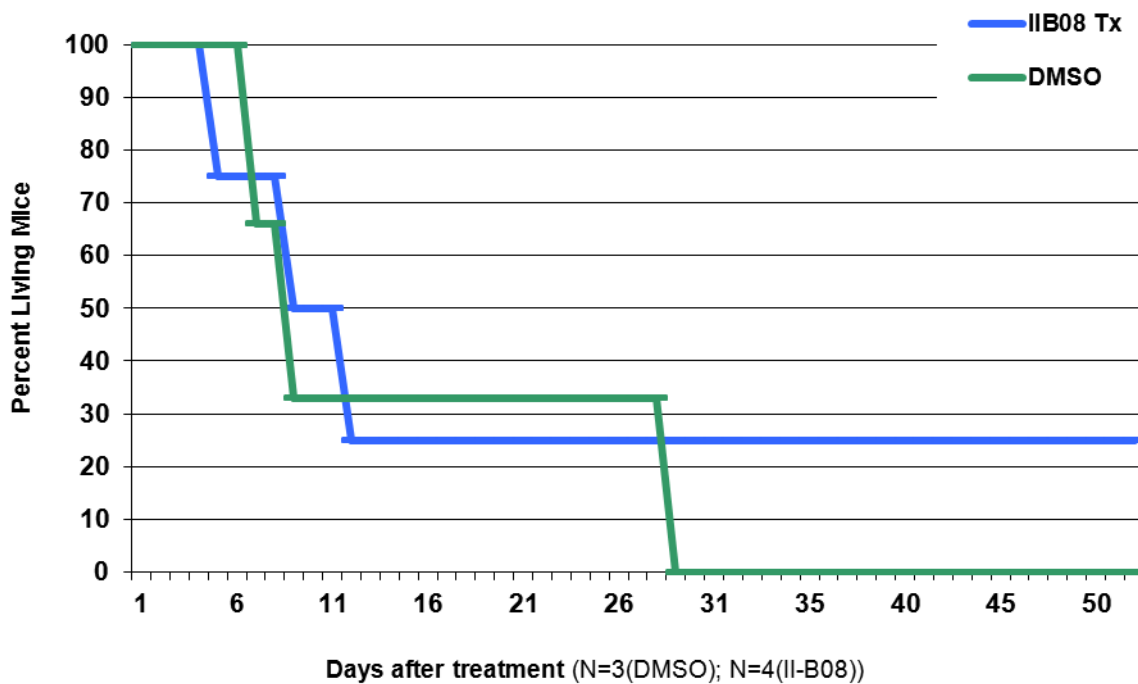
Figure 5.7: Overall survival of animals with established N51-FLT3-induced MPD treated with II-B08 or vehicle

Survival curve of animals treated with either 100mg/kg daily or the equivalent volume of 50% DMSO:PBS. Animals were started on the treatment when their peripheral blood draw displayed significant EGFP-positive expression (established disease).

Animal N125 demonstrated 15% positive EGFP at the initiation of II-B08

therapy, and demonstrated a marked reduction in EGFP expression after 1 week of

treatment with II-B08 (Figure 5.8A). N125 was treated with II-B08 for a total of 20 days.

The reduction of GFP+ expressing cells was sustained long-term, up to the last blood

draw at 20 weeks post-transplant (Figure 5.8A). Even after II-B08 treatment was

terminated, animal N125 continued to live for another 4 months. At the time of elective

euthanasia, the spleen weight was moderately enlarged at 0.15g. Upon examination of

the histopathology, the spleen had fairly normal splenic architecture with well-defined

red and white pulp (Figure 5.8B). The femur, however, demonstrated many mitotic

figures as well as an over-abundance of neutrophils, indicative of MPD (Figure 5.8C).

The white blood cell count of N125, however, remained relatively low (7.58-13.64

thousand wbc/ml), indicating indolent, rather than aggressive, disease. While the

description of this one animal's response to II-B08 is anecdotal, it is possible that the

15% EGFP+ population of cells was modest enough that II-B08 was able to effectively

suppress the growth and expansion of the N51-FLT3-expressing cells and thus permit

substantially increased survival.
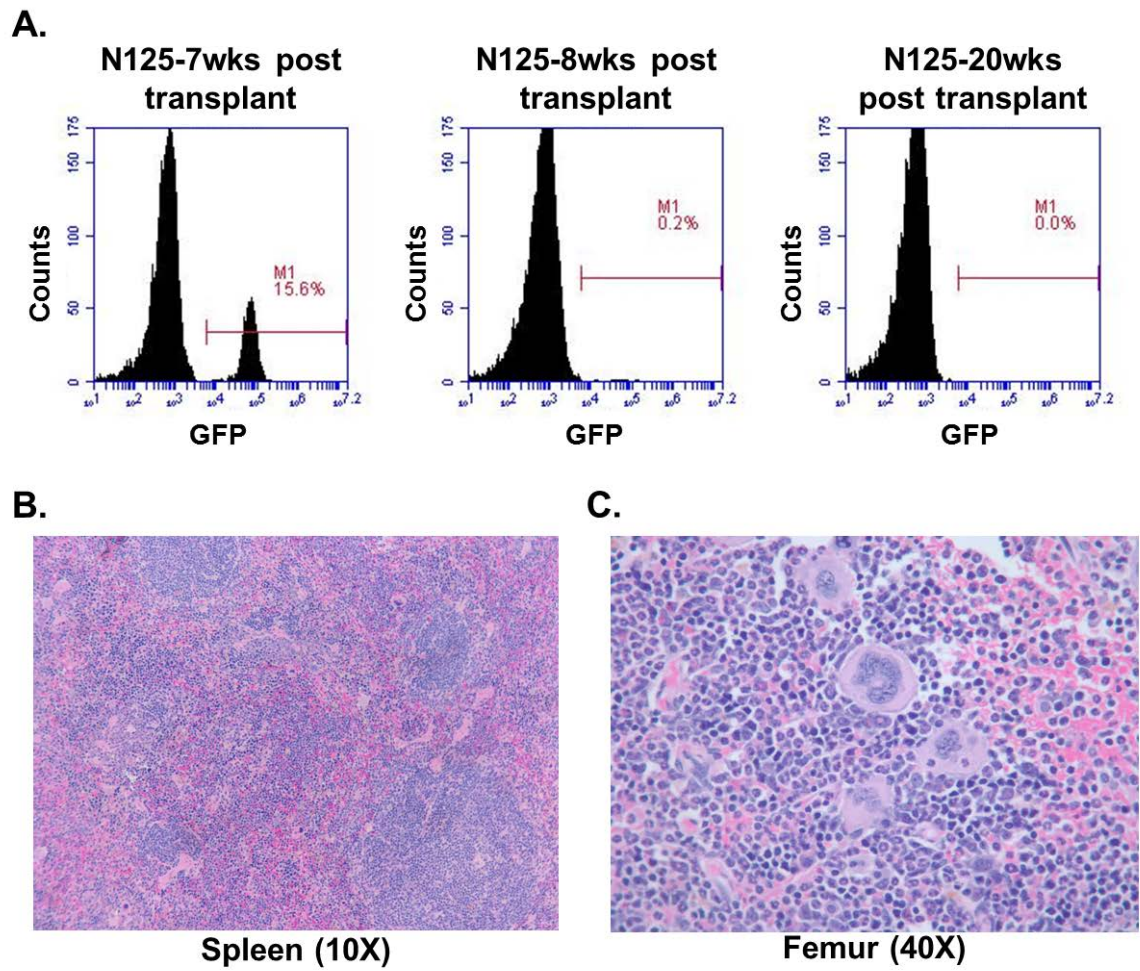
Figure 5.8: N51-FLT3 syngeneic transplant animal, N125, had increased life span after II-B08 treatment

(A) EGFP+ expression of peripheral blood 7, 8, and 20 weeks post-transplant. II-B08 treatment started after the 7 week blood draw demonstrating 15% EGFP+ cells and continued for 20 days. **(B)** H&E staining of the spleen was relatively normal, while the bone marrow **(C)** demonstrated leukemia.

Conclusions

FLT3-ITDs have been a popular target of many researchers seeking to find better therapies for FLT3-ITD-positive AML. Many FLT3 inhibitors have been tried and thus far FLT3-ITDs remain a difficult target rendering FLT3-ITD-positive AML patients challenging to treat with generally poor outcomes. Therefore, we are particularly interested in testing the Shp2 inhibitor, II-B08, as we have demonstrated that using biochemical and genetic studies that Shp2 plays a role in FLT3-ITD-signaling. In testing a pharmacologic inhibitor, there are several levels of interrogation.

We demonstrated that N51-FLT3-expressing primary cells are more sensitive to II-B08 treatment than their WT-FLT3-expressing counterparts. The hyperproliferation of N51-FLT3-expressing primary cells is significantly reduced in a dose-dependent manner when these cells are treated with increasing concentrations of II-B08. The proliferation of WT-FLT3-expressing cells however, is slightly but not statistically significantly reduced with increasing concentrations of II-B08. Biochemically II-B08 reduces hyperphosphorylation of STAT5 and Shp2 and of sustained Ras activation induced by N51-FLT3. In addition, N51-FLT3-positive cells have a higher increase in II-B08-induced apoptosis than WT-FLT3-positive cells.

In vivo we have treated a small cohort of N51-FLT3-ITD-positive animals with II-B08 who had begun to show signs of MPD. While this study is very preliminary, we did observe one animal that had a long term survival as a result of II-B08 treatment, rendering II-B08, or future derivative drugs with higher potency and specificity for Shp2, as attractive pharmacologic agents as we consider future studies using Shp2 inhibitors in FLT3-ITD-induced leukemia. Currently, Jackson Laboratories has FLT3-ITD knock-in

mice. These animals would be an ideal alternative to the syngeneic transplant animals and could potentially be used for II-B08 treatment directly to test the efficiency of the Shp2 inhibitor.

By defining targetable molecules in the FLT3-ITD-leukemogenic pathway, we can begin to uncover the options in finding better therapeutic targets which will lead to the development of better therapeutic options for the thousands of FLT3-ITD-positive AML patients desperately awaiting a cure. While our data demonstrated a benefit of using II-B08 *in vitro,* the *in vivo* data is still too young to determine if II-B08 could have some therapeutic benefits.

It has been demonstrated that II-B08 binds the catalytic pocket of Shp2 blocking its phosphatase activity (Zhang, He et al.). Just because II-B08 binds the catalytic site of Shp2 and has an effect on downstream signaling, does not necessarily imply that all Shp2-related functions are blocked. The SH2 domains of Shp2 in particular are used to help Shp2 dock to other phosphorylated proteins and causes signaling cascades. In prolactin signaling, the C-SH2 domain has been shown to be important in positively regulating STAT5 (Chughtai, Schimchowitsch et al. 2002). Therefore, while we are able to exhibit a decrease in N51-FLT3-induced STAT5 activation by blocking the phosphatase activity of Shp2 with II-B08 treatment, it may be possible to further reduce STAT5 activation by also abrogating the C-SH2 domain of Shp2.

We have demonstrated that Shp2 is an attractive target for treating FLT3-ITD-positive AML patients. While we have data which supports further investigation of II-B08, it is highly likely that it will be insufficient in curing FLT3-ITD-positive AML in its entirety, but may be useful for combination therapy. As we know, combination therapy

is becoming more prevalent and necessary to treat diseases with poor prognosis, therefore it may be beneficial to consider the inhibition of Shp2 for treating FLT3-ITD-positive AML.

CHAPTER SIX

DISCUSSION

Despite vigorous efforts to develop better treatments and therapies, the current treatment options for FLT3-ITD+ AML patients remain limited, especially in the elderly population where the disease is most prevalent. To date, the survival rates of FLT3-ITD+ patients remain significantly lower than FLT3-ITD- AML patients (Abu-Duhier, Goodeve et al. 2000). In order to better understand the molecular mechanisms contributing to FLT3-ITD-induced malignancy, we have investigated the role of Shp2 in FLT3-ITD-positive cell lines, primary cells, and in an *in vivo* mouse model.

Using Baf3 cells expressing WT-FLT3, N51-FLT3, or N73-FLT3, we demonstrated that N51-FLT3 and N73-FLT3 induce cellular hyperproliferation (Figure 3.1A), and hyperactivation of Stat5 (Figure 3.1C). Furthermore, we found that Shp2 is constitutively associated to N51-FLT3 (Figure 3.2A) and N73-FLT3 (Figure 3.2B) in Baf3 cells as well as to FLT3-ITDs in human cells (Figure 3.3B). Upon shRNA-targeted knock down of Shp2, we found a significant decrease in the hyperproliferation induced by N51-FLT3 (Figure 3.6C) and N73-FLT3 (Figure 3.6D). Finally, our findings demonstrate that Shp2 immunoprecipitates with STAT5 (Figure 3.4) as well as co-localizes with STAT5 in the nucleus of FLT3-ITD positive hematopoietic cells (Figure 3.7). Most novel, however, is the finding that Shp2 is found in a complex at the STAT5-regulated promoter sequence of *BCL2L1*, which controls the transcription of the pro-survival gene Bcl-X_L (Figure 3.8B). This mechanism is strikingly different than the well-known role of Shp2 as a cytosolic signaling molecule and implies a novel function and mechanism of Shp2 in combination with STAT5 in FLT3-ITD positive AML. These data

demonstrate that Shp2 plays an important role in FLT3-ITD-induced cellular proliferation, and that the implications extend beyond findings in transduced Baf3 cells, as we have also demonstrated that Shp2 is associated to FLT3-ITD in human cells expressing endogenous FLT3-ITD, supporting the general idea that Shp2 is important for FLT3-ITD-induced cellular transformation and leukemogenesis.

Future experiments may include further investigation of the role of Shp2 in the nucleus of leukemic cells. Since we exhibited Shp2 at the promoter sequence of STAT5 target, Bcl-X_L, it would be informative to see which (if any) other STAT5 transcriptional targets Shp2 may act on and/or if it is recruited to any other nuclear proteins. We demonstrated that Shp2 and STAT5 form a complex at the promoter of STAT5 transcriptional target, Bcl-X_L, however we have yet to elucidate the full function of Shp2 in the nucleus and/or which domain of Shp2 may be responsible for this interaction. It is possible that Shp2 acts as a scaffolding protein within a larger transcriptional complex which also contains STAT5. Alternatively, Shp2 may function to dephosphorylate an unknown protein substrate, permitting constitutive phosphorylation and activation of STAT5 at STAT5-responsive promoters. To test the role of Shp2 on the activation of Bcl-X_L, another possible experiment is to perform luciferase assays with luciferase expression linked to the Bcl-X_L promoter sequence and express a dominant-negative form (either C-SH2, N-SH2, or phosphatase domain mutant) of Shp2 in MV411 cells, with the hypothesis that Bcl-X_L-driven luciferase activity will decrease in the presence of dominant-negative Shp2 compared to wild type Shp2. The use of Shp2-C-SH2-, N-SH2-, and phosphatase-domain mutants, will allow us to determine which of these three Shp2

domains is most important for the co-localization of Shp2 with STAT5 and with the

activation of STAT5 target, Bcl-X$_L$ in FLT3-ITD-positive hematopoietic cells.

Using primary murine bone marrow low density mononuclear cells (LDMNCs)

transduced with WT-FLT3 or N51-FLT3, we were able to confirm the data generated in

Baf3 cells, that N51-FLT3 induces hyperproliferation (Figure 4.1B) and hyperactivation

of Stat5 (Figure 4.2) compared to WT-FLT3. One of the biggest benefits of using

primary cells is that, unlike heterologous cell lines, they are not transformed and, thus,

are less likely to yield misleading experimental results. That in mind, the primary cell

experiments presented played a vital role in setting up the fundamental experimental

model to progress and use the Shp2$^{flox/flox}$;Mx1-Cre+ mouse model, which demonstrated

that loss of physiologic Shp2 (polyI/polyC-treated Shp2$^{flox/flox}$;Mx1-Cre+ LDMNCs)

reduces N51-FLT3-induced hyperproliferation and hyperactivation of STAT5 *in vitro*

(Figures 4.6-4.8).

Given that Shp2 has been shown to interact with tyrosine 599 (Y599) of WT

FLT3, some future experimental goals using primary cells include the modification of

Y599 to phenylalanine (Y599F) in the first, second or both Y599 residues of N51-FLT3

followed by transduction of the modified N51-FLT3-Y599F constructs into primary cells

to determine which residue(s) is(are) most important for N51-FLT3-induced cellular

hyperproliferation and activation of STAT5. Furthermore, since the C-SH2 domain of

Shp2 has been implicated in the phosphorylation of and association with STAT5 in

mammary epithelial cells (Chughtai, Schimchowitsch et al. 2002), I would like to mutate

the N-SH2, C-SH2, or phosphatase domains of Shp2 (all of these constructs have been

made and are available in the Chan lab), co-transduce these mutant Shp2 constructs with

N51-FLT3 into primary cells, and use functional and biochemical assays to determine which domain of Shp2 is most important for proliferation and STAT5 constitutive activation. Given that the C-SH2 domain of Shp2 has been implicated in the Shp2-STAT5 interaction, I hypothesize that in the presence of N51-FLT3 and C-SH2 Shp2 domain mutant, the mutant Shp2 would be unable to properly phosphorylate and/or associate with STAT5 and therefore result in reduced hyperproliferation and hyperactivation of STAT5 compared to cells co-expressing N51-FLT3 and wild type Shp2. These experiments would be very informative in further understanding which domains of Shp2 are responsible for recruitment to Y599 of FLT3 as well as the promiscuous activation of STAT5. A better understanding of the function of Shp2 in this model system would yield implications and potentially a paradigm for Shp2 function in a multitude of malignant diseases.

Using the *in vivo* model, we found that a loss of Shp2 in the bone marrow of N51-FLT3 transplant recipients led to bone marrow failure and death in some recipients (Figures 4.15 and 4.16); however, those animals that did not succumb to bone marrow failure early-on did demonstrate a statistically significant increase in survival due to increased latency to malignancy, compared to N51-FLT3 transplant recipients with wildtype levels of Shp2 (Figure 4.18). Furthermore, in one experiment directly comparing polyI/polyC-treated animals transplanted with Cre+N51-FLT3- v. Cre+ WT-FLT3-transduced cells, animals transplanted with the Cre+N51-FLT3-transduced cells tended to be more sensitive to loss of Shp2 and succumb to bone marrow failure (2 of 7 animals), whereas polyI/polyC-treated Cre+ WT-FLT3 transplant recipients did not (0 out of 7 animals). While these data (polyI/polyC-treated Cre+N51-FLT3 vs.

polyI/polyC-treated WT-FLT3) were generated with a small sample size, it does suggest

that N51-FLT3 is more dependent on Shp2 than WT-FLT3 in transplant recipients, which

implicates a fundamental difference in the signaling mechanisms in N51-FLT3 compared

to WT-FLT3.

While these *in vivo* data are informative, and suggest that targeting Shp2 may be

useful, it is likely not the hallmark cure for FLT3-ITD+ AML. It has been well

established that Shp2 is important in hematopoietic stem cells and normal hematopoiesis

(Qu, Shi et al. 1997; Qu, Yu et al. 1998; Chan, Johnson et al. 2003; Chan, Li et al. 2006;

Chan, Cheung et al. 2011; Zhu, Ji et al. 2011), nevertheless, we hypothesized that in the

presence of N51-FLT3, loss of Shp2 could correct N51-FLT3-induced malignancy.

While the loss of Shp2 increased the latency to N51-FLT3-induced leukemic phenotype,

Shp2 is still essential for normal hematopoiesis, therefore it also caused bone marrow

failure. Targeting Shp2 in FLT3-ITD+ patients could be potentially beneficial, but the

therapeutic window may be narrow. Therefore, it is likely that targeting Shp2 will need

to be carefully titrated in order to reduce Shp2 to a level that is low enough to diminish

the penetration of N51-FLT3-induced transformation and be therapeutically beneficial,

but to maintain an adequate Shp2 level to prevent bone marrow failure and subsequent

death.

In targeting Shp2 pharmacologically with novel Shp2 inhibitor, II-B08, we were

able to demonstrate that inhibition of the phosphatase activity of Shp2 in primary cells

expressing N51-FLT3 results in a dose-dependent and statistically significant reduction in

hyperproliferation with increasing concentrations of II-B08 (Figure 5.2A).

Biochemically, we demonstrated that 15µM of II-B08 was sufficient to reduce the

promiscuous activation of STAT5, reduce phospho-Shp2, and phospho-Akt levels

(Figure 5.2B). The percent increase in apoptosis in cells expressing N51-FLT3 increases

significantly in N51-FLT3-expressing cells upon increasing concentrations of II-B08,

while this increase in apoptosis is not evident in WT-FLT3-expresssing cells (Figure 5.4).

These functional and biochemical data suggested that Shp2 inhibition *in vitro* with II-B08

successfully inhibited FLT3-ITD-induced hyperproliferation, leading us to test its

potential efficacy *in vivo.*

Syngeneic N51-FLT3 transplant recipients succumb to FLT3-ITD-induced

malignancy approximately 40% of the time. Four out of seven of those leukemic mice

were treated with 100mg/kg II-B08 by daily IP injection for up to 20 days. While our

subset of animals was limited, one of the animals had long-term survival (Figure 5.7) and

went into a remission-like state as its peripheral blood percent EGFP population dropped

from 15.6% (prior to II-B08 treatment) to 0.2% one week after starting treatment (Figure

5.8). This low EGFP percentage was maintained until the animal's euthanasia

approximately 4 months following II-B08 therapy. While this finding is highly

preliminary, it suggests further investigation and/or development of more specific and

potent Shp2 inhibitors may improve the efficacy of Shp2 inhibition *in vivo* and improve

its potential therapeutic benefits.

Taken together, our data demonstrate a novel role of Shp2 in a complex with

STAT5 in the nucleus of FLT3-ITD-expressing cells. Additionally, both of our *in vivo*

studies (genetic knock out of Shp2 and pharmacologic Shp2 inhibition with II-B08)

suggest that a controlled loss of Shp2 expression/function could provide a therapeutic

benefit to FLT3-ITD-positive AML patients. While much is known about Shp2 in

cancers, our current findings contribute significantly to the greater Shp2 research

community, as they provide a novel Shp2 mechanism in myeloid malignancies and yield

a potential novel therapeutic approach in FLT3-ITD+ AMLs.

Overall Conclusions and Significance

Internal tandem duplications in FLT3 (FLT3-ITDs) account for approximately 30% of the mutations reported in AML patients, are associated with poor clinical prognosis, and the molecular mechanism of how they signal to induce leukemogenesis is poorly understood. In the process to further understand their molecular mechanisms, we expected to observe that Shp2 is important for FLT3-ITD-induced proliferation, activation of STAT5, and the development and/or progression of N51-FLT3-induced MPD *in vivo*. We further expected that loss or reduction of Shp2 expression and/or function would at least partially correct the cellular hyperproliferation, constitutive activation of STAT5, and either prevent the onset or increase the latency to N51-FLT3-induced malignancy *in vivo*.

We discovered several novel findings regarding the molecular mechanisms of FLT3-ITD-induced malignancy. While Shp2 is normally localized to the cytoplasm and functions as a cytosolic signaling molecule, in the presence of FLT3-ITD-activing mutations we demonstrated that Shp2 co-localizes with STAT5 in the nucleus, at the *BCL2L1* promoter region which activates STAT5-responsive transcriptional target, Bcl-X_L. To our knowledge, this is the first time Shp2 has been found at a STAT5 promoter in leukemic cells and suggests a novel role of Shp2 in the nucleus where it likely functions to drive transcription of pro-leukemic proteins. This novel role of Shp2 as an important co-molecule in a complex with STAT5 at STAT5-responsive genes leads us to consider other potential gene response elements where Shp2 may function and/or other potential transcription factors Shp2 may cooperate with to promote pro-leukemic signals. Future

investigation is needed to address these questions and to better understand the implications of the Shp2-STAT5 complex in the setting of leukemogenesis.

In addition to Bcl-X$_L$, Stat5 also up-regulates cell cycle promoting gene, Cyclin-D1, and the proto-oncogene, Pim-1, therefore it would be interesting to test for a similar Shp2-STAT5 complex at the promoter sequences of Cyclin-D1 and Pim-1 which would support our novel finding that Shp2 acts in cooperation with transcription factor STAT5 in the nucleus. STAT family member, Stat3 regulates cell cycle progression genes Fos, Cyclin-D, and c-Myc as well as anti-apoptotic genes BCL2 and Bcl-X$_L$. Data suggests that Shp2 gain-of-function mutations negatively regulate STAT3, and that Shp2 gain-of-function mutations are associated with decreased binding between STAT3 and DNA (Zhang, Chan et al. 2009). Therefore, it may be relevant to test nuclear co-localization of STAT3 and Shp2 in leukemic cells.

In vivo, we discovered that transplant of Shp2-deficient N51-FLT3-expressing cells results in increased latency and decreased severity of FLT3-ITD-induced malignancy which suggests that inhibiting Shp2 may have therapeutic benefit to FLT3-ITD+ AML patients. In addition, animals transplanted with N51-FLT3-expressing cells seemed to be much more sensitive to loss of Shp2, as they more commonly succumb to bone marrow failure and subsequent death compared to animals transplanted with WT-FLT3-expressing cells. This increased sensitivity of FLT3-ITD-expressing cells to loss of Shp2 implies that targeting Shp2 could be used as a therapeutic advantage to selectively target FLT3-ITD+ cells over WT cells.

Collectively we demonstrated a novel role of Shp2 in the nucleus at Stat5-responsive gene elements and show convincing evidence that targeting Shp2 may provide

therapeutic benefit to treat FLT3-ITD-positive AML. While these findings are vital to better understand the role of Shp2 in FLT3-ITD-induced leukemogenesis, they have a broader impact because mutations in Shp2 are present in about 50% of patients with the congenital disorder, Noonan Syndrome (NS), which have an increased susceptibility in the pediatric disease, juvenile myelomonocytic leukemia (JMML). Although it is a rare disease, approximately 30% of JMML patients (who do not have NS) also have causative Shp2 mutations. My studies demonstrate that FLT3-ITDs constitutively recruit Shp2 and result in increased Shp2 activity. This increase in Shp2 activity could be paralleled with gain-of-function Shp2 mutations found in NS and JMML in the sense that both diseases have increased Shp2 function. In addition to the role of Shp2 in leukemogenesis, further understanding of the molecular mechanisms of aberrantly activated Shp2 may have implications in other types of malignancies in which Shp2 has been implicated including breast, lung, and gastric cancers. For example, Shp2 is essential for the transformation of breast cancer cells and inhibition of Shp2 reverts diseased tissue back to a normal breast epithelial phenotype (MET) (Zhou and Agazie 2008). Also, suppression of Shp2 in lung cancer cell lines results in reduced proliferation and c-Myc expression which may suggest that Shp2 positively cooperates with STAT3 at STAT3 transcriptional target, c-Myc (Ren, Chen et al. 2010). While these diseases are phenotypically distinct, greater understanding of the molecular mechanisms surrounding Shp2 could provide further insight into treating these diseases.

As medical technologies advance, the implication and use of personalized medicine is becoming more essential and moving toward being the "new" standard of care. It is currently a routine practice to receive molecular testing as part of a traditional

cancer work-up in order to dictate which cocktail of drugs and treatments will best attack

one's specific molecular aberrations. This molecular diagnosis is even more specific than

a general phenotypic diagnosis of AML, CML, breast cancer, or the like, and allows for

much more targeted and specialized treatment. While there are trends and common

mutations within patients with the same disease, each patient has a unique set of

molecular markers rendering them more or less likely to benefit from each particular

therapy. Therefore, a further understanding of the molecular mechanisms surrounding

FLT3-ITDs and Shp2, including the multitude of diseases Shp2 has been implicated in is

of the upmost importance as the field of personalized medicine advances.

REFERENCES

Abu-Duhier, F. M., A. C. Goodeve, et al. (2000). "FLT3 internal tandem duplication mutations in adult acute myeloid leukaemia define a high-risk group." <u>Br J Haematol</u> **111**(1): 190-195.

Ali, S., Z. Chen, et al. (1996). "PTP1D is a positive regulator of the prolactin signal leading to beta-casein promoter activation." <u>Embo J</u> **15**(1): 135-142.

Bentires-Alj, M., S. G. Gil, et al. (2006). "A role for the scaffolding adapter GAB2 in breast cancer." <u>Nat Med</u> **12**(1): 114-121.

Bentires-Alj, M., J. G. Paez, et al. (2004). "Activating mutations of the noonan syndrome-associated SHP2/PTPN11 gene in human solid tumors and adult acute myelogenous leukemia." <u>Cancer Research</u> **64**(24): 8816-8820.

Berchtold, S., S. Volarevic, et al. (1998). "Dominant negative variants of the SHP-2 tyrosine phosphatase inhibit prolactin activation of Jak2 (janus kinase 2) and induction of Stat5 (signal transducer and activator of transcription 5)-dependent transcription." <u>Mol Endocrinol</u> **12**(4): 556-567.

Beverly, L. J. and H. E. Varmus (2009). "MYC-induced myeloid leukemogenesis is accelerated by all six members of the antiapoptotic BCL family." <u>Oncogene</u> **28**(9): 1274-1279.

Chan, G., L. S. Cheung, et al. (2011). "Essential role for Ptpn11 in survival of hematopoietic stem and progenitor cells." <u>Blood</u> **117**(16): 4253-4261.

Chan, R. J. and G. S. Feng (2007). "PTPN11 is the first identified proto-oncogene that encodes a tyrosine phosphatase." <u>Blood</u> **109**(3): 862-867.

Chan, R. J., S. A. Johnson, et al. (2003). "A definitive role of Shp-2 tyrosine phosphatase in mediating embryonic stem cell differentiation and hematopoiesis." <u>Blood</u> **102**(6): 2074-2080.

Chan, R. J., M. B. Leedy, et al. (2005). "Human somatic PTPN11 mutations induce hematopoietic-cell hypersensitivity to granulocyte-macrophage colony-stimulating factor." <u>Blood</u> **105**(9): 3737-3742.

Chan, R. J., Y. Li, et al. (2006). "Shp-2 heterozygous hematopoietic stem cells have deficient repopulating ability due to diminished self-renewal." <u>Exp Hematol</u> **34**(9): 1230-1239.

Chen, L., S. S. Sung, et al. (2006). "Discovery of a novel shp2 protein tyrosine phosphatase inhibitor." <u>Mol Pharmacol</u> **70**(2): 562-570.

Chen, Y., R. Wen, et al. (2003). "Identification of Shp-2 as a Stat5A phosphatase." <u>J Biol Chem</u> **278**(19): 16520-16527.

Choudhary, C., C. Brandts, et al. (2007). "Activation mechanisms of STAT5 by oncogenic Flt3-ITD." <u>Blood</u> **110**(1): 370-374.

Choudhary, C., J. V. Olsen, et al. (2009). "Mislocalized activation of oncogenic RTKs switches downstream signaling outcomes." <u>Molecular cell</u> **36**(2): 326-339.

Chughtai, N., S. Schimchowitsch, et al. (2002). "Prolactin induces SHP-2 association with Stat5, nuclear translocation, and binding to the beta-casein gene promoter in mammary cells." <u>J Biol Chem</u> **277**(34): 31107-31114.

Chung, K. Y., G. Morrone, et al. (2005). "Enforced expression of an Flt3 internal tandem duplication in human CD34+ cells confers properties of self-renewal and enhanced erythropoiesis." <u>Blood</u> **105**(1): 77-84.

Deschler, B. and M. Lubbert (2006). "Acute myeloid leukemia: epidemiology and etiology." Cancer **107**(9): 2099-2107.

Estey, E. and H. Dohner (2006). "Acute myeloid leukaemia." Lancet **368**(9550): 1894-1907.

Feng, G. S. (1999). "Shp-2 tyrosine phosphatase: signaling one cell or many." Experimental cell research **253**(1): 47-54.

Fukuda, S., H. E. Broxmeyer, et al. (2005). "Flt3 ligand and the Flt3 receptor regulate hematopoietic cell migration by modulating the SDF-1alpha(CXCL12)/CXCR4 axis." Blood **105**(8): 3117-3126.

Georgiades, P., S. Ogilvy, et al. (2002). "VavCre transgenic mice: a tool for mutagenesis in hematopoietic and endothelial lineages." Genesis **34**(4): 251-256.

Georgiou, G., V. Karali, et al. (2006). "Serial determination of FLT3 mutations in myelodysplastic syndrome patients at diagnosis, follow up or acute myeloid leukaemia transformation: incidence and their prognostic significance." Br J Haematol **134**(3): 302-306.

Griffith, J., J. Black, et al. (2004). "The structural basis for autoinhibition of FLT3 by the juxtamembrane domain." Mol Cell **13**(2): 169-178.

Heiss, E., K. Masson, et al. (2006). "Identification of Y589 and Y599 in the juxtamembrane domain of Flt3 as ligand-induced autophosphorylation sites involved in binding of Src family kinases and the protein tyrosine phosphatase SHP2." Blood **108**(5): 1542-1550.

Irusta, P. M., Y. Luo, et al. (2002). "Definition of an inhibitory juxtamembrane WW-like domain in the platelet-derived growth factor beta receptor." J Biol Chem **277**(41): 38627-38634.

Joung, Y. H., E. J. Lim, et al. (2005). "Hypoxia activates the cyclin D1 promoter via the Jak2/STAT5b pathway in breast cancer cells." Experimental & molecular medicine **37**(4): 353-364.

Kato, Y., A. Iwama, et al. (2005). "Selective activation of STAT5 unveils its role in stem cell self-renewal in normal and leukemic hematopoiesis." J Exp Med **202**(1): 169-179.

Ke, Y., J. Lesperance, et al. (2006). "Conditional deletion of Shp2 in the mammary gland leads to impaired lobulo-alveolar outgrowth and attenuated Stat5 activation." J Biol Chem **281**(45): 34374-34380.

Kelly, L. M., Q. Liu, et al. (2002). "FLT3 internal tandem duplication mutations associated with human acute myeloid leukemias induce myeloproliferative disease in a murine bone marrow transplant model." Blood **99**(1): 310-318.

Kiyoi, H. and T. Naoe (2002). "FLT3 in human hematologic malignancies." Leukemia & lymphoma **43**(8): 1541-1547.

Kiyoi, H., R. Ohno, et al. (2002). "Mechanism of constitutive activation of FLT3 with internal tandem duplication in the juxtamembrane domain." Oncogene **21**(16): 2555-2563.

Koch, S., A. Jacobi, et al. (2008). "Abnormal localization and accumulation of FLT3-ITD, a mutant receptor tyrosine kinase involved in leukemogenesis." Cells, tissues, organs **188**(1-2): 225-235.

Kuhn, R., F. Schwenk, et al. (1995). "Inducible gene targeting in mice." Science **269**(5229): 1427-1429.

Lee, B. H., Z. Tothova, et al. (2007). "FLT3 mutations confer enhanced proliferation and survival properties to multipotent progenitors in a murine model of chronic myelomonocytic leukemia." Cancer Cell **12**(4): 367-380.

Li, L., H. Modi, et al. (2011). "A critical role for SHP2 in STAT5 activation and growth factor-mediated proliferation, survival, and differentiation of human CD34+ cells." Blood **118**(6): 1504-1515.

Maroun, C. R., M. A. Naujokas, et al. (2000). "The tyrosine phosphatase SHP-2 is required for sustained activation of extracellular signal-regulated kinase and epithelial morphogenesis downstream from the met receptor tyrosine kinase." Molecular and cellular biology **20**(22): 8513-8525.

Melchert, M. (2006). "Managing acute myeloid leukemia in the elderly." Oncology (Williston Park) **20**(13): 1674-1682; discussion 1683-1674, 1687.

Mizukawa, B., J. Wei, et al. (2011). "Inhibition of Rac GTPase signaling and downstream prosurvival Bcl-2 proteins as combination targeted therapy in MLL-AF9 leukemia." Blood **118**(19): 5235-5245.

Mizuki, M., J. Schwable, et al. (2003). "Suppression of myeloid transcription factors and induction of STAT response genes by AML-specific Flt3 mutations." Blood **101**(8): 3164-3173.

Mohi, M. G., I. R. Williams, et al. (2005). "Prognostic, therapeutic, and mechanistic implications of a mouse model of leukemia evoked by Shp2 (PTPN11) mutations." Cancer Cell **7**(2): 179-191.

Neel, B. G., H. Gu, et al. (2003). "The 'Shp'ing news: SH2 domain-containing tyrosine phosphatases in cell signaling." Trends Biochem Sci **28**(6): 284-293.

Qu, C. K., Z. Q. Shi, et al. (1997). "A deletion mutation in the SH2-N domain of Shp-2 severely suppresses hematopoietic cell development." Molecular and cellular biology **17**(9): 5499-5507.

Qu, C. K., W. M. Yu, et al. (1998). "Biased suppression of hematopoiesis and multiple developmental defects in chimeric mice containing Shp-2 mutant cells." Molecular and cellular biology **18**(10): 6075-6082.

Ren, Y., Z. Chen, et al. (2010). "Critical role of Shp2 in tumor growth involving regulation of c-Myc." Genes Cancer **1**(10): 994-1007.

Rocnik, J. L., R. Okabe, et al. (2006). "Roles of tyrosine 589 and 591 in STAT5 activation and transformation mediated by FLT3-ITD." Blood **108**(4): 1339-1345.

Saxton, T. M., M. Henkemeyer, et al. (1997). "Abnormal mesoderm patterning in mouse embryos mutant for the SH2 tyrosine phosphatase Shp-2." The EMBO journal **16**(9): 2352-2364.

Schmidt-Arras, D., S. A. Bohmer, et al. (2009). "Anchoring of FLT3 in the endoplasmic reticulum alters signaling quality." Blood **113**(15): 3568-3576.

Schmidt-Arras, D. E., A. Bohmer, et al. (2005). "Tyrosine phosphorylation regulates maturation of receptor tyrosine kinases." Molecular and cellular biology **25**(9): 3690-3703.

Schubbert, S., K. Lieuw, et al. (2005). "Functional analysis of leukemia-associated PTPN11 mutations in primary hematopoietic cells." Blood **106**(1): 311-317.

Schuringa, J. J., K. Y. Chung, et al. (2004). "Constitutive activation of STAT5A promotes human hematopoietic stem cell self-renewal and erythroid differentiation." The Journal of experimental medicine **200**(5): 623-635.

Shi, Z. Q., D. H. Yu, et al. (2000). "Molecular mechanism for the Shp-2 tyrosine phosphatase function in promoting growth factor stimulation of Erk activity." Molecular and cellular biology **20**(5): 1526-1536.

Small, D. (2006). "FLT3 mutations: biology and treatment." Hematology Am Soc Hematol Educ Program: 178-184.

Tartaglia, M., C. M. Niemeyer, et al. (2003). "Somatic mutations in PTPN11 in juvenile myelomonocytic leukemia, myelodysplastic syndromes and acute myeloid leukemia." Nature genetics **34**(2): 148-150.

Whitman, S. P., K. J. Archer, et al. (2001). "Absence of the wild-type allele predicts poor prognosis in adult de novo acute myeloid leukemia with normal cytogenetics and the internal tandem duplication of FLT3: a cancer and leukemia group B study." Cancer Res **61**(19): 7233-7239.

Xu, R., Y. Yu, et al. (2005). "Overexpression of Shp2 tyrosine phosphatase is implicated in leukemogenesis in adult human leukemia." Blood **106**(9): 3142-3149.

Yu, C. L., Y. J. Jin, et al. (2000). "Cytosolic tyrosine dephosphorylation of STAT5. Potential role of SHP-2 in STAT5 regulation." J Biol Chem **275**(1): 599-604.

Zhang, E. E., E. Chapeau, et al. (2004). "Neuronal Shp2 tyrosine phosphatase controls energy balance and metabolism." Proc Natl Acad Sci U S A **101**(45): 16064-16069.

Zhang, S. and H. E. Broxmeyer (1999). "p85 subunit of PI3 kinase does not bind to human Flt3 receptor, but associates with SHP2, SHIP, and a tyrosine-phosphorylated 100-kDa protein in Flt3 ligand-stimulated hematopoietic cells." Biochem Biophys Res Commun **254**(2): 440-445.

Zhang, S. and H. E. Broxmeyer (2000). "Flt3 ligand induces tyrosine phosphorylation of gab1 and gab2 and their association with shp-2, grb2, and PI3 kinase." Biochem Biophys Res Commun **277**(1): 195-199.

Zhang, S., C. Mantel, et al. (1999). "Flt3 signaling involves tyrosyl-phosphorylation of SHP-2 and SHIP and their association with Grb2 and Shc in Baf3/Flt3 cells." J Leukoc Biol **65**(3): 372-380.

Zhang, W., R. J. Chan, et al. (2009). "Negative regulation of Stat3 by activating PTPN11 mutants contributes to the pathogenesis of Noonan syndrome and juvenile myelomonocytic leukemia." J Biol Chem **284**(33): 22353-22363.

Zhang, X., Y. He, et al. "Salicylic acid based small molecule inhibitor for the oncogenic Src homology-2 domain containing protein tyrosine phosphatase-2 (SHP2)." J Med Chem **53**(6): 2482-2493.

Zhou, X. D. and Y. M. Agazie (2008). "Inhibition of SHP2 leads to mesenchymal to epithelial transition in breast cancer cells." Cell Death Differ **15**(6): 988-996.

Zhu, H. H., K. Ji, et al. (2011). "Kit-Shp2-Kit signaling acts to maintain a functional hematopoietic stem and progenitor cell pool." Blood **117**(20): 5350-5361.

CURRICULUM VITAE

Sarah Cassidy Nabinger

EDUCATION

2005-2012   Indiana University, Indianapolis, IN
Ph.D. Medical and Molecular Biology w/ Minor in Life Sciences
Dissertation: Understanding the Mechanisms of FLT3-ITD-Induced
Leukemogenesis
Advisor: Rebecca J. Chan, MD/PhD

2003-2005   Indiana University Purdue University Indianapolis, B.S. Biology
Indianapolis, IN

2001-2003   University of Indianapolis; Indianapolis, IN Biology; Transferred

HONORS AND AWARDS

2010   Sigma Xi Graduate Student Biomedical Research Competition – 2nd place
of Senior Graduate Students, 2010
2009   Travel Award to attend the annual meeting of the American Society of
Hematology, New Orleans, LA
2009   First prize for poster presentation at "Cancer Research Day"
2008   Travel Award from Indiana University School of Medicine to attend
ISEH, Boston, MA
2008   Travel Award to attend the annual meeting of the International Society of
Hematology (ISEH), Boston, MA
2005   Outstanding Researcher Award
2002   Induction into Phi Alpha Epsilon (Freshmen Honor Society) at Univ. of
Indianapolis
2001-2003   Dean's Scholarship; University of Indianapolis (50% of tuition)

ABSTRACTS PRESENTED (ORAL PRESENTATION)

2012   Midwest Blood Club Symposium, Indianapolis, IN, 2012. **Nabinger SC**,
XJ Li, S Goenka, GS Feng, M Yu, GE Sandusky, R Kapur, and RJ Chan.
The Protein Tyrosine Phosphatase, Shp2, Positively Contributes to FLT3-
ITD-Induced Hematopoietic Progenitor Hyperproliferation and Malignant
Disease *In Vivo.*

2011   Sigma Xi Graduate Research Competition, Indianapolis, IN, 2011.
Nabinger SC. Shp2/STAT5 Nuclear Co-Localization in FLT3-ITD-
Expressing Leukemic Cells.

2010   Midwest Blood Club, Indianapolis, IN, 2010. **Nabinger SC**, Y He, F Yin, B Ramdas, X Zhang, LT Senbanjo, S Fukuda, M Yu, HS Boswell, GS Feng, ZY Zhang, R Kapur, and RJ Chan. Targeting the Protein Tyrosine Phosphatase, Shp2, May be a Future Therapeutic for FLT3-ITD-Positive AML.

2010   Sigma Xi Graduate Biomedical Research Competition, Indianapolis, IN 2010. **Nabinger SC**. Shp2 May be a Future Therapeutic Target for FLT3-ITD-Positive AML.

2009   American Society of Hematology, New Orleans, LA 2009. **Nabinger SC**, Y He, F Yin, X Zhang, LT Senbanjo, S Fukuda, M Yu, GS Feng, ZY Zhang, R Kapur, and RJ Chan. Targeting the Protein Tyrosine Phosphatase, Shp2, Reduces FLT3-ITD-Induced Hyperproliferation of Murine Hematopoietic Progenitors.

2008   International Society of Experimental Hematology (ISEH), Boston, MA, 2008. **Nabinger SC**, S Fukuda, R Kapur, RJ Chan. The Role of Shp2 in FLT3-ITD-Induced Leukemogenesis.

ABSTRACTS PRESENTED (POSTER PRESENTATIONS)

2011   International Society of Hematology, Vancouver, B.C., Canada, 2011. **Nabinger SC**, X Li, and RJ Chan. The Protein Tyrosine Phosphatase, Shp2, Demonstrates Interaction with STAT5 and Nuclear Localization in FLT3-ITD-Expressing Leukemic Cells.

2011   Midwest Blood Club, Cincinnati, OH, 2011. **Nabinger, SC**, X, Li, and RJ Chan. 2011. The Protein Tyrosine Phosphatase, Shp2, Demonstrates Interaction with STAT5 and Nuclear Localization in FLT3-ITD-Expressing Leukemic Cells.

2011   Cancer Research Day, Indianapolis, IN 2011. **Nabinger SC**, X Li, and RJ Chan. The Protein Tyrosine Phosphatase, Shp2, Demonstrates Interaction with STAT5 and Nuclear Localization in FLT3-ITD-Expressing Leukemic Cells.

2009   Midwest Blood Club, Cincinnati, OH, 2009. **Nabinger SC**, S Fukuda, R Kapur, RJ Chan. Shp2 Plays a Key Role in FLT3-ITD-Induced Leukemogenesis.

2008   American Society of Hematology, San Francisco, CA, 2008. **Nabinger SC**, S Fukuda, R Kapur, and RJ Chan. The Role of Shp2 in FLT3-ITD-Induced Leukemogenesis.

GRANTS AND FELLOWSHIPS

Improved Therapies for AML in the Elderly
Principal Investigator, Sarah C. Nabinger
Agency: NIH/Institute of Aging

PUBLICATIONS

1.   **Nabinger SC**, Chan RJ. Shp2 Function in Hematopoietic Stem Cell Biology and Leukemogenesis. "Invited Review", Current Opinion in Hematology. Submitted.

2.   **Nabinger SC**, Li X, Ramdas B, He Y, Zhang X, Fukuda S, Goenka S, Feng GS, Yu M, Sandusky GE, Boswell HS, Zhang ZY, Kapur R, and Chan RJ. The Protein Tyrosine Phosphatase, Shp2, Positively Contributes to FLT3-ITD-Induced Hematopoietic Progenitor Hyperproliferation and Malignant Disease *In Vivo.* Leukemia, revision invited.

3.   Ma P, R Mali, L-F Zeng, H Martin, B Ramdas, Y He, E Sims, J Ghosh, **SC Nabinger**, J Ghosh, N Sharma, V Munugalavadla, A Chatterjee, S Li, G Sandusky, AW Craig, KD Bunting, GS Feng, RJ Chan, Z-Y Zhang, and R Kapur. 2012. Role of SHP2 phosphatase in KIT induced transformation: Identification of SHP2 as a druggable target in diseases involving oncogenic KIT. Blood, revision submitted.

4.   Mali, R, B Ramdas, P Ma, J Shi, V Munugalavadla, E Sims, L Wei, S Vemula, **SC Nabinger**, CB. Godwin, RJ Chan, F Traina, V Visconte, RV. Tiu, TA Lewis, AM Stern, Q Wen, JD Crispino, HS Boswell, and R Kapur. Rho kinase regulates the survival and transformation of cells bearing oncogenic forms of KIT, FLT3, and BCR-ABL. Cancer Cell, 2011 Sep 13.

5.   Sayar H, Chan RJ, Orschell CM, Chan EM, Yu Z, Hood D, Plett A, Yang Z, Hui CL, **Nabinger SC**, Kohlbacher KJ, West ES, Walter A, Sampson C, Wu J, Cripe LD. Thrice weekly azacitidine does not improve hematological responses in lower-risk myelodysplastic syndromes: A study of the Hoosier Oncology Group. Leuk Res. 2011 Mar 18.

6.   Ranahan WP, Han Z, Smith-Kinnaman W, **Nabinger SC**, Heller B, Herbert BS, Chan R, Wells CD. The adaptor protein AMOT promotes the proliferation of mammary epithelial cells via the prolonged activation of the extracellular signal-regulated kinases. Cancer Res. 2011 Mar 15;71(6):2203-11.

7.   Zhang X, He Y, Liu S, Yu Z, Jiang ZX, Yang Z, Dong Y, **Nabinger SC**, Wu L, Gunawan AM, Wang L, Chan RJ, Zhang ZY. (2010). Salicylic acid based small molecule inhibitor for the oncogenic Src homology-2 domain containing protein tyrosine phosphatase-2 (SHP2). J Med Chem. 53(6):2482-93.

8.   Yang Z, Kondo T, Voorhorst CS, **Nabinger SC**, Ndong L, Yin F, Chan EM, Yu M, Würstlin O, Kratz CP, Niemeyer CM, Flotho C, Hashino E, Chan RJ. (2009). Increased c-Jun expression and reduced GATA2 expression promote aberrant monocytic differentiation induced by activating PTPN11 mutants. Mol Cell Biol. (16):4376-93.

9.   Witting SR, Brown M, Saxena R, **Nabinger S**, Morral N. (2008). Helper-dependent adenovirus-mediated short hairpin RNA expression in the liver activates the interferon response. J Biol Chem. 283(4):2120-8.

10.   Bard M, Sturm AM, Pierson CA, Brown S, Rogers KM, **Nabinger S**, Eckstein J, Barbuch R, Lees ND, Howell SA, Hazen KC. (2005). Sterol uptake in Candida glabrata: rescue of sterol auxotrophic strains. Diagn Microbiol Infect Dis. 52(4):285-93.